5-907

A REPORT

TO CANMET

ON

THE EVALUATION OF GROUT FILLED LIGHTWEIGHT TUBULAR STEEL AS AN ALTERNATIVE TO CONVENTIONAL SUPPORT IN LARGE EXCAVATIONS IN COAL MINES OR OTHER PLACES SUBJECT TO HIGH STRESS

Department of Supply and Services
Contract Number 0ST85-00120

Prepared by

D.S. Jones
Department of Mining and Metallurgical Engineering
Technical University of Nova Scotia

181 pp

EXECUTIVE SUMMARY

The use of conventional steel supports (rolled steel joists - RSJ) in mine tunnels subjected to high stress zones requires the application of 'heavy' support sets. The complexity of fabrication and the additional time required to install these supports increases the tunnel development cycle time and consequently increases the tunnel development cost. A proposal to use light weight hollow tubes which could be quickly erected in the mine tunnel and subsequently filled with a stiffening agent (grout) would alleviate this current problem if the composite support member provided adequate support strength. An investigation of this new support member was conducted in the Department of Mining and Metallurgical Engineering at the Technical University of Nova Scotia, Halifax Nova Scotia.

A review of the design criteria for RSJ mine supports is presented as a basis to compare support capacity of the composite support member with the RSJ supports. Four RSJ design techniques are discussed.

The technology of grout filled tubular column and column-beam structural members is discussed. A limited

amount of this information is transferrable to the subject study; however, this review provides an introduction to the technology of grout filled tubular structures.

A series of grout filled hollow structural steel (HSS) beam members were tested in one and three-point, simply supported bend tests. A range of grout cure times of 1,3,7 and 28 days were investigated. Additional tests on steel reinforced beam members and a pressurized grout core composite beam member were conducted.

Laterally constrained beam tests were conducted using a specially constructed rigid test frame to investigate the effect of restricting the end rotation of the simply supported beam as may be provided by a rigid joint in RSJ support work.

A discussion of the test results is presented and conclude that for the composite member researched, a 37% weight reduction for support installation can be achieved without any loss of ultimate support strength.

Material cost estimates are made for the equivalent ultimate strength grout filled HSS beam and

RSJ beam. No estimate of the potential labour savings for installation of the lighter weight 'empty' HSS section has been predicted.

Other advantages of the composite HSS beam are presented such as the potential to significantly increase the section modulus (Syy) and improve the lateral strength of the composite support member over an equivalent support strength RSJ support.

The connections and bracing method for tubular sections are reviewed to demonstrate that fabrication techniques are in place to accommodate both the assembly of multi-piece mine support tubular structures and the strutting of these supports.

It was demonstrated that conventional composite beam design methods by material transformation principles cannot be used to accurately predict the performance of a grout filled HSS beam.

Final recommendations are made to conduct ultimate (collapse) load investigations of the composite beam member in an arch support structure. It is proposed that this support configuration would derive significantly greater benefit from the grout core than the simply supported straight beam members that were investigated.

RESUME DES RECOMMANDATIONS

L'utilisation de supports d'acier classiques (poutrelles d'acier laminé) dans les tunnels de mine où sont exercées de fortes contraintes nécessite la mise en place d'une série de supports lourds. Puisque leur fabrication est compliquée et qu'il faut plus de temps pour les installer, ces supports prolongent les opérations liées au creusement du tunnel et, par conséquent, augmentent les coûts pertinents. De légers poteaux en profils creux qui prendraient peu de temps à dresser dans le tunnel et qui seraient ensuite remplis d'un raidisseur (coulis de béton) pourraient être une solution si la force portante du support composite était suffisante. Des recherches ont été faites sur ce nouveau support au Department of Mining and Metallurgical Engineering à la Technical University of Nova Scotia, à Halifax, en Nouvelle-Ecosse.

Un énoncé des critères de conception pour les poutrelles d'acier laminé dans les mines sert à comparer la force portante du support composite avec celle des supports d'acier classiques. Quatre techniques de conception relatives aux poutrelles d'acier laminé sont également traitées.

La technique des poteaux tubulaires remplis de béton et des éléments d'ossature du genre poteau-poutre est décrite. Même si une quantité limitée de données seulement se rapporte au sujet à l'étude, l'énoncé sert néanmoins d'introduction à la technique des structures tubulaires de béton.

Une série de poutres creuses en profils et remplies de béton ont subi des essais de flexion sur des appuis simples, soit des essais où la charge était concentrée en un point et, ensuite, en trois points. La cure du béton a été étudiée pendant des périodes de 1, 3, 7 et 28 jours. D'autres essais ont été réalisés sur des poutres à armature en acier et sur une poutre composite dont l'âme a été remplie de béton sous pression.

Des essais de contrainte latérale ont été entrepris sur la poutre à l'aide d'un cadre rigide conçu tout spécialement pour les essais. Il s'agissait de déterminer comment réagirait la poutre sur des appuis simples si la rotation à son extrémité était restreinte comme c'est le cas dans un ouvrage de soutènement à poutrelles d'acier laminé en raison d'un assemblage rigide.

Les résultats des essais sont expliqués, et il en ressort que , dans le cas de la poutre composite mise à l'essai, il est possible de mettre en place ce genre de supports et de diminuer leur poids de 37 % sans qu'il y ait perte de tension de rupture.

Des prévisions sur les frais en matériaux sont établies pour la poutre en profils creuse remplie de béton et pour la poutrelle d'acier laminé ayant la même tension de rupture. Aucune prévision n'a a été avancée sur la diminution des frais de main-d'oeuvre qui pourrait résulter de la mise en place de la section en profils creuse et légère.

D'autres avantages de la poutre composite en profils creuse sont traités, tels que la possibilité d'augmenter de façon considérable le moment de section et de donner plus de force latérale au support composite par rapport à une poutrelle d'acier laminé ayant la même force portante.

Les raccords et la méthode d'entretoisement pour les sections tubulaires sont également traités pour montrer qu'il existe des techniques de fabrication pour permettre à la fois l'assemblage des structures de soutènement composées de plusieurs pièces tubulaires, de même que leur étayage.

Il a été démontré que les techniques classiques, soit les principes de la transformation de matériaux, qui s'appliquent à la conception de la poutre composite, ne permettent pas de prédire avec exactitude la performance d'une poutre en profils creuse remplie de béton.

Selon les dernières recommandations, la poutre composite devrait subir des essais de charge de rupture dans un soutènement par cadre. Ces essais viseraient à démontrer que le coulis de béton présenterait beaucoup plus d'avantages pour ce mode de soutènement que pour les poutres sur des appuis simples sur lesquelles ont porté les recherches.

TABLE OF CONTENTS

	Page
EXECUTIVE SUMMARY	i
1.0 INTRODUCTION	1
1.1 Purpose of Study	1
1.2 Scope of Study	2
2.0 A REVIEW OF DESIGN CRITERIA FOR RSJ SUPPORTS	4
2.1 Engineering Mechanics of Beam Structures	6
2.1.1 Elastic Bending of a Straight Beam	8
2.1.2 Inelastic Bending of a Straight Beam	9
2.1.3 Curved Beams	13
2.1.4 Composite Beams	16
2.2 RSJ Design Criteria	20
2.2.1 NCB Design of RSJ Supports (Newson, 1985)	23
. 'Square work' Supports	23
. Cambered Supports	25
. Semi-circular Arch Supports	27
2.2.2 Biron and Arioglu Arch Design Technique	29
2.2.3 Proctor and White Arch Design Technique	33
2.2.4 Empirical arch design criteria-Choquet	45
3.0 GROUT FILLED TUBULAR STEEL	51
3.1 A Review of Current R & D work	51
3.2 A Discussion of the current contract-Steel Encased Concrete Beam	53
3.3 Concrete Encased Steel Beam Composite Member	59
4.0 LABORATORY INVESTIGATIONS	62
4.1 Selection of the HSS Section Size	63
4.1.1 Computation of Composite Beam Properties	65
4.1.2 Selection of Beam Length	69
4.2 Selection of Grout Material	69
4.3 Method of Preparation and Placement of Grout in HSS Sections	71

Page

4.4 Testing of Beam Sections 76
4.4.1 Simply supported beam tests 78
4.4.2 Laterally constrained beam tests 78

4.5 Results of Laboratory Testing 84
4.5.1 Selection of the grout material to be used in beam tests 85
4.5.2 Performance of grout filled (4.0 1 M-Bed) HSS sections 89
4.5.3 Performance of pressurized grout filled HSS section beam 91
4.5.4 Performance of reinforced grout beam members 93
4.5.5 Performance of laterally constrained beams 96

4.6 Theoretical Analysis of Laboratory Testing Through Engineering Mechanics of Beam Structures 99
4.6.1 One and three point bend tests 99
4.6.2 Laterally constrained beam tests 102
4.6.3 Theoretical prediction of beam performance 103

4.7 Comparison of the Composite Beam Theoretical Predictions versus Test Results of Composite HSS beams 107
4.7.1 Comparision of empty beam performance . 112
4.7.2 Comparison of grout filled HSS beam performance (theoretical predictions vs test results) 114
4.7.3 Comparision of theoretical predictions vs test results for reinforced, grout filled HSS beams 116
4.7.4 Conclusions on the proposed theoretical models for composite HSS beam performance 116

4.8 Comparison of the Collapse Loads for Simply Supported RSJ Beams and for Composite HSS Beams 119
5.0 EVALUATION OF THE COMPOSITE HSS BEAM MEMBER FOR MINE SUPPORT 122

5.1 Assembly of Tubular Supports 123

5.2 Strutting of Tubular Supports 127

Page

6.0 CONCLUSIONS 130

7.0 RECOMMENDATIONS 133

REFERENCES 136
APPENDIX I 140
APPENDIX II 144

LIST OF FIGURES

Figure 2.1	Simply Supported Beam in Bending ...	7
Figure 2.2	Elastic and Inelastic Deformation in Simply Supported Beams	10
Figure 2.3	Perfect Elastoplastic Behaviour	12
Figure 2.4	Transition from Elastic to Plastic Bending in a Simply Supported Rectangular Beam	12
Figure 2.5	Curved Beam	14
Figure 2.6	Transformed Area Technique for Stress Analysis in Beams	17
Figure 2.7	Beams of two materials	19
Figure 2.8	RSJ Support Profiles, Listed in Order of Increasing Support Strength	24
Figure 2.9	Effect of End Restraint on Bending Moments	26
Figure 2.10	Cambered RSJ Supports-Simply Supported Minimum Radius of Curvature (10x Depth) for Various RSJ Section Sizes	28
Figure 2.11	Static Model of an idealized Rigid Steel Arch	32
Figure 2.12	Moment and Normal Loads on a Rigid Steel Arch plotted in Polar Coordinates	32
Figure 2.13	Forces Acting at Overbreak Blocking Point	35
Figure 2.14	Limit of Rotation of the Passive Force in the Rock (F_p) to 25° ..	36
Figure 2.15	Resolution of Forces at Overbreak Blocking Points	38
Figure 2.16	Action of Forces at Blocking Point 3 in Figure 2.15	39
Figure 2.17	Example of the Determination of Stresses in an Arch by the Force Polygon Method	41

		Page
Figure 2.18	Representation of the STRESS/ DEFORMATION of an Underground Arch Support Member	48
Figure 2.19	Relation between Deflection and the Product of the Intrinsic Characteristic x The Global Stiffness of the Arch	50
Figure 3.1	Pure Bending Tests on Concrete Filled Pipe (Kato, 1981)	54
Figure 3.2	Two designs - Reinforced Concrete Encased RSJ Beams (MRDE, NCB, 1980)	60
Figure 4.1	Hollow Structural Steel (HSS) Section used in Laboratory Investigations	64
Figure 4.2	Transformed Area Calculations for 3 Cases of Grout Filled HSS Beams ..	68
Figure 4.3	M-Bed Standard	70
Figure 4.4	Talygrout 100	72
Figure 4.5	Laterally Confined Beam Test Frame .	83
Figure 4.6	Instrumentation Used in Beam Tests .	86
Figure 4.7	Effect of Grout Strength on Deflection of Composite Beam in 1-Point Bend Tests	88
Figure 4.8	1 & 3 Point Bend Tests on Simply Supported Composite Beam	90
Figure 4.9	1-Point Bend Test on Pressurized (200psi) Grout Core in HSS Section	92
Figure 4.10	1-Point Bend Tests on Grout Filled HSS with 1/2 inch diameter Rebar- normal and Pressurized (200psi) Grout Core	94
Figure 4.11	Lateral Deflection of Bottom Fibre of Composite Beams for Laterally Confined vs. Unconfined Beam Tests	97

Page

Figure 4.12 Beam Deflection for Laterally-Confined vs. Unconfined Composite Beams-Grout Filled HSS Section ... 98

Figure 4.13 Loading, Shear and Moment Diagrams . 101

Figure 4.14 Laterally Confined Beams and Similarities To Rigid-End Beams .. 104

Figure 4.15 Loading, Shear and Moment Diagrams For Rigid Beam 105

Figure 4.16 Theoretical Load vs. Deflection (Elastic) Curves For HSS Sections Under Study 111

Figure 4.17 Comparison of Theoretical Predictions and Actual Bend Test Results on Empty HSS Beams withinthe Elastic Range 113

Figure 4.18 Comparison of Theoretical Predictions and Actual Bend Test Results For Grout Filled HSS Sections within the Elastic Range 115

Figure 4.19 Comparison of Theoretical Predictions and Actual Bend Test Results on Grout Filled HSS Section with 1/2 inch Diameter Rebar (within the Elastic Range) 117

Figure 5.1 Welded End-Plate Connections for Tubular to Tubular Junctions 125

Figure 5.2 Standard Beam Connections To Concrete Filled HSS Columns 128

Page

LIST OF TABLES

Table 2.1	Specifications for Mining Steel as Designated By British Standards, BS4; 1980, Part 1	22
Table 2.2	NCB Allowable 'H' Section RSJ for Mine Support Arches	22
Table 2.3	Estimated Collapse Loads (kN) for Standard Arch and Simply Supported Beams With Single Point Loading Acting at the Centre	30
Table 2.4	Design Table for Semi-Circular Arch Continuous Ribs	46
Table 4.1a	Theoretical beam Performance For Beams in 1-Point Loading	108
Table 4.1b	Theoretical Beam Performance For Beams in 3-Point Loading	109
Table 4.1c	Theoretical Beam Performance For Beams in Laterally Confined Beam Test (Simulated by Rigid-Ended Beam; 3-Point Loading)	110

LIST OF PHOTOGRAPHS

Photo 1. Double turbine grout mixer mounted on a variable speed drill press for mixing grout 73

Photo 2. Moyno 2L4 Progressing Cavity Pump equipped with a 1 ft^3 grout hopper .. 74

Photo 3. HSS tube pumping setup 75

Photo 4. In-Line isolated pressure Sensor and Valve for the pressurized grout core filling procedures 77

Photo 5. One-Point Bend Test on a Simply Supported Composite Beam 79

Photo 6. Reinforcement Rod (1/2 inch diameter) installed in the bottom of the Beam with 1/2 inch cover on the sides and bottom 80

Photo 7. Laterally confined stiff test frame ... 81

Photo 8. Three-point Bend Test on a Laterally Constrained Beam 82

1.0 INTRODUCTION

Conventional support in coal mine access tunnels which are required to provide long service-life or at roadway junctions subjected to high ground stresses is provided by various profile RSJ section supports. When there is 'heavy' loading of these support structures it is necessary to use heavy duty supports or to fabricate a composite beam section by bolting or welding steel beam components together. The heavy-duty supports create a problem with handling and installation within the mine openings. The composite beam sections require significant fabrication within the mine environment which in the case of welding generates an open-flame that presents an environmental hazard requiring special operating procedures. Both of these support alternatives represent a significant delay in the support installation phase of the tunnel development cycle.

1.1 Purpose of Study

The purpose of this study is to investigate the potential to use a lightweight, hollow-structural steel (HSS) support member which can be installed in the mine opening without creating a delay in the tunnel development cycle. Subsequent to the installation, the

HSS support member would be filled with a pumpable grout material to provide the added support strength required to resist the 'heavy' loading to be accepted by the support member.

1.2 Scope of Study

The study was initiated by reviewing the design principles used in the specification of steel RSJ support members for mine openings. Four support design techniques are reviewed to establish the engineering criteria used in this design work and to guide the evaluation of the engineering properties of the grout filled HSS support members.

A review was also conducted on the existing work with grout (concrete) filled steel tubular structures used in the construction industry. This review indicated the extensive use of these structures as column members subjected to axial compressive loading. In general, the current design work on grout filled tubular structures permits very limited bending moments to be induced into the structure though an eccentrically applied axial load on the composite column. In recognition of the potential for large bending moments to be exerted on the mine support members being

evaluated, limited design principles could be extracted from the review which was conducted.

Laboratory testing of grout filled HSS straight beam sections was conducted to evaluate the engineering properties of the composite beam members in various states of bending. These investigations included testing of simply supported beams in one and three-point bending and also testing of laterally constrained beams in three-point bending. Pressurized grout core HSS members and steel reinforced core beams were also investigated.

Following this testing, an evaluation of the potential to use the composite structural member for an underground support member is presented. This evaluation also discusses connections, bracing and assembly of the support sections as required for use underground.

2.0 A REVIEW OF DESIGN CRITERIA FOR RSJ SUPPORTS

Fundamental to a discussion on the design of steel supports in high stress zones in coal mines is the basic concept of the support strength versus the applied loads on the various elements of the support member. The evaluation of the material strength used in steel supports is determined through standard testing procedures established by such agencies as the Canadian Standards Association (CSA), the American Society for the Testing of Materials (ASTM), the American Iron and Steel Institute (AISI), and the British Standards (BS). Conversely, an estimate of the applied loads on the support members is difficult to predict given the variability of the in situ stress field created by the inhomogeneous, anisotropic behavior of coal measure rocks and the post-mining redistribution of stresses around mine openings. When possible, empirical and theoretical information is combined with field load tests to determine the loading anticipated on the underground opening support structures.

Underground support design is conducted in two ways - empirical and rational. Civil Engineers have developed a rational analysis for the design of steel

supports for geotechnical structures in rock based on classic engineering mechanics theories. This technique is used to design critical structures where support deformation is intolerable and long term usage of the structure is planned. The theory is based on an early and complete blocking of the supports against the opening profile and the elimination of impact loading from falls of 'loose zone' material around the support. Mine supports are not held to such rigid restrictions and often minor damage and limited permanent deformation of mine supports are tolerated, provided the support member maintains the general integrity of the opening. As a result, a largely empirical approach to support design in mines has evolved as opposed to the more theoretical, rational approach in Civil Engineering. Despite the more empirical approach of mine support current literature discusses the application of rational planning for RSJ supports in mines.

One further issue with RSJ support structures in rock openings, which complicates the design of optimally sized support members, is the rock support-interaction phenomenon with arch shaped members. Based on theories to be discussed later in this report, the arch support member is able to shed some of the load exerted on the member back into the rock mass and

thereby enhance its support capacity beyond that which would be predicted for a free-standing arch structure.

2.1 Engineering Mechanics of Beam Structures

A beam is defined as a structural member that supports transverse loads. Beams resist external shearing forces which are held in equilibrium by resisting shear stresses exerted by the fibres of the beam. The analysis of beams is conducted by a determination of the bending stresses set up in the beam fibres that resist the applied bending moments caused by the transverse loads. This principle is best demonstrated with a simple beam acted on by a central concentrated load P as shown in Figure 2.1, where for equilibrium to exist:

Bending Moments = Resisting Moments

For the discussion of steel structures in underground support members, it is necessary to consider several issues which related to beam theory. The theories summarized in the following text include:

- elastic bending of a straight beam
- inelastic bending of a straight beam
- curved beam structures

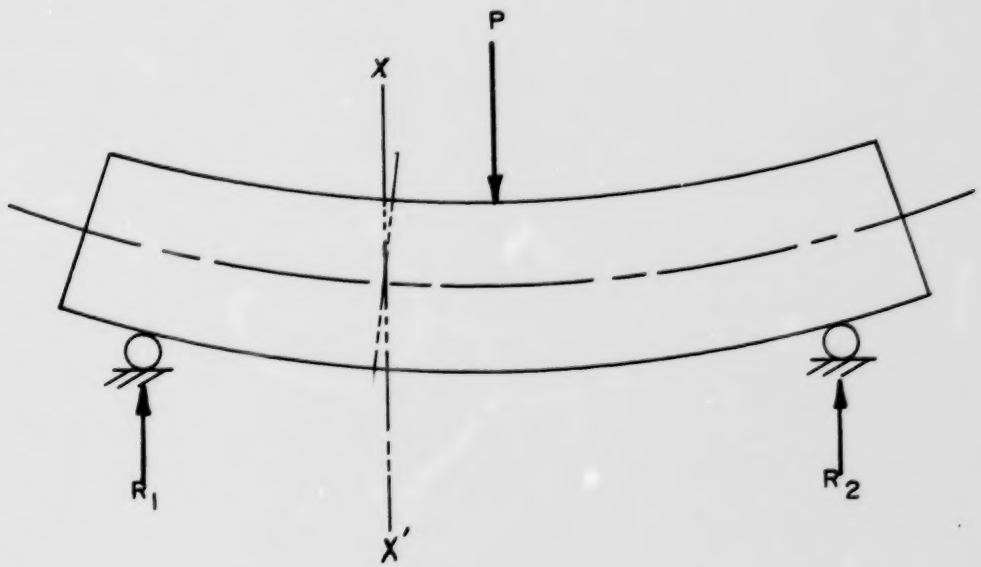

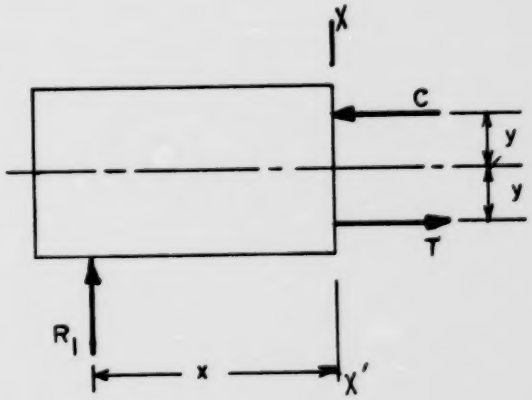

$$R_1 \cdot x = T \cdot y + C \cdot y$$

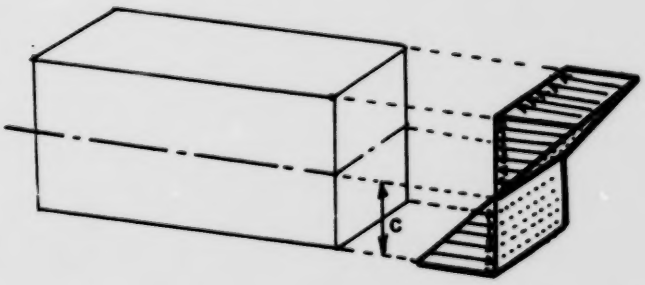

Stress distribution across beam section

Extreme Fibre Stress

FIGURE 2·1 Simply Supported Beam in Bending

Of special consideration for the subject study is the theory of composite beam (steel encased concrete) structures which is also introduced for future reference in this report.

2.1.1 Elastic Bending of a Straight Beam

The investigation of beam structures is based on the **flexure formula** which states that for beams which are deformed elastically the maximum bending moment is defined by the formula:

$$M = \frac{fI}{C}$$

where M = maximum bending moment,
f = maximum allowable fibre stress,
I = moment of inertia,
C = distance from neutral axis to extreme fibre of the beam.

Utilizing the relationship between the moment of inertia and the section modulus of a beam member:

$$S = \frac{I}{C}$$

where S = section modulus (elastic),

the more common form of the flexure formula becomes:

$$S = \frac{M}{f}$$

This formula is used to determine the desired section modulus of a beam member based on a calculated bending moment (M) created by the external load and the known maximum fibre stress (f) for the beam material.

The preceding analysis is based on the fact that the beam is deformed elastically; that is, if the external load is removed from the beam, the beam will return to its original shape (straight). Analysis of beam structures for mining applications should also consider the case where the beam is stressed beyond its elastic limit and is in fact plastically deformed as is shown in Figure 2.2.

2.1.2 Inelastic Bending of a Straight Beam

The analysis of the inelastic bending of a simple beam is referred to as **plastic analysis.**

The point at which plastic analysis is used in beam design instead of elastic analysis is when the

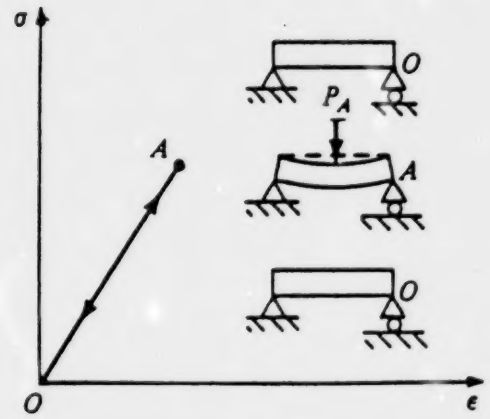

ELASTIC DEFORMATION

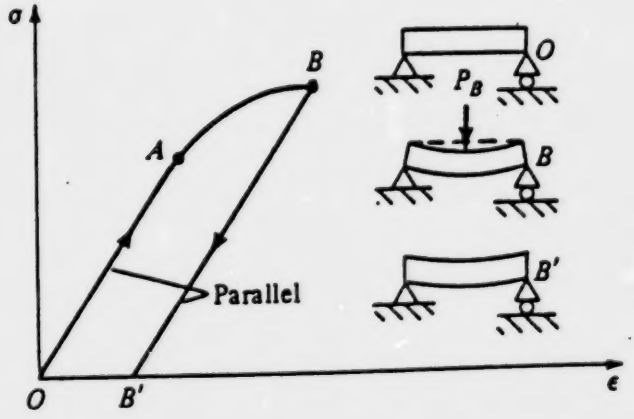

INELASTIC DEFORMATION

FIGURE 2.2 ELASTIC AND INELASTIC DEFORMATION IN SIMPLY SUPPORTED BEAM (WILLIAM, EASLEY, ROLFE, 1984)

external fibres of the beam are stressed to the yield strength, σ_{ys}, of the beam material, Figure 2.3. At this point, the bending moment in the beam is referred to as the **yield moment,** M_{ys}, and:

$$M_{ys} = S \times \sigma_{ys}$$

where M_{ys} - yield moment,

σ_{ys} - yield strength,

S - elastic section modulus.

As the bending moment is increased the yielding will migrate toward the interior of the beam until the complete depth of the beam is fully yielded. When the entire depth of the beam is at the yield strength the bending moment in the beam is called the plastic moment, Mpl. A diagram showing this migration of the yield stress, σ_{ys}, through the beam as a result of an increased bending moment from M_{ys} to Mpl is shown in Figure 2.4. for a rectangular beam section.

The plastic analysis of beams establishes a relationship between the plastic moment, Mpl and the yield moment, M_{ys}, called the **shape factor** , f, where:

$$f = \frac{M_{pl}}{Mys}$$

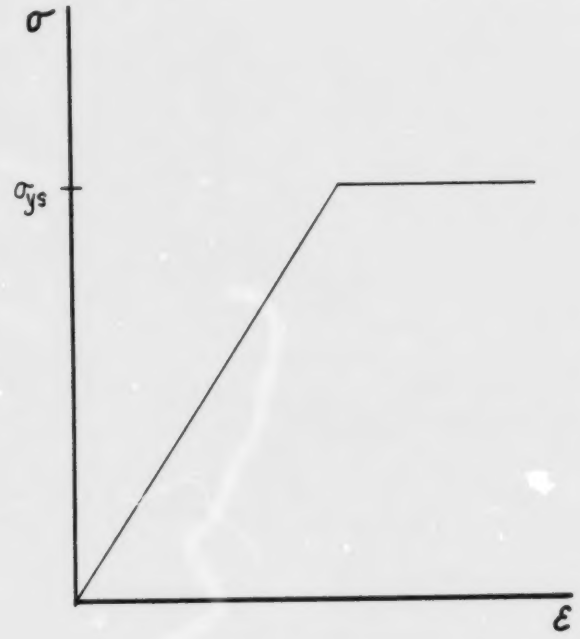

FIGURE 2·3 Perfect Elastoplastic Behaviour

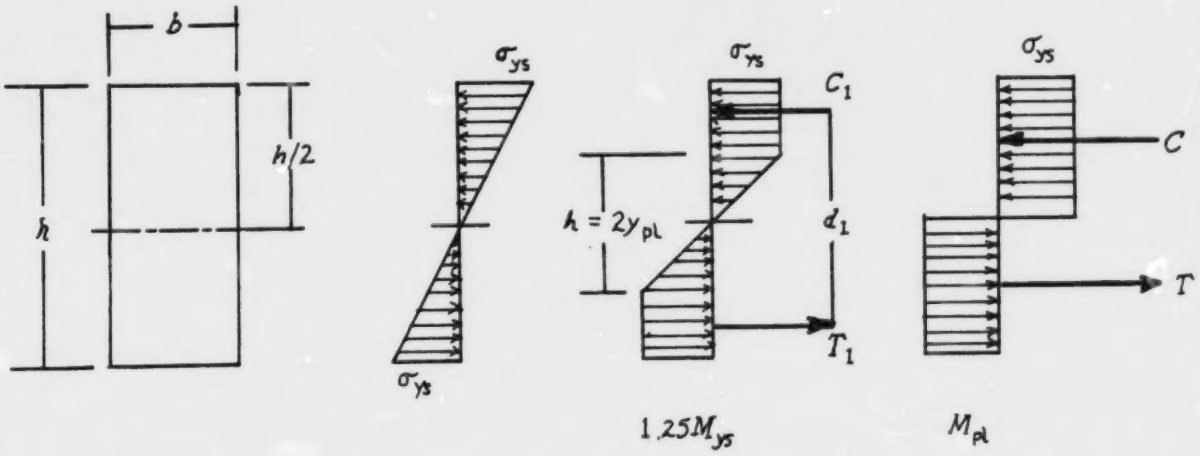

FIGURE 2·4 Transition From Elastic To Plastic Bending in A Simply Supported Rectangular Beam

The plastic moment in a beam can be determined by

$$M_{pl} = Z \times \sigma_{ys}$$

where Z = plastic modulus

Consequently, the shape factor, f, for a beam can be determined by

$$f = \frac{Z.\sigma_{ys}}{S.\sigma_{ys}} = \frac{Z}{S} = \frac{\text{plastic modulus}}{\text{elastic section modulus}}$$

2.1.3 Curved Beams

The previous discussion of beams makes the assumption that the neutral axis of the beam and the centroidal axis coincide. A curved beam will not exhibit this property due to the curvature in the beam. The general relationship between the centroidal and neutral axes of a curved beam are shown in Figure 2.5.

Based on the curved beam theory, the neutral axis in the beam can be determined by

$$r_n = \frac{A}{\int_A (dA/r)}$$

where A - area of beam

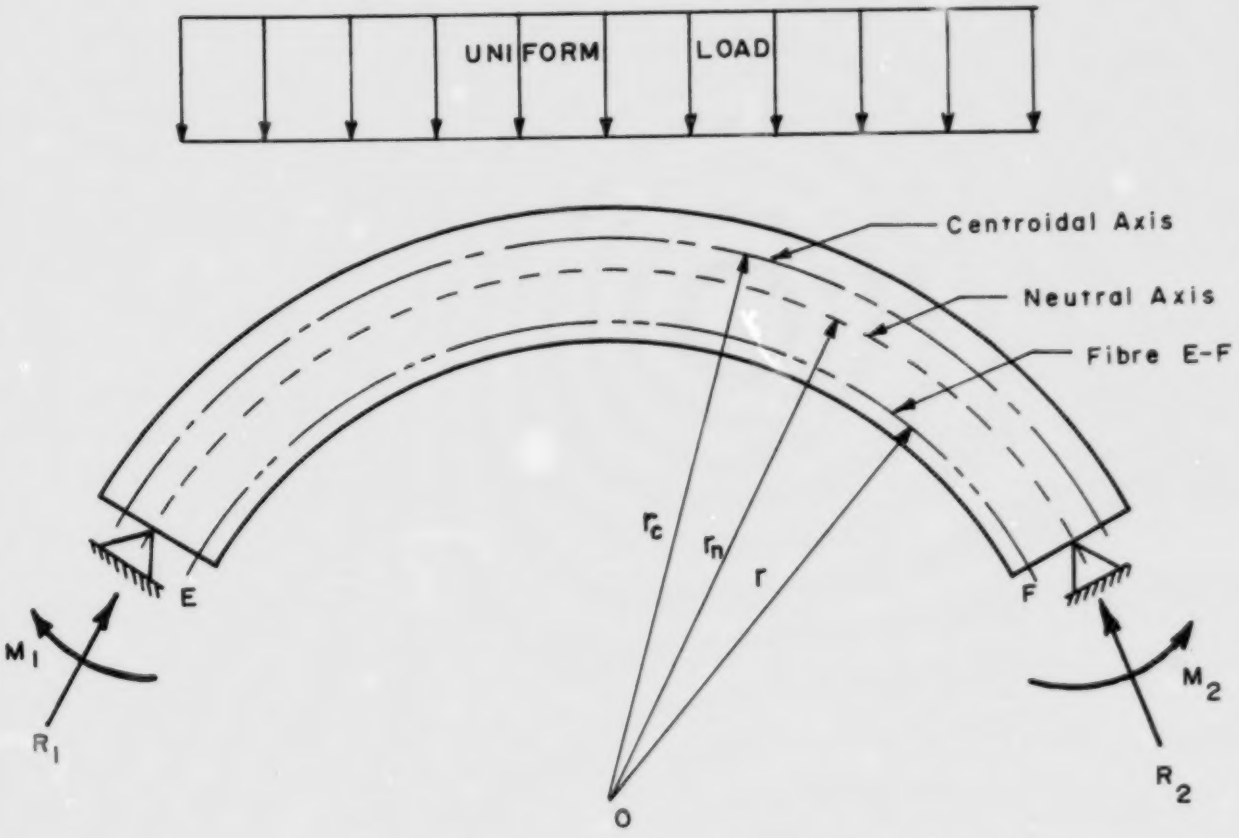

where r_n – neutral axis radius

r_c – centroidal axis radius

r – radius to a particular fibre E-F

O – denotes centre of curvature

FIGURE 2·5 CURVED BEAM

Once the neutral axis radius is calculated, the fibre stresses through the depth of the beam can be determined by

$$\sigma = \frac{M_z (r_n - r)}{r A (r_c - r_n)}$$

where: σ = fibre stress at radius r from the centre of curvature,

M_z = bending moment in the beam about the z-axis.

A = area of the beam

r_n, r_c, r (Figure 2.5)

As would be anticipated, the outside fibres of the beam are in compression while the inside fibres are in tension. Based on the above relationship, the inside fibres of the beam will be under a numerically larger load (tension) than the outside fibres (compression). The difference in these fibres stresses will be greater as the radius of curvature of the beam is decreased. With large radius of curvature beams limited error is introduced if a straight beam analysis is employed to determine fibre stresses. This fact explains the minimum radius of curvature for a cambered RSJ as discussed in section 2.2.1.

More detailed analysis of curved beam structures are available using statically indeterminant structural

analysis techniques. One such technique employs the theorem of Castigliano, and is detailed by Timoshenko, 1968 for semi-circular arch structures based on a single point load at the crown of the arch. Work has been done by the N.C.B. (Sadler and Campbell, 1965) to utilized this technique to investigate the collapse loads for other arch shaped profiles.

2.1.4 Composite Beams

Composite beams are those which are composed of more than one material with different moduli of elasticity. The technique of analysing the stress distribution (elastic) within a composite beam member is known as the **transformed-area** method.

The transformed area method works on the principle that the beam must first be transformed into an equivalent beam of one material based on a ratio of the moduli of elasticity of the two materials

$$n = \frac{E_1}{E_2}$$

Figure 2.6 illustrates this principal. Note the area changes must be made in a direction perpendicular to the bending plane of the beam.

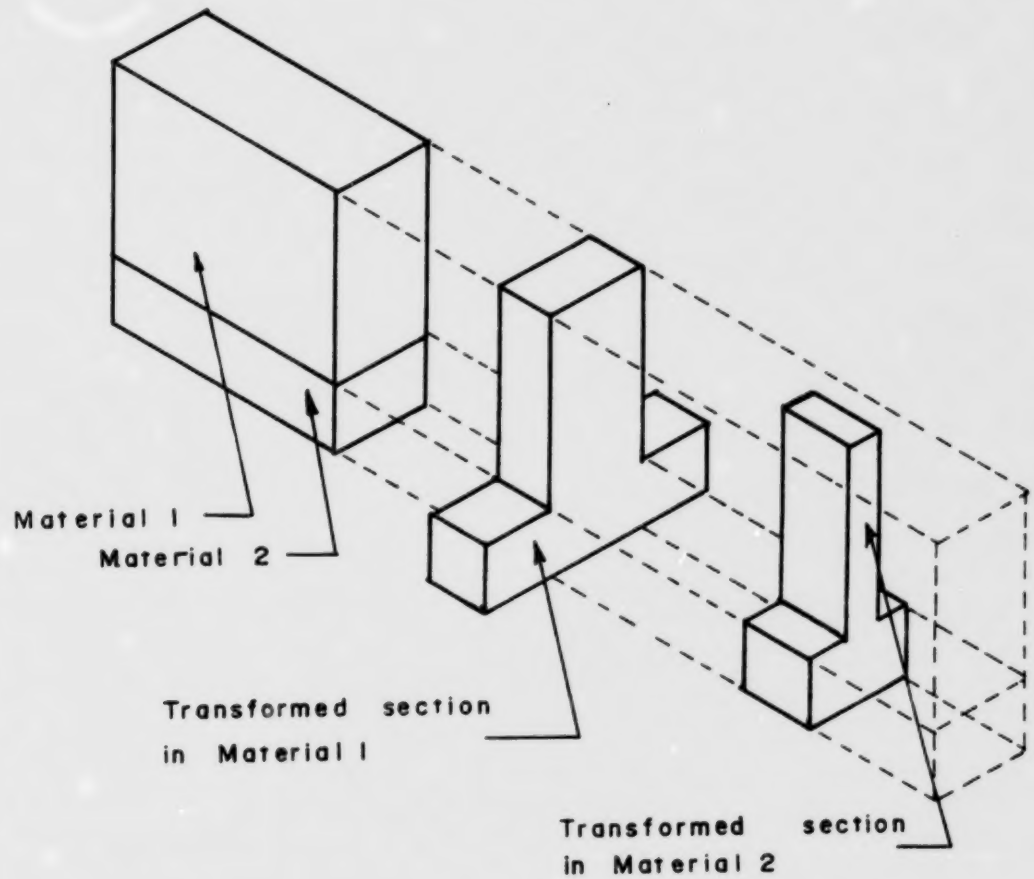

where: $n = E2 / E1 = 2$

FIGURE 2·6 TRANSFORMED AREA TECHNIQUE FOR STRESS ANALYSIS IN BEAMS

Following the transformation of the areas, it is necessary to determine the neutral axis of the transformed area and the moment of inertia of the transformed section. Utilizing the illustration given in Figure 2.7, the location of the neutral axis is given by $\bar{y}$ and is determined by

$$\bar{y} = \frac{A_{tr_1}(1)\, y_1 + A_{tr_1}(2)\, y_2}{A_{tr_1}(1) + A_{tr_2}(2)}$$

where $A_{tr_1}(1)$ - transposed Area for material 1 into material 1 (i.e unchanged Area 1)

$A_{tr_1}(2)$ - transposed Area for material 2 into material 1 (i.e. $A_{tr_1}(2)=nA_2$)

y_1 - distance from bottom of beam to centroid of Area 1

y_2 - distance from bottom of beam to centroid of Area 2.

The moments of inertia of the transformed sections are denoted

I_{tr_1} - moment of inertia for material 2 transformed into material 1.

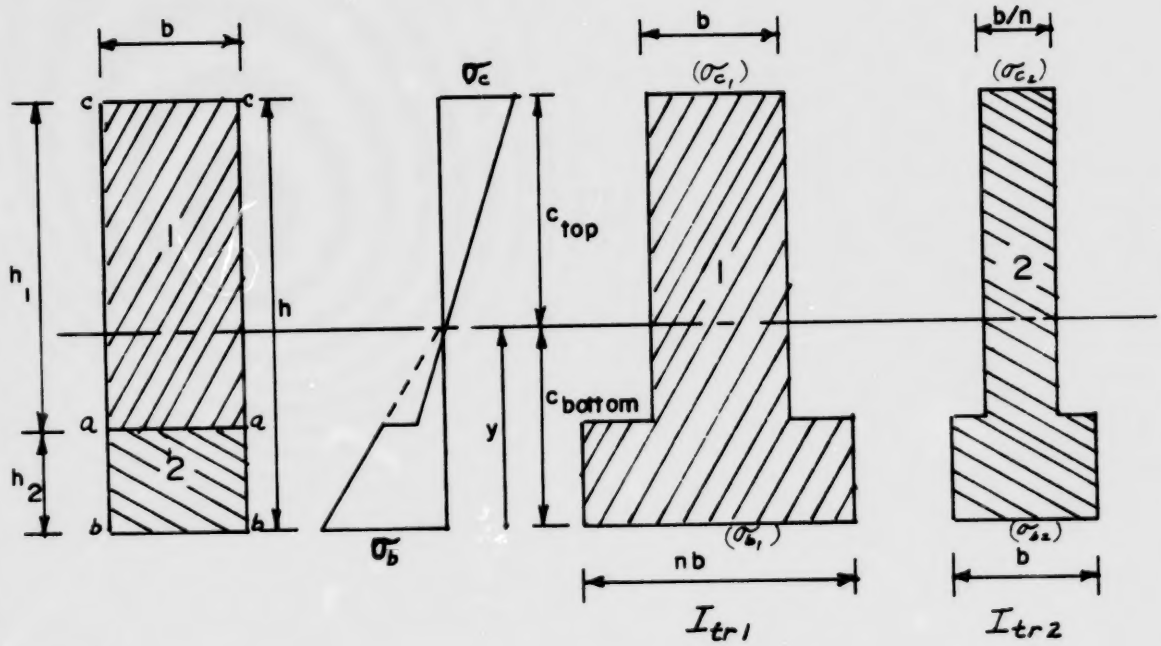

where : $n = E_2 / E_1 = 2$

FIGURE 2·7 BEAMS OF TWO MATERIALS

I_{tr_2} - moment of inertia for material 1 transformed into material 2.

Using previously defined stress equations

$$\sigma_{c1} = \frac{MC(top)}{Itr_1} \quad \text{and} \quad \sigma_{b1} = \frac{MC(bottom)}{Itr_1}$$

it is possible to determine the stress level at the extreme fibres of the beam subjected to moment (M) in the equivalent material. To determine the stress level in original beam materials

$$\sigma_c = \frac{MC(top)}{I_{tr1}} \quad \text{and} \quad \sigma_b = \frac{nMC(bottom)}{I_{tr1}}$$

Similar determinations can be made for the reverse material transformation (i.e. Material 1 transformed to Material 2).

2.2 RSJ Design Criteria

The application of Rolled Steel Joist (RSJ) steel sections for mine supports is practiced extensively in the United Kingdom. In particular the "H" section support members dominate the roadway support applications of the NCB. Based on this extensive use

of steel supports by the NCB, standards have been established with respect to material specification and support design criteria which will be summarized in this section of the report.

The British Standards, BS4;1980: Part 1 designates 3 steel products as suitable for mine support members. These specifications are shown in Table 2.1; however, the 'standard' RSJ material is the 'Grade 250' having a minimum yield strength of 250 N/mm^2 (16 $tons/in^2$) and minimum collapse strength of 430 N/mm^2 (28 $tons/in^2$).

The National Coal Board Specification 114 designates a group of 'H shaped' RSJ sections which are outlined in Table 2.2, for use in RSJ support fabrication.

Steel support design criteria of the NCB uses several basic guidelines:

- design is based on plastic beam failure not the elastic theory as employed by Civil Engineers,

- loading is considered to be the 'worst case scenario' where the load is a single point load acting at the center of a flat

TABLE 2.1 SPECIFICATIONS FOR MINING STEEL AS DESIGNATED BY BRITISH STANDARDS, BS4; 1980; PART 1 (NEWSON, 1985)

GRADE	TYPICAL COMPOSITION						MINIMUM TENSILE PROPERTIES	
	% C	% Si	% Mn	% Nb	% V	% N^2	YIELD STRESS N/mm^2 ($Tons/in^2$)	TENSILE STRENGTH N/mm^2 ($Tons/in^2$)
250	.18	.25	.65	-	-	.008	250 (16)	430 (28)
350	.16	.25	1.30	.02	-	.008	350 (22)	490 (32)
450	.14	.25	1.30	-	.13	.020	450 (29)	550 (36)

TABLE 2.2 NCB ALLOWABLE 'H' SECTION RSJ FOR MINE SUPPORT ARCHES

Section (mm)	Weight per metre run (kg)	Web Thickness (mm)	Section Modulus (mm^3 x 10-3)	
			XX	YY
89 x 89	19.35	9.5	67.4	22.4
102 x 102	23.06	9.5	97.0	37.4
114 x 114	26.78	9.5	132.0	47.2
127 x 114	29.76	10.2	158.0	52.4
152 x 127	37.20	10.4	248.0	59.6
127 x 114	26.78	7.6	152.4	50.8
204 x 152	52.08	8.9	457.8	106.4

beam or at the crown of a curved beam depending on the support being evaluated,

- the section modulus of the beam section is taken as a direct indication of the strength of the beam member,

- the support profiles utilized in the NCB coal mines, and shown in Figure 2.8, have support strength of increasing value in the order shown (i.e. the square work is the lowest strength profile while the circular profile is the strongest).

2.2.1 NCB Design of RSJ Supports (Newson, 1985)

Based on work conducted by the NCB and presented by Newson, 1985 the following guidelines have been established for design of various profile RSJ support members for coal mines:

(1) 'Square Work' supports:

A simply supported straight beam with center point loading exhibits the following yield and collapse load

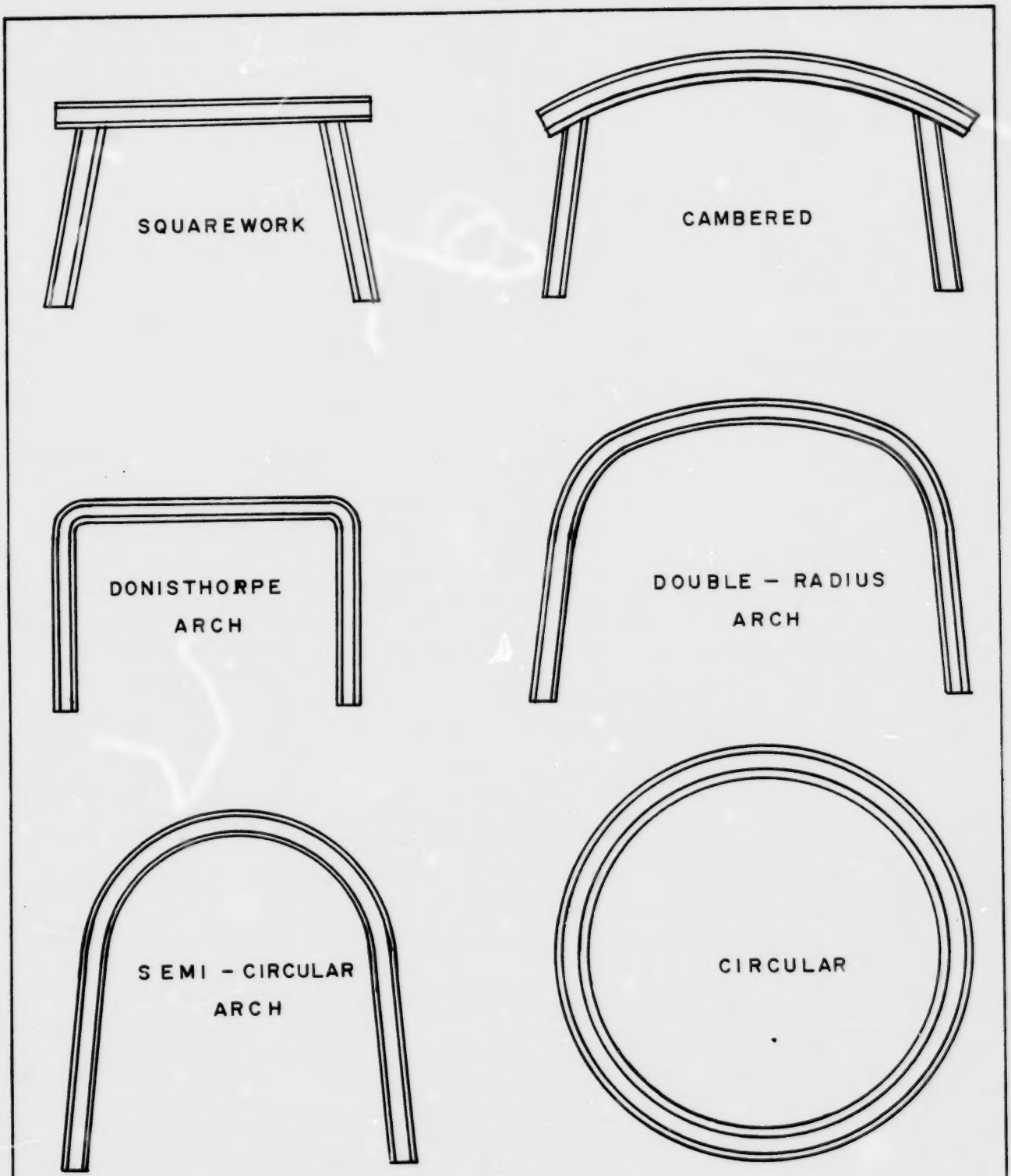

FIGURE 2·8 RSJ SUPPORT PROFILES – LISTED IN INCREASING ORDER OF SUPPORT STRENGTH (Newson, 1985)

relationships using plastic beam theory or limit design principles:

$$\text{Yield Load (kN)} = \frac{\text{Section Modulus (cm}^3\text{)} \times 1020}{\text{Span (mm)}}$$

$$\text{Collapse Load (kN)} = \frac{\text{Section Modulus (cm}^3\text{)} \times 1980}{\text{Span (mm)}}$$

The NCB 'square work' supports are usually end restrained using one of a variety of rigid joints (such as the Hollybank rigid joint). This end confinement renders the beam a rigid ended beam which significantly improves the yield and collapse loads of the beam by reducing the bending moment in the beam by an amount equal to the bending moment applied through the joint. Consequently higher loads can be sustained by a rigid ended beam. This principle is outlined in Figure 2.9. Work conducted by the NCB has shown that rigid end joints on 'squarework' beams increases the ultimate loads (yield and collapse) by approximately 37% (Newson, 1985).

(2) Cambered Supports:

It has been proven that if a simply supported cambered beam has a radius of curvature larger than 10X the depth of the beam (i.e. for a 114 x 114 mm RSJ,

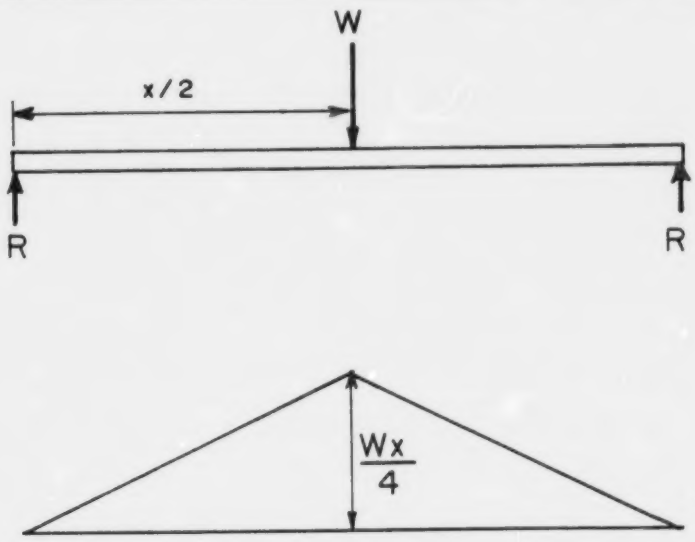

Simply supported beam

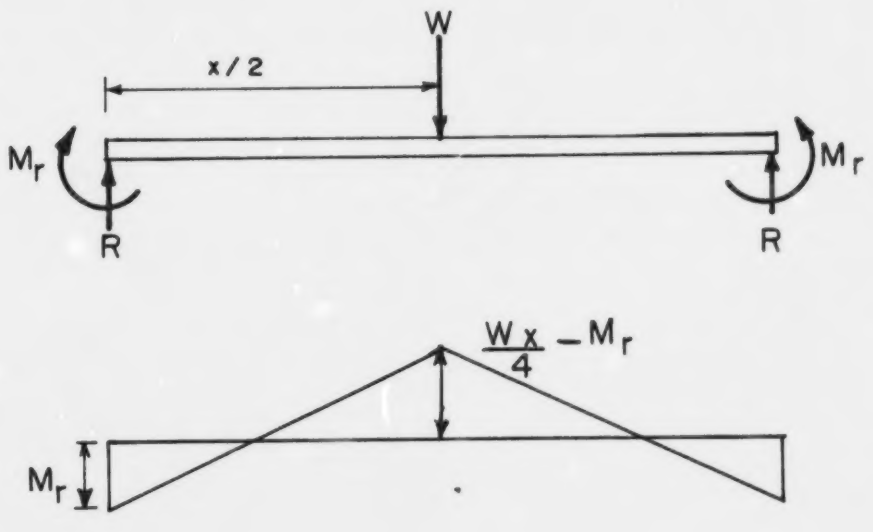

Rigid ended beam

FIGURE 2·9 EFFECT OF END RESTRAINT ON BENDING MOMENTS (Newson, 1985)

if the radius of curvature of the cambered beam is >1.14 m) then the cambered beam has the same load bearing capacity to a central point load as a 'square work' beam (Newson, 1985), Figure 2.10.

It is commented that corner bracing on a cambered beam presents significant strength advantages although no documented literature can be cited for this work.

(3) Semi-circular Arch Supports

Semi-circular RSJ section arches with splayed legs (2,3 piece and even 4 piece) with wrap around fishplate joints are the standard roadway arch for the NCB. Newson, 1985 documents a single formula developed by the NCB to calculate the collapse load for a point load at the crown of the arch:

$$P = 5.1 \frac{S}{D}$$

Where: P = load in (kN)

S = section modulus (mm^3)

D = roadway width (mm)

A summary of the calculated collapse loads for RSJ supports (2 piece arches, 3 piece arches and simply supported beams) have been published by Newson, 1985 and are included in Table 2.3.

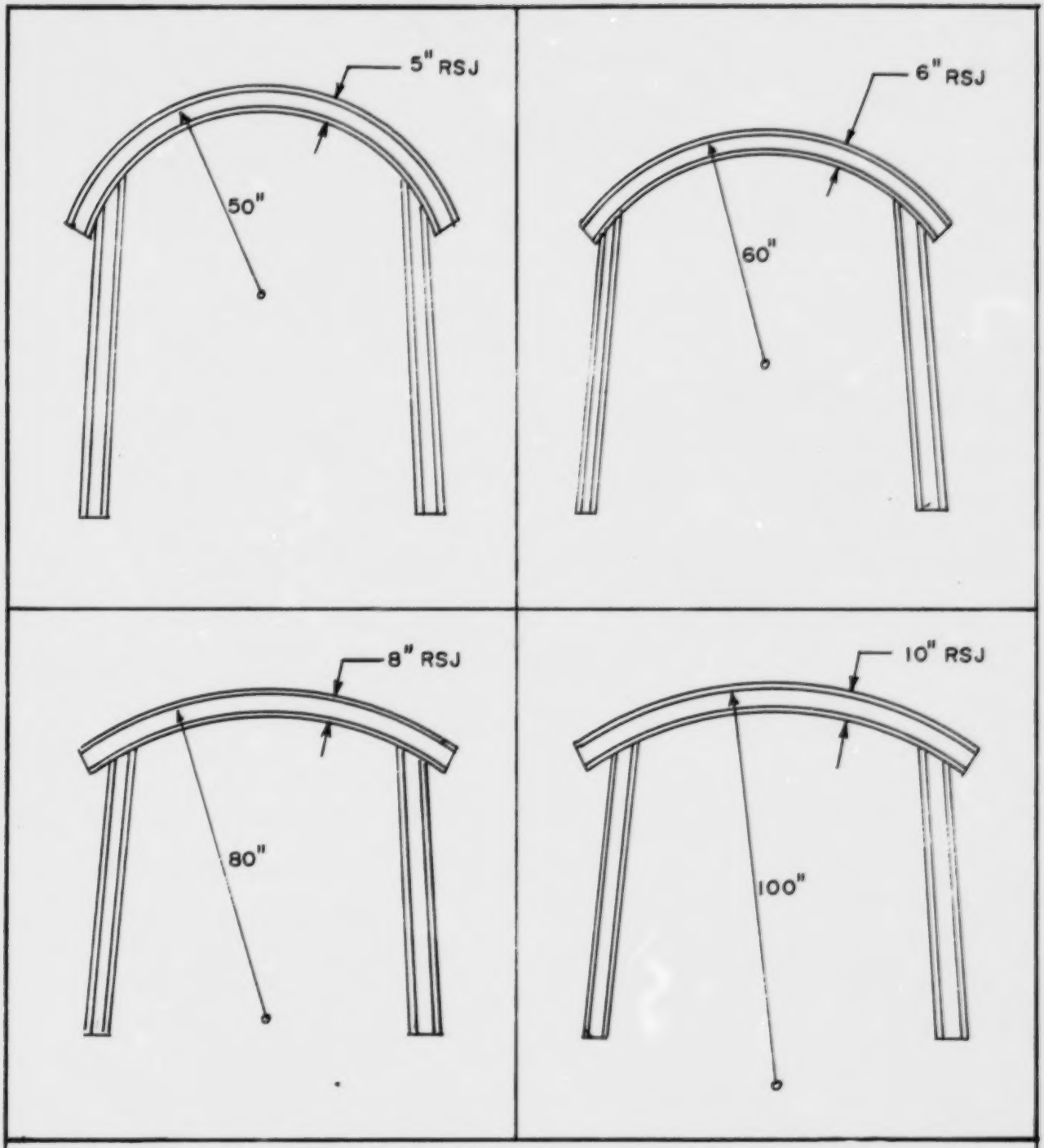

FIGURE 2.10 CAMBERED RSJ SUPPORT - SIMPLY SUPPORTED MINIMUM RADIUS OF CURVATURE (10x DEPTH) FOR VARIOUS RSJ SECTION SIZES

Two non-standardized arch profiles are discussed by Newson, 1985 which are the Donisthorpe and the Double Radius Arch. Usually of special design, these arches are quite costly and provide limited support advantage to the 'square work' arch (unless the camber in the Double Radius is large; i.e. less than 10 times the RSJ depth). Greater collapse loads are achieved by semi-circular arch profiles with splayed legs than by either of these non-standardized arch profiles.

2.2.2 Biron and Arioglu Arch Design Technique

Biron and Arioglu, 1982 propose a more detailed evaluation of stresses in a semi-circular rigid arch based on a uniformly distributed load acting over the arch. This situation is shown in Figure 2.11 and arch section design is based on determination of maximum moment and normal force in the arch structure. These values are determined as:

Side reactions (A_y, B_y):

$$A_y = B_y = \frac{(0.785h' + 0.666r)\, q_t r^3}{(0.666\, h'^3 + \pi r h'^2 + 4h'r^2 + 1.57r^3)}$$

TABLE 2.3 ESTIMATED COLLAPSE LOADS (kN) FOR STANDARD ARCHES AND SIMPLY SUPPORTED BEAMS WITH SINGLE POINT LOADING ACTING AT THE CENTRE

(1) Two Piece Arches
(2) Three Piece Arches
(3) Simply Supported Beam

Beam or Arch Span (mm)		Section Size (mm)									
		89 x 89 (3.1/2x3.1/2in)		102 x 102 (4 x 4in)		114 x 114 (4.1/2x4.1/2in)		127 x 114 (5 x 4.1/2in)		152 x 127 (6 x 5 in)	
		Yield	Ult	Yield	Ult	Yield	Ult	Yield	Ult	Yield	Ult
2440 (8ft)	1	100	145	140	200						
	2	-	-	-	-						
	3	30	55	40	80						
2745 (9ft)	1	90	125	125	175						
	2	-	-	-	-						
	3	25	50	35	70						
3050 (10ft)	1	80	115	110	160	150	215				
	2	-	-	70	160	-	-				
	3	25	45	30	65	45	85				
3355 (11ft)	1	75	105	100	145	-	-				
	2	-	-	65	145	85	195				
	3	20	40	30	55	40	80				
3660 (12ft)	1	65	95	95	130	-	-	150	215		
	2	-	-	60	130	75	180	95	215		
	3	20	35	30	50	35	70	45	85		
3960 (13ft)	1					-	-	-	-		
	2					70	165	85	195		
	3					35	65	40	80		
4265	1			80	115	105	150	130	185	-	-
	2			50	115	65	150	80	185	125	285
	3			25	45	30	60	40	75	60	115
4570 (15ft)	1					-	-	-	-	-	-
	2					60	140	75	170	115	265
	3					30	55	35	70	55	105
4875 (16ft)	1							-	-	-	-
	2							70	160	110	245
	3							35	65	50	100
5180 (17ft)	1									-	-
	2									100	235
	3									50	95
5485 (18ft)	1							-	-	-	-
	2							60	140	95	220
	3							30	60	45	90
6096 (20ft)	1							-	-	-	-
	2							55	125	85	200
	3							25	50	40	80

Bending Moment around arch (M):

$$M = 0.5\, q_t\, r^2 \sin^2\alpha - A_y\,(h' + r \sin\alpha)$$

Normal Force on Arch (N):

$$N = -q_t\, r \cos^2\alpha - A_y \sin\alpha$$

and are plotted on the polar coordinates of the arch. A typical diagram of such a plot is given in Figure 2.12. The maximum values of bending moment and normal force can be determined by

Maximum bending Moment (Mmax):

$$Mmax = -A_y\left[h' + \frac{0.5\, Ay)}{q_t}\right]$$

Maximum normal force (N_1) to arch profile:

$$N_1 = -q_t r$$

The stress in the semi-circular arch support is calculated by

$$\sigma = \frac{q_t r}{0.149\, S + 9.780\, S} + \frac{A_y\,(h' + 0.5\, A_y/qt}{S}$$

Note: the symbols for the Biron formulae are shown in Figure 2.12.

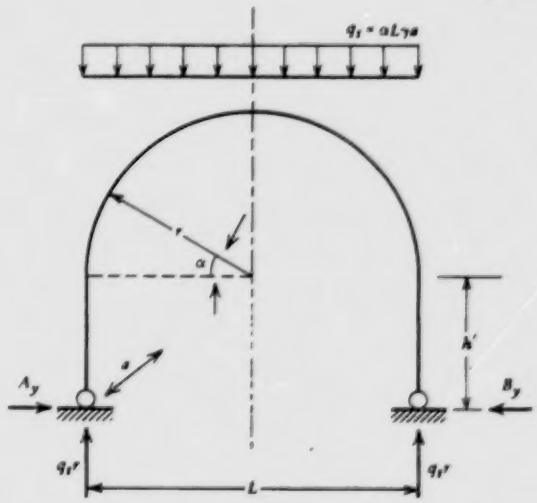

where $A_y = B_y$ side reactions, in tonnes
h' = vertical distance of the arch, in meters
r = radius of the arch, in meters
α = angle from horizontal, in degrees
q_t = uniform roof load, in tonnes per meter
M = moment, in tonnes · meter
N = normal force to the profile, in tonnes

FIGURE 2.11 STATIC MODEL OF AN IDEALIZED RIGID STEEL ARCH (BIRON, ARIOGLU: 1983)

where $|\sigma|$ = absolute stress value, in tonnes per square meter
F = section area of the profile, in square meters
S = section modulus of the profile, in cubic meters
σ_{zf} = allowable stress in steel for mine supports, 1400 kg/cm² or 14000 t/m²

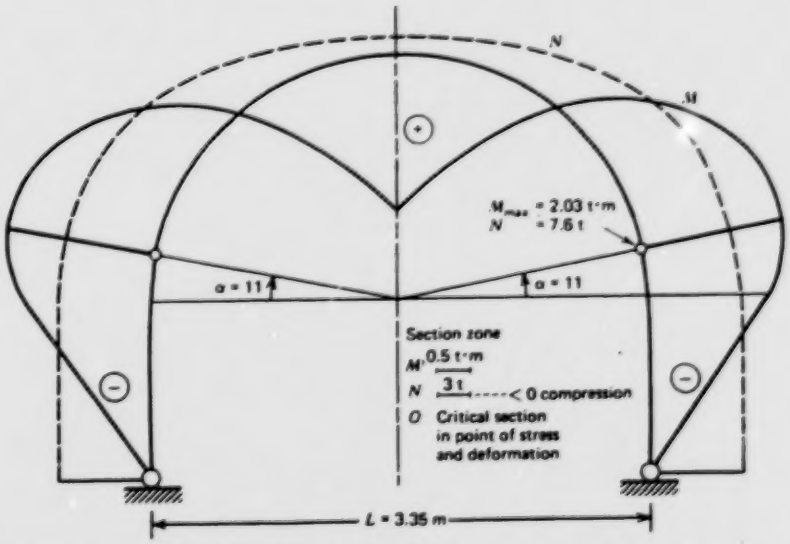

FIGURE 2.12 MOMENTS AND NORMAL LOADS ON A RIGID STEEL ARCH PLOTTED IN POLAR COORDINATES (BIRON, ARIOGLU; 1983)

This solution process is used to calculate the appropriate section modulus(S) for the support requirements imposed.

2.2.3 Proctor and White Arch Design Technique

Proctor and White, 1977 presented a technique for the design of steel arches in rock tunnels using a graphical solution process. This technique has been adopted by the U.S. Army Corp of Engineers (EM 1110-2-2901, 1978) and is also summarized briefly by Peng, 1978. The technique is based on elastic theory NOT plastic theory as is most commonly practiced in mine support design work. It is, however, a very useful technique and provides a method to determine the stresses within an underground steel support structure.

The technique presented by Proctor and White emphasizes some very important principles related to steel arches for underground rock support:

- wedging a block between the steel set and the tunnel profile is critical to the strength of the arch through the creation of an ACTIVE FORCE exerted on the rock mass by a slight elastic deformation (spring action) in the arch,

- blocking point spacing is critical to the minimization of bending moments being exerted in the arch by the rock load. The wider the blocking spacing the higher the bending moments and the lower the load carrying capacity of the rib. The relationship cited is that the bending moment increases as the square of the distance between the blocking points,

- if proper blocking practices are used, the rock load can be transmitted in the arch as compression thrust forces, NOT bending moments.

The theory recognizes the importance of the rock-support interaction and identifies both ACTIVE and PASSIVE forces acting at each blocking point to establish equilibrium. A history of the development of the forces at a blocking point are illustrated by a sequence of diagrams extracted from Proctor and White, 1977 and shown in Figure 2.13. One qualification to the concept that the passive force in the rock (F_p) rotates with an increased active rock load (W) is that F_p can only rotate to 25° from the horizontal due to frictional forces within the rock mass that would restrain rock moment beyond this angle as shown in Figure 2.14. A resolution of the forces acting at four

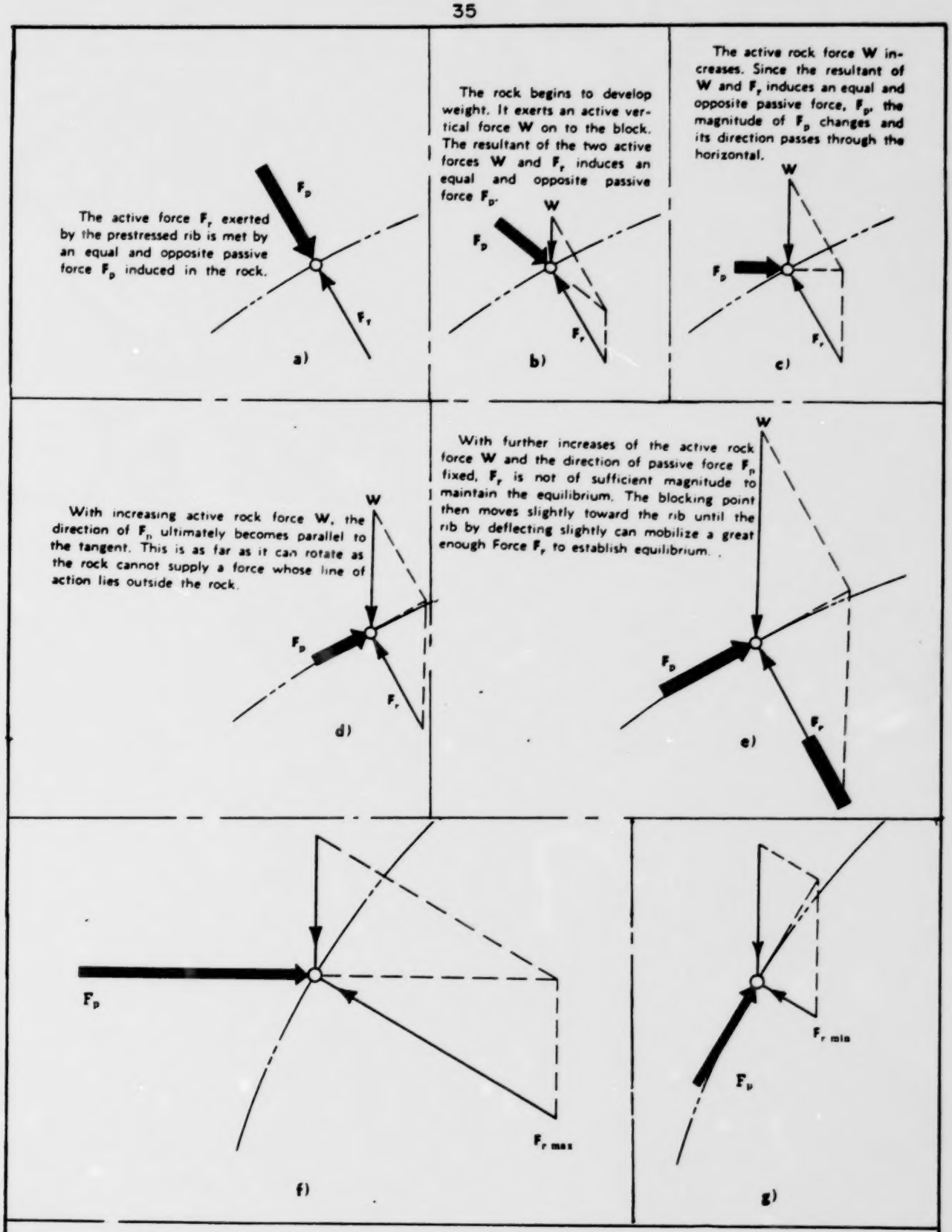
The active force F_r exerted by the prestressed rib is met by an equal and opposite passive force F_p induced in the rock.
F_p
F_r
a)
The rock begins to develop weight. It exerts an active vertical force W on to the block. The resultant of the two active forces W and F_r induces an equal and opposite passive force F_p.
W
F_p
F_r
b)
The active rock force W increases. Since the resultant of W and F_r induces an equal and opposite passive force, F_p, the magnitude of F_p changes and its direction passes through the horizontal.
W
F_p
F_r
c)
With increasing active rock force W, the direction of F_p ultimately becomes parallel to the tangent. This is as far as it can rotate as the rock cannot supply a force whose line of action lies outside the rock.
W
F_p
F_r
d)
With further increases of the active rock force W and the direction of passive force F_p fixed, F_r is not of sufficient magnitude to maintain the equilibrium. The blocking point then moves slightly toward the rib until the rib by deflecting slightly can mobilize a great enough Force F_r to establish equilibrium.
W
F_p
F_r
e)
F_p
$F_{r\,max}$
f)
$F_{r\,min}$
F_p
g)

FIGURE 2.13 FORCES ACTING AT OVERBREAK BLOCKING POINT (PROCTOR AND WHITE, 1977)

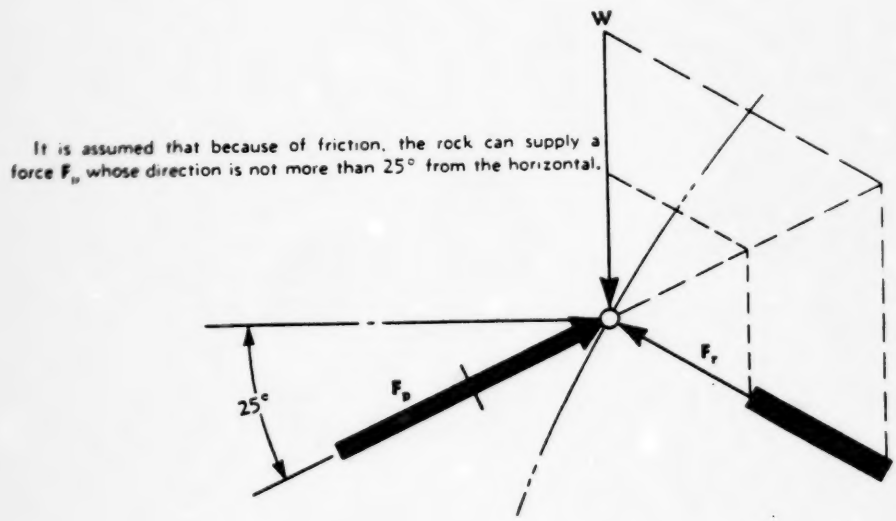
It is assumed that because of friction, the rock can supply a force F_p whose direction is not more than 25° from the horizontal.
W
25°
F_p
F_r

FIGURE 2.14 LIMIT OF ROTATION OF THE PASSIVE FORCE IN THE ROCK (F_p) TO 25° (PROCTOR AND WHITE, 1977)

(4) blocking points in one quadrant of a semi-circular arch is shown in Figure 2.15. The radial component of the active weight (load force) must be resisted by the arch, while the tangential component is offset by the mobilized passive rock force (F_p). The steel arch resists the load force by exerting two thrust forces (T_{2-3}, T_{3-4}) as shown in Figure 2.16. Note that these thrust forces are controlled by the other blocking points around the arch. In the case shown in Figure 2.16, the resultant of these arch thrust forces (F_r - rib force) is greater than the load force and consequently, an additional passive rock force is setup in the rock mass to offset the excess support resistance from the rib.

If the blocking points are kept closely spaced then the bending moment induced into the rib is limited. However, to ensure that the actual fibre stress of the rib is calculated, the bending moment created by the curvature of the arch is included through the following calculations:

$$f_r = \frac{T}{A} + \frac{Mmax}{S}$$

where fr = stress in arch portion of rib

T = Thrust in arch portion of rib

A = Sectional area of the beam

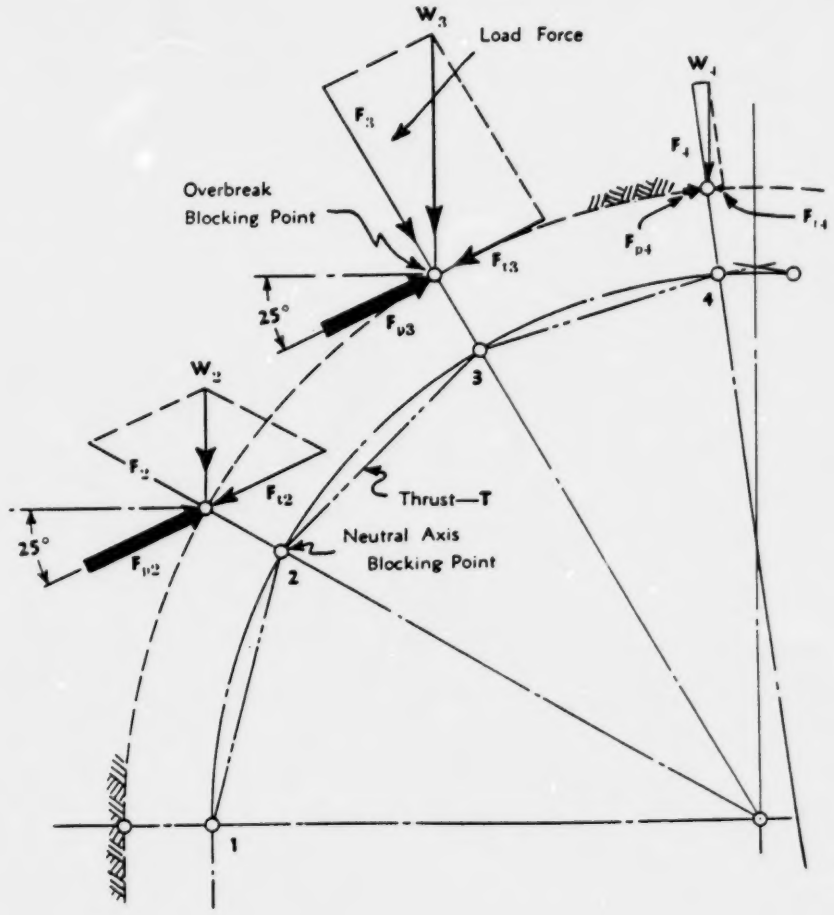

The assumed active vertical force **W** at each blocking point is resolved into two components, a radial load force **F** and a componant force F_t, acting at 25° to the horizontal or at the slope angle of the tangent, whichever is smaller. The force F_t induces an equal and opposite passive force F_p in the rock which can be of any required magnitude. Hence F_t is disregarded. The radial load force **F** either induces or opposes the rib force (F_r, Fig 2·13$_a$) exerted through the block.

FIGURE 2.15 RESOLUTION OF FORCES AT OVERBREAK BLOCKING POINTS (PROCTOR AND WHITE, 1977)

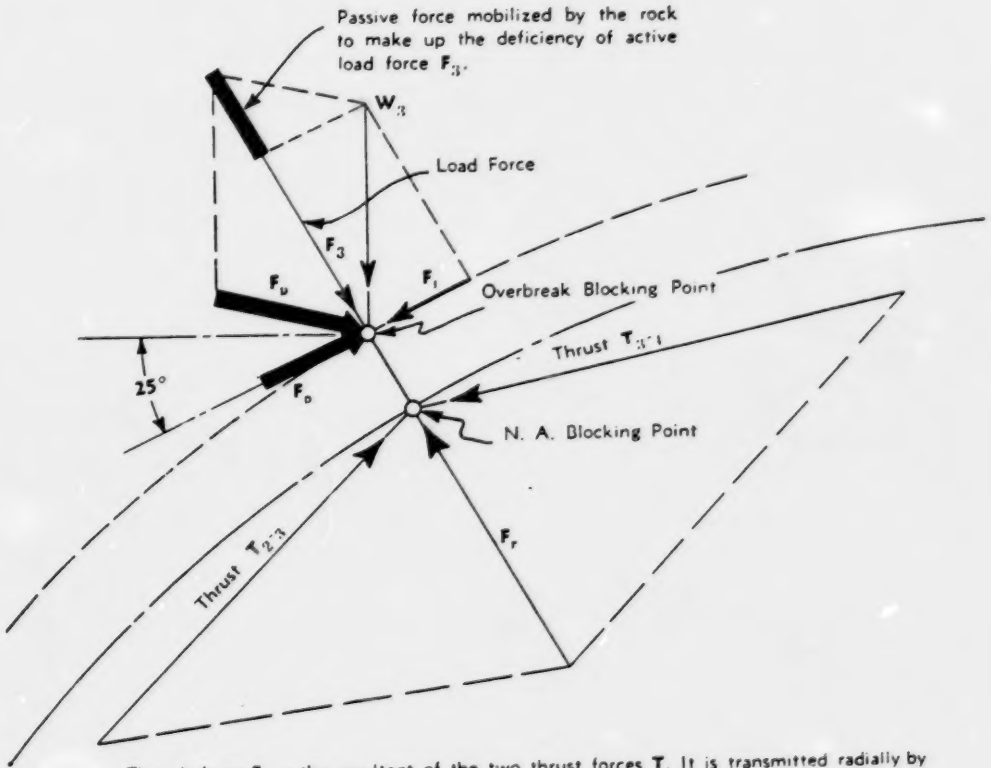

The rib force F_r is the resultant of the two thrust forces **T**. It is transmitted radially by the block to the rock where it is met by the active load force **F**. This in turn is the radial component of the active vertical load force **W**. If **F** is less than the rib force F_r, the rock mobilizes additional passive force by changing the direction and magnitude of passive force F_p so that the resultant of F_p and **W** is equal to F_r.

FIGURE 2.16 ACTION OF FORCES AT BLOCKING POINT 3 IN FIGURE 2.15 (PROCTOR AND WHITE, 1977)

Mmax = Maximum bending moment in arch

S = Section Modulus of beam

Mmax = 0.86 M_t

where M_t = theoretical bending moment for a pinned connection arch

M_t = ht

where h = rise of arc between blocking points

$$h = R - \sqrt{R^2 - \left(\frac{C}{2}\right)^2}$$

where R = radius of neutral axis of rib

C = chord length between blocking points

An analysis of the Thrust forces within the arch member is conducted using a graphical procedure referred to as a force polygon. A typical presentation of this solution technique is shown in Figure 2.17. The process of solution is as follows:

- plot the physical structure including overbreak line, rib, center of rotation (pole),
- locate blocking points on flanges of the rib,

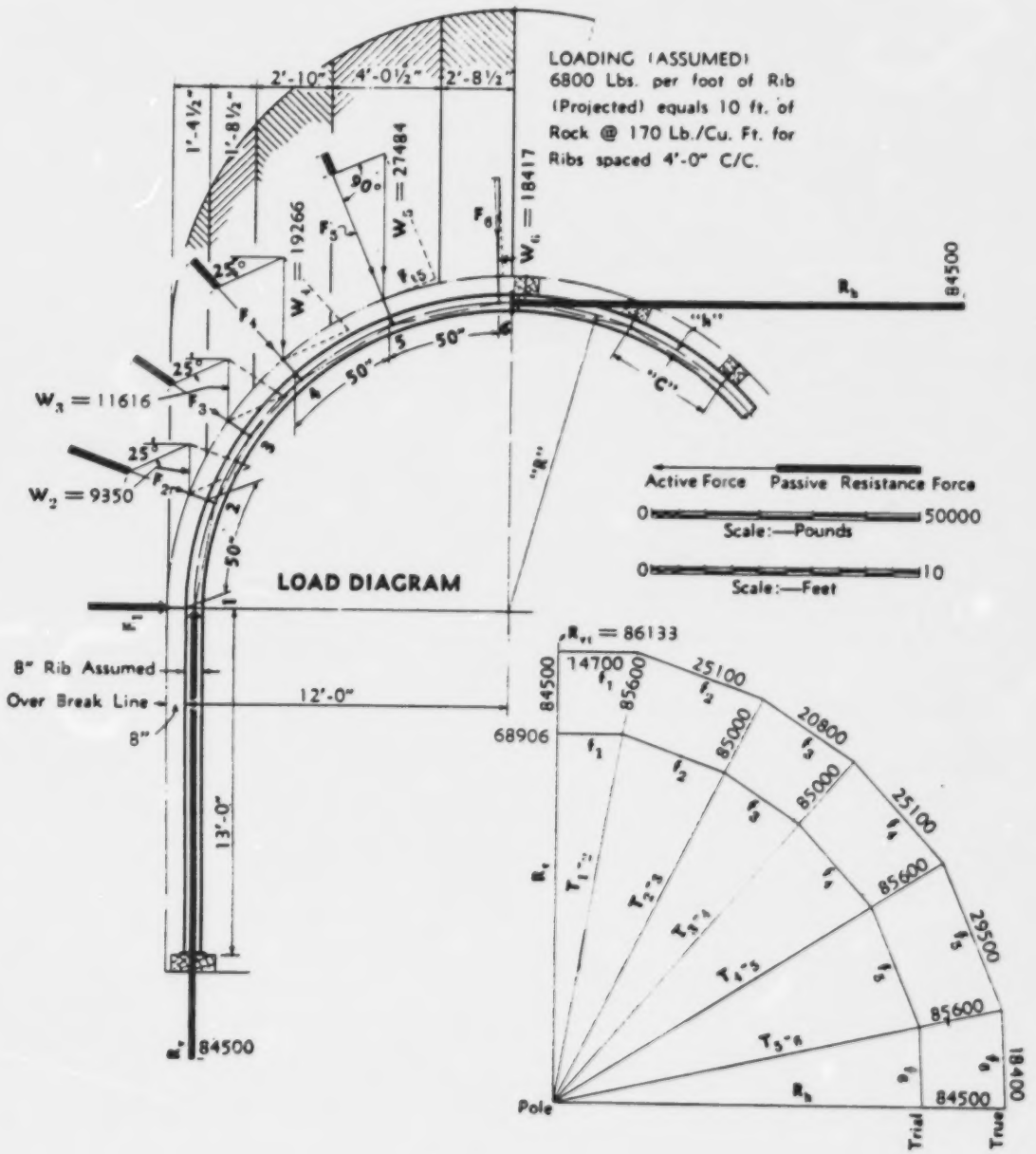

FIGURE 2.17 EXAMPLE OF THE DETERMINATION OF STRESSES IN AN ARCH BY THE FORCE POLYGON METHOD (PROCTOR AND WHITE, 1977)

- identify the rock loading distribution above the tunnel and subdivide it evenly between the blocking points (vertical lines half-way between blocking points),
- construct the force polygon (trial),
- assume pole for polygon,
- draw thrust line rays in the direction of the thrust line in the arch,
- construct a trial polygon using .8 x ΣW (weight forces acting on the arch) as a starting point for R_V and then construct all other force lines (f, f_2....) parallel to the rock force lines in the schematic,
- transfer all rock forces (F_1, F_2....) which are greater than (f_1,f_2....) to the trial polygon,
- using the force (F) with the largest difference to the trial polygon (f) construct the True Polygon for the arch with force lines parallel to the force lines in the trial force polygon.

Using the results of this force polygon analysis and the arch radius and section modulus, the fibre stress of the arch is computed. It is commented that worked examples for a semi-circular arch, a double radius arch and a cambered tunnel support structure are done in Proctor and White, 1977. The U.S. Army Corp of Engineers (El 1110-2-2901) does a worked example of a

horseshoe arch which could be modified for a splayed leg arch support analysis.

The foregoing analysis also evaluates the strength of the arch legs against buckling. Two cases are examined;

- the legs are acted on only by the thrust and bending moment carried at the springline of the arch,
- the legs are exposed to external side loading as well as the thrust and bending moment from the arch.

The reader is encouraged to refer to Proctor and White for the columnar analysis of stresses in the leg. A summary of the calculations are:

Bending moment in leg at springline (M_1):

$$M_1 = .67\ M_t = .67\ ht$$

Stress in leg at the springline (f_1):

$$f_1 = \frac{T}{A} + \frac{M_1}{S}$$

where T = thrust in rib at springline

A = area of rib member

S = section modulus

Deflection caused by Bending Moment only (d_1):

$$d_1 = .0642 \frac{M_1 l^2}{EI}$$

where: l - length of leg

E - Modulus of Elasticity

I - Moment of Inertia

Bending Moment at point of maximum deflection (M_c):

$$Mc = \frac{(.578\ M_1)^2}{(.578\ M_1 - d_1 R_V)}$$

where: R_V - thrust acting on the leg.

Stress in the leg at the point of maximum deflection (fc):

$$f_c = \frac{R_V}{A} + \frac{M_c}{S}$$

It is required that the fibre stress in the leg of the arch must be less than the reduced allowable fibre stress for the given length of arch leg (l)

$$f_c < f(red)$$

$$\text{where } f(red) = \left[\frac{f(all)}{1 + \frac{l^2}{f(all)\ r^2}}\right]$$

where f(all) = allowable fibre stress for steel

r = radius of gyration for the major axis of the beam section

Proctor and White (1977) have developed a set of Tables that can be used in the design of arch supports for rock tunnels and shown in Table 2.4. This table gives the maximum blocking point spacing for each tunnel width from 14 feet to 44 feet and for a wide range of support member sizes (4"I-beam to a 12"x12"W.F). The Table presents the maximum capacity in pounds per foot of tunnel width that can be supported. Therefore if the ground pressures are known, the correct beam size can be selected for a given tunnel width.

2.2.4 Empirical arch design criteria - Choquet

Choquet, 1982 has proposed a failure criterion for underground tunnel arch supports based on an evaluation of results from laboratory testing of full size arch supports. This criterion is based on a linear regression analysis of the arch crown deflection versus the product of two physical parameters of the arch member. The two physical parameters which were defined by Choquet are:

- the 'intrinsic characteristic' of the arch which accounts for both the dimensions of the arch profile as well as the rigidity of the profile, and is determined by the following formula:

TABLE 2.4 DESIGN TABLE FOR SEMI-CIRCULAR ARCH CONTINUOUS RIBS (PROCTOR AND WHITE, 1977)

CAPACITY IN POUNDS PER FOOT OF TUNNEL WIDTH **MAXIMUM FIBER STRESS—27000 LBS. PER SQ. IN.**

BEAM		Width of Tunnel to Outside Design Concrete Line															
Nominal Depth, Flange Width & Type	Wt. Per Foot	14'-0"	16'-0"	18'-0"	20'-0"	22'-0"	24'-0"	26'-0"	28'-0"	30'-0"	32'-0"	34'-0"	36'-0"	38'-0"	40'-0"	42'-0"	44'-0"
		40"	42"	44"	46"	48"	50"	52"	54"	56"	58"	60"	62"	64"	66"	68"	70"
		Maximum Blocking Point Spacing															
4" I	7.7	3090	2780														
4" x 4" H	13.0	5380	4850	4400	4020												
5" I	10.0	4530	4070	3690	3360												
5" x 5" Stanchion	16.0	7780	7000	6330	5770												
5" x 5" H	18.9	8840	7940	7190	6550												
6" I	12.5	6290	5660	5110	4650	4260											
6" I	17.25	7990	7180	6490	5920	5430	5010										
6" x 4" Light Beam	12.0	6200	5560	5020	4570	4200											
6" x 4" " "	16.0	8480	7600	6870	6270	5740	5300										
6" x 6" Stanchion	15.5	8380	7500	6780	6180	5660	5230										
6" x 6" H	20.0	10740	9630	8710	7930	7270	6700	6220	5780								
6" x 6" H	25.0	13270	11890	10770	9800	8980	8280	7680	7140	6670							
7" I	15.3			6740	6130	5610	5190										
8" I	18.4			8590	7820	7170	6610										
8" I	23.0			10240	9330	8550	7890	7310	6790	6340	5940	5580	5250				
8" x 4" Light Beam	15.0			7110	6470	5930	5470										
8" x 8" H	34.3			16820	15310	14020	12940	12000	11160	10410	9750	9170	8640	8180	7740	7350	6990
8" x 5¼" W.F.	17.0			8220	7510	6880	6360	5890									
8" x 5¼" " "	20.0			9820	8940	8160	7550	7010	6500	6070							
8" x 6½" " "	24.0			11920	10860	9930	9170	8500	7900	7380	6920	6490	6120	5790	5490		
8" x 6½" " "	28.0			14010	12670	11600	10710	9930	9220	8610	8070	7580	7150	6770	6410		
8" x 8" " "	31.0			15550	14160	12970	11970	11090	10300	9630	9020	8470	7990	7560	7150	6790	6470
8" x 8" " "	35.0			17590	16030	14750	13540	12550	11670	10900	10200	9600	9040	8550	8100	7680	7310
8" x 8" " "	40.0			20100	18300	16750	15470	14330	13320	12430	11650	10960	10330	9760	9250	8770	8350
8" x 8" " "	48.0				22090	20240	18670	17310	16080	15030	14070	13230	12480	11690	11070	10510	10000
8" x 8" " "	58.0					24410	22530	20880	19390	18120	17000	15990	15070	14240	13500	12810	12180
8" x 8" " "	67.0					28240	26090	24190	22470	20980	19650	18470	17410	16480	15610	14800	14110
10" I	25.4					10810	9970	9240	8580	8020	7510	7060	6660	6300	5970	5670	5400
10" I	35.0					14080	12980	12080	11180	10450	9790	9190	8670	8200	7760	7370	7010
10" x 5¾" W.F.	21.0					9250	8530	7900	7330	6850	6420	6040	5690	5390	5100	4850	4610
10" x 5¾" " "	25.0					11100	10260	9510	8840	8260	7740	7280	6860	6510	6180	5860	5580
10" x 8" " "	33.0					14770	13590	12610	11730	10960	10270	9650	9100	8610	8160	7750	7380
10" x 8" " "	39.0					17580	16220	15030	13960	13040	12230	11490	10840	10260	9720	9240	8790
10" x 8" " "	45.0					20360	18760	17380	16170	15100	14150	13310	12550	11870	11250	10690	10170
10" x 10" " "	49.0						20580	19090	17740	16570	15550	14610	13780	13030	12350	11730	11170
10" x 10" " "	54.0						22720	21090	19590	18300	17170	16130	15220	14390	13650	12960	12330
10" x 10" " "	66.0						28070	25760	23940	22350	20960	19710	18580	17570	16660	15830	15060
12" x 8" " "	45.0									15940	14940	14050	13260	12540	11890	11310	10750
12" x 10" " "	53.0									18980	17800	16740	15790	14940	14170	13450	12820
12" x 12" " "	65.0									23380	21940	20620	19450	18420	17470	16590	15810

Values shown are for stress of 27 Kips
For 24 Kips multiply by .889

$$\text{'intrinsic characteristic'} = \frac{1}{(Sx+Sy).Area}$$

where Sx - Section Modulus on the X-X axis

Sy - Section Modulus on the Y-Y axix

Area - inner area bounded by the arch

. the 'global stiffness' of the arch which is determined by the following formula

$$k(arch) = \sum \frac{Forces}{Def}$$

where $\sum$Forces - the total forces acting on the arch at collapse,

Def - deflection in the arch crown at collapse

These two terms are illustrated in Figure 2.18 and the ratio $\sum$ FORCES/DEF is designated as the 'global stiffness' of the arch member k(arch).

The regression analysis developed between the arch crown deflection on the ordinate and the product of the two physical parameters of the arch member on the absissa; i.e.:

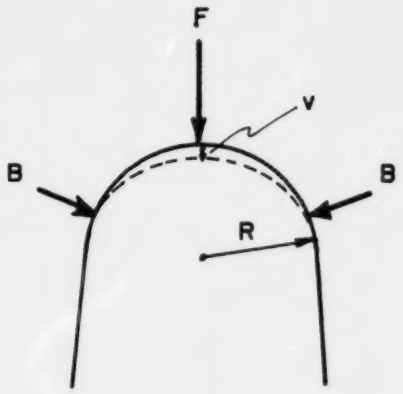

where R - arch radius

v - deflection at the crown

F - active load on the arch

B - passive reaction loads produced at the abutments due to the active load F

STRESS ON AN ARCH SUPPORT BLOCKED AT ABUTMENTS

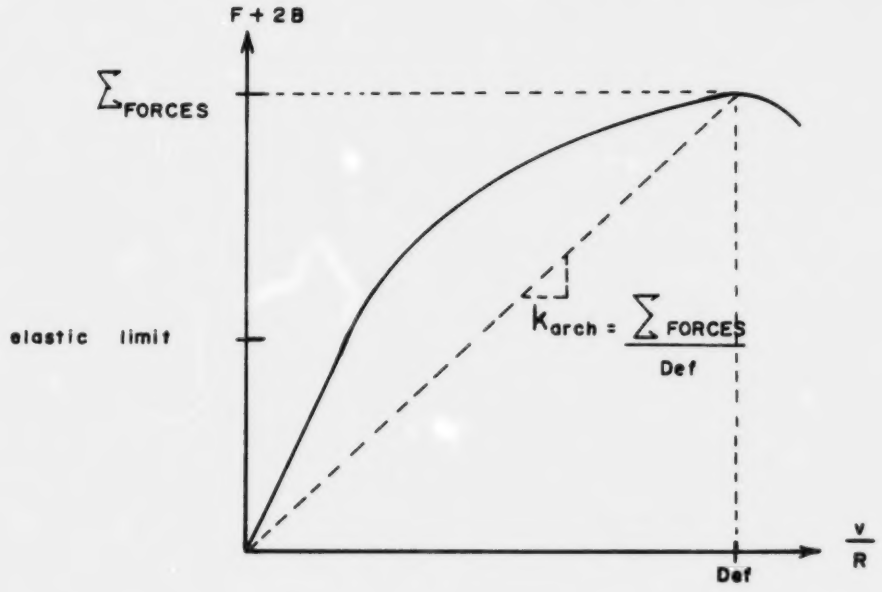

FIGURE 2·18 REPRESENTATION OF THE STRESS / DEFORMATION OF AN UNDERGROUND ARCH SUPPORT MEMBER

(Chequet, 1982)

ARCH DEFLECTION vs Product of two physical parameters

OR

$$\frac{V}{R} \quad \text{vs} \quad \left[\frac{1}{(Sx+Sy).Area} \times \sum \frac{FORCES}{Def} \right]$$

has produced a failure criterion which states that:

$$Def = -3.48 \times 10^{-9} \left[\frac{1}{(Sx+Sy).Area} \times \sum \frac{Forces}{Def} \right] + 0.090$$

This relationship is presented in graphical form in Figure 2.19.

It is proposed by Choquet that this regression equation can be used for both preliminary design work of arch supports as well as for the insitu determination of the margin of safety against collapse of the arch. The insitu arch evaluation is conducted through measurement of the crown deflection (V) and the loads in the arch ($\sum$FORCES) (determined by strain measurements of the arch).

An interesting suggestion of this regression equation is that the two profiles of arch sections investigated by Choquet (H shaped RSJ profile the Toussaint-Heintzman profile) exhibit identical behaviour at the collapse load of the arch.

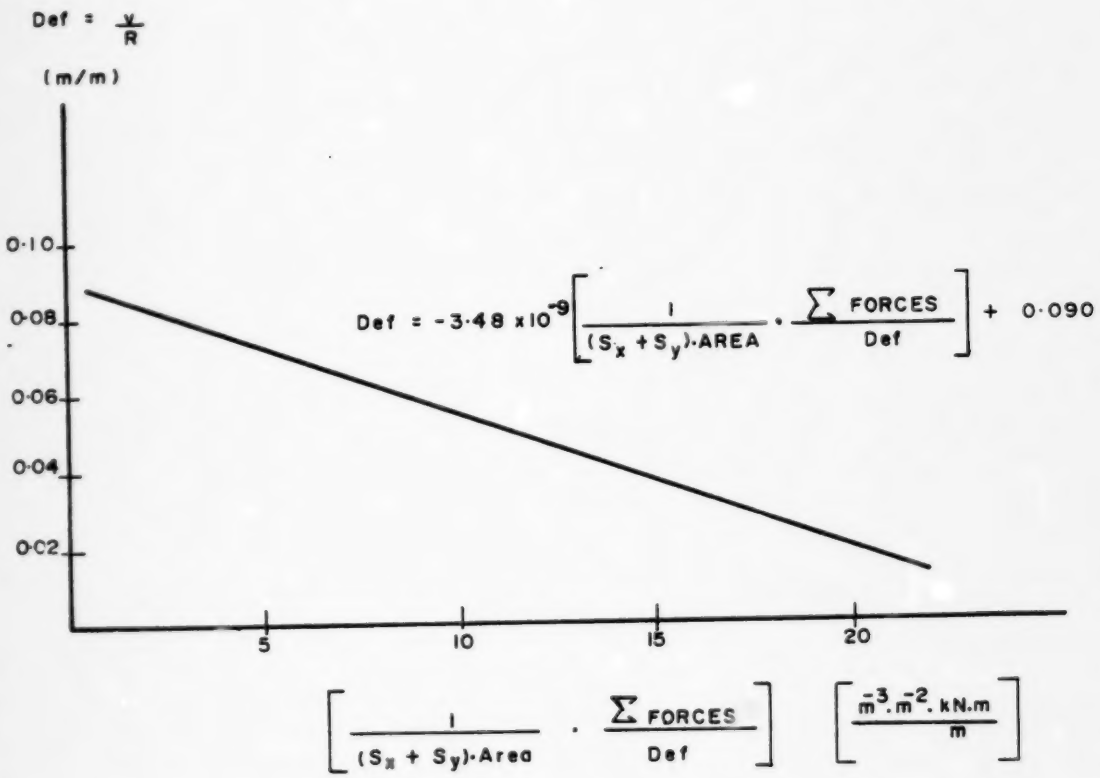

FIGURE 2·19 RELATION BETWEEN DEFLECTION AND THE PRODUCT OF THE INTRINSIC CHARACTERISTIC x THE GLOBAL STIFFNESS OF THE ARCH (Choquet, 1982)

3.0 GROUT FILLED TUBULAR STEEL

3.1 A Review of Current Research and Development Work

Grout (concrete) filled tubular steel sections have been extensively investigated to define their mechanical properties as compression members for column or column-beam elements in building structures. At the current time the work being conducted comprises the following four segments:

- axially loaded sections,
- eccentrically loaded columns under uniaxial bending,
- eccentrically loaded columns under biaxial bending,
- thin walled sections - circular steel sections.

One other major use of concrete filled tubular steel is in offshore oil production platform legs. The concrete filled tubular leg provides improved structural properties through increased flexural rigidity and increased unit area strength and it also prevents the corrosion of the leg structures on the inside of the leg tubing which significantly extends the life of the leg structures when compared with empty tubular leg structures.

In 1963 an organization of 17 member countries was formed to investigate and develop the use of tubular sections in structures. The organization was called the International Committee for the Development and Study of Tubular Structures (CIDECT). The committee members are mostly European Countries and Japan; however, Canada is represented through the interest and participation of a private corporation, STELCO. One of the areas of R & D work by CIDECT is in concrete filled hollow structural steel columns. Design criteria were developed by CIDECT for these composite columns and published in a French Monograph #5 - "Calcul des poteaux en profils creux remplies de beton - methode de calcul et technologie de mise en oeuvre" (Design of Concrete-Filled Hollow Section Columns - Calculation method and Application Technology).

A Canadian version of the CIDECT Monograph #5 was published by STELCO in January, 1981 entitled "Hollow Structural Sections - Design Manual for Concrete Filled HSS Columns" which at this time constitutes a design manual for Canadian work on this composite column member. Selected sections of this design manual by STELCO are included in APPENDIX I. It is commented that the Canadian Building Code does not permit the use of eccentrically loaded columns due to the bending moment created by the eccentric load and the resultant

tensile stress imposed on the column. Based on current Canadian Building Codes (Section 17.8 of CAN3-S16.1M84, Steel Structures for Buildings) all bending moments and tensile stress must be maintained by the steel section alone and not by the concrete inside the composite column. This code assumes that concrete in the tube has no tensile strength and as such the composite member must be designed as a hollow structural member without allowance for the concrete core.

3.2 A Discussion of the Current Contract - Steel Encased Concrete Beam

The current contract is to investigate a grout filled HSS beam section in pure bending. None of the foregoing literature or research has pursued this area of mechanical properties investigation for a concrete filled HSS section. In fact, only one source (Kato, et al., 1981) has been found that discusses any bending tests on a concrete filled steel tube. This testing was done to evaluate a newly developed pipe with raised checker projections on the inside of the pipe to improve the steel-concrete interface strength. No significant investigation of the mechanical properties of the beam members was conducted as the sole purpose of the work was to highlight the advantages of this new steel tube with raised checker projections. The results which can be cited are included in Figure 3.1

STEEL PIPE - Unfilled steel pipe
NBD - Compound pile using NEW CHECKERED PIPE
OBD - Compound pile using CONVENTIONAL CHECKERED PIPE
FBD - Compound pile using ORDINARY PIPE

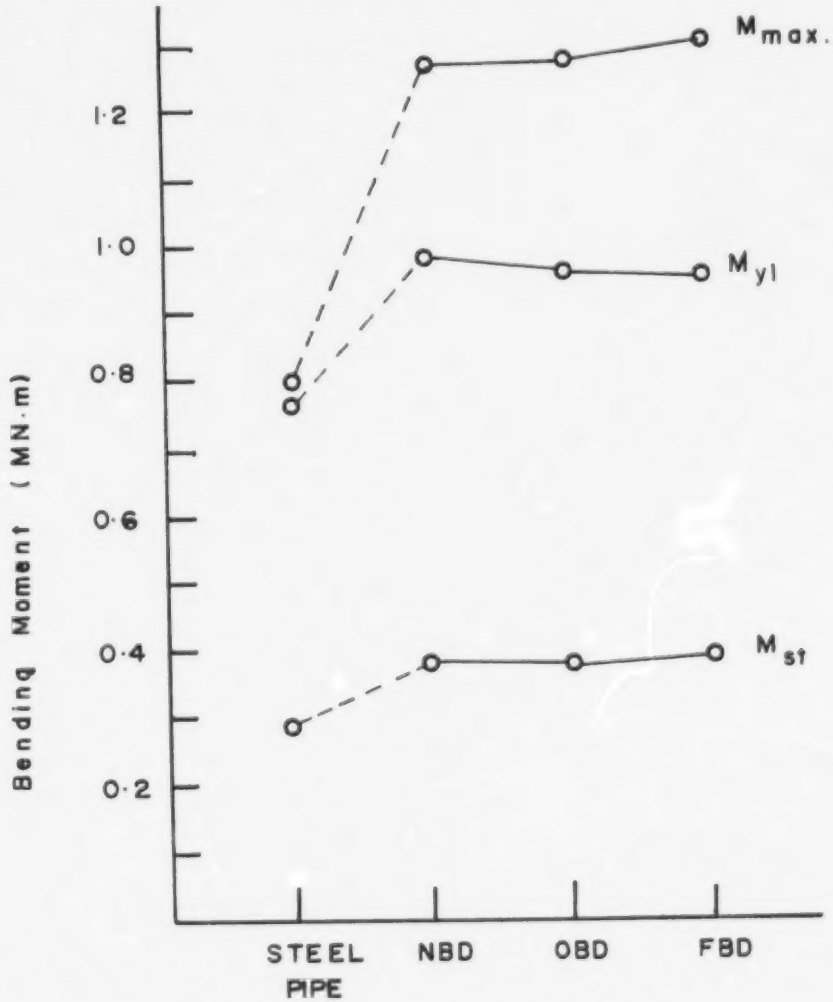

Mmax - Bending Moment at Ultimate Load on beam

M_{yi} - Bending Moment with extreme fibres at yield point (0.2% offset)

M_{st} - Bending Moment with extreme fibres at 140 MPa

FIGURE 3.1 PURE BENDING TESTS ON CONCRETE FILLED PIPE (KATO, 1981)

which indicates an increased resistance to bending, of approximately 50% at ultimate load, of a concrete filled beam versus an unfilled steel pipe. Very limited differences in flexural strength resulted from the variety of steel-concrete interface strengths being investigated in the (Kato) work.

Based on this summary of work which has been performed on the mechanical properties investigation of concrete filled HSS sections, no developed theory can be used to predict the performance of the composite beam member in the pure bending tests undertaken in this contract.

The only work which possibly has some relationship to the current contract is on eccentrically loaded columns where bending moments are induced into the composite member. Unfortunately, these bending moments are evaluated concurrently with an axial load and therefore eliminates a direct transfer of information. The Structural Stability Research Council, Subcommittee 20 Composite Columns (Iyengar et al., 1981) has proposed an approximating formula for pure flexure (which is acknowledged by the Subcommittee as being "in

lieu of an analytically accurate specification for flexural failure in composite columns"):

$$M_o = F_y S_m = S_{sc} F_y + \frac{1}{3} A_{cr} F_{cr} (h_2 - 2C_r) + A_w F_y \left(\frac{h_2}{2} - \frac{A_w F_y}{1.7 f'_c h_1} \right)$$

where:

M_o = Moment capacity in the absence of axial thrust (kip - ft.)

F_y = Specified minimum yield stress of the steel (Kips/in^2)

S_m = Modified Section Modulus about the axis of bending of a composite column (in^3)

S_{sc} = Elastic Section Modulus of structural shapes pipe or tube about the axis of bending (in^3)

A_{cr} = Area of longitudinal bar reinforcement in a composite column cross section (in^2)

F_{cr} = Specified yield strength of longitudinal reinforcement (kips per in^2 - not greater than 55 Ksi)

h_2 = Overall thickness of a composite cross section in the plane of bending (in)

C_r = Average of distance from compression face to longitudinal reinforcement in that face and distance from tension face to longitu dinal reinforcement in that face (in)

A_w = Web area; for girders or rolled shapes A_w = d tw (in^2) (d = depth of beam or girder)

Note: A_w = 0 for steel pipes or tubes

F_y = Specified minimum yield stress of the type of steel being used (kips per in^2)

f'_c = Specified compressive strength of concrete (kips per in^2)

h_1 = Overall thickness of a composite cross section perpendicular to the plane of bending (in)

This formula predicts the flexural capacity of the composite member to be comprised of:

- the steel shape,
- the longitudinal reinforcement,
- the concrete which is compressed along one edge of the cross-section.

Several other issues were detailed by the Subcommittee 20 work:

- the cross-section area of the steel shape must comprise at least 4% of the total composite column cross-section, which would require that

$(A_s/(A_s + A_{cr}+A_{cc}) > 0.04)$. If this condition is not met, the member must be considered a reinforced concrete member for design work.

where:

A_s - Area of steel tube (in^2)

A_{cr} - Area of reinforcing rods (in^2)

A_{cc} - Area of concrete (in^2)

- reinforcement rods must be tied together,
- concrete strengths in compression can range between 3000 psi to 8000 ksi,
- the design yield strength of structural steel is not to exceed 55 ksi,
- the steel tube wall thickness is restricted by the following relationship:

$$t \geq b \ (F_y/3E)^{\frac{1}{2}}$$

for each face of width b in rectangular sections.

where: t = thickness of tube wall

b = effective width of member (in)

F_y = Specified minimum yield of steel ($kips/in^2$)

E = Elastic modulus of steel (29,000 $kips/in^2$)

- the allowable flexural stress is only 75% of the allowable yield stress of the specified steel:

$$F_b = 0.75\ F_y$$

where F_y = axial stress permitted in absence of bending (ksi)

F_b = bending stress permitted in absence of axial force (ksi)

3.3 Concrete Encased Steel Beam Composite Member

One other form of a concrete - steel composite beam member is the concrete encased structural steel beam employing a significant quantity of reinforcing rods to strengthen the concrete envelope. Though this structural member is considered to be outside the terms of this contract some interesting work in the mining field has been conducted by enclosing a steel RSJ with concrete. Initially, it is reported by Colcrete Limited (UK) that an application of shotcrete to the web of an RSJ will increase its flexure strength. Also, work conducted by the Mining Research and Development Establishment of the National Coal Board (MRDE, 1981) reports information on concrete encased RSJ beams of several designs (Figure 3.2). The reported results are that the ultimate strength of the beams increased relative to the strength of the plain

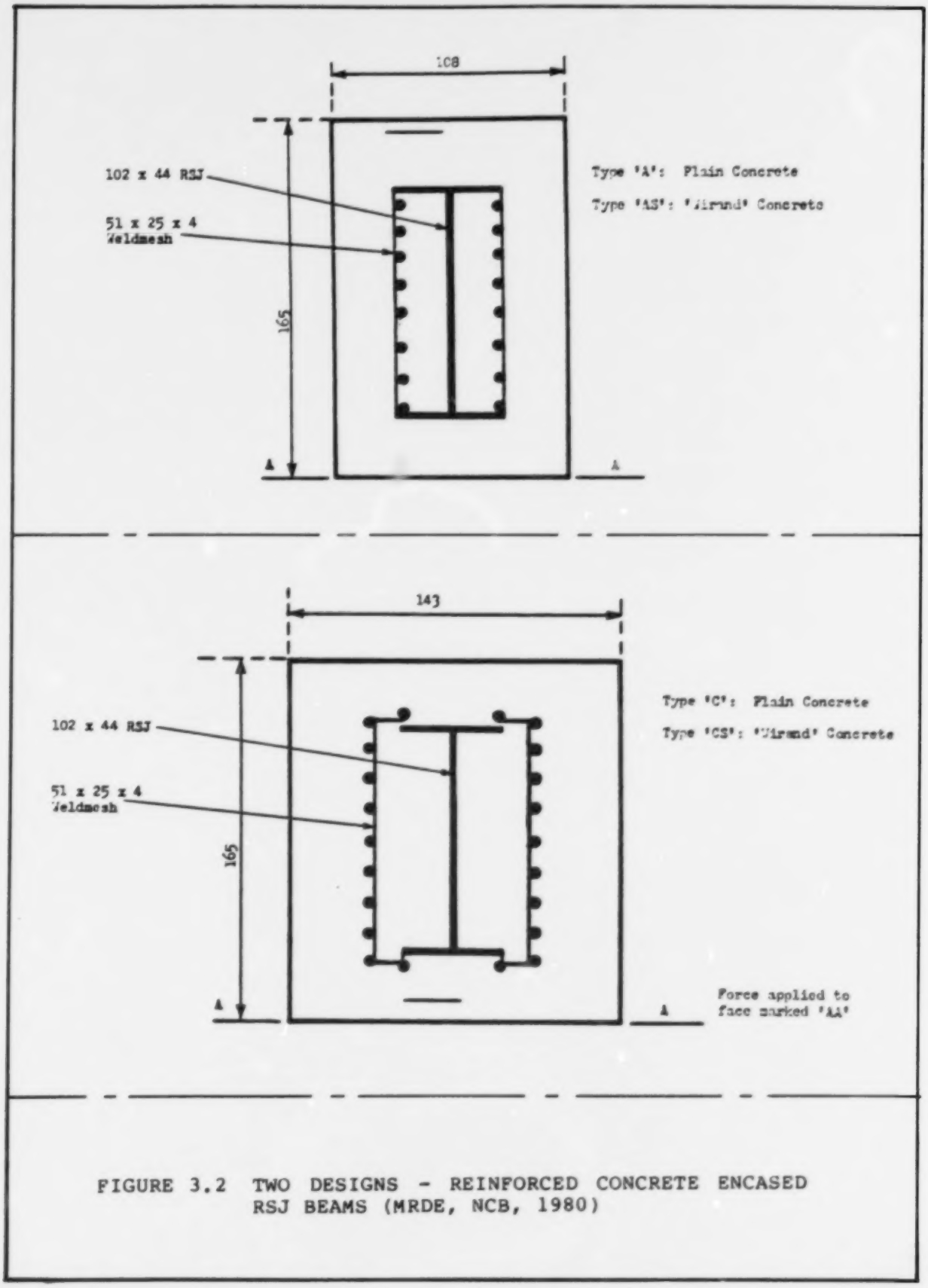

FIGURE 3.2 TWO DESIGNS - REINFORCED CONCRETE ENCASED RSJ BEAMS (MRDE, NCB, 1980)

RSJ by 46%; however, this result required an average increase in the weight of the beam of 700%.

As the current contract work is to investigate a steel encased concrete beam, this concrete encased RSJ member will not be discussed further in this report.

4.0 LABORATORY INVESTIGATION

The evaluation of the mechanical properties of a straight beam member was investigated in laboratory testing at the Technical University of Nova Scotia, Halifax, Nova Scotia. The tests which were conducted included:

- simply supported beam members with single point (mid-point) loading,
- simply supported beam members with three point loading,
- laterally confined beam members with three point loading.

It was identified from the literature review that extensive debates have been conducted on whether the testing of the subject composite beam member should be controlled by standard tests for structural steel or concrete (reinforced). The one and three point bending tests are consistent with both standards and pose no difficulty for this study. However, the laterally confined beam test was conducted to specifically investigate the properties of the grout core inside the steel tube. The laterally confined beam test was designed to simulate the testing fixture for roof strata and is not a recognized standard test at this time. Further discussion of this test will be conducted in a subsequent section of this report.

4.1 Selection of HSS Section Size

It was decided at the outset of the project to restrict testing of the beam members to a single HSS section size. This decision was made in consideration of the contract budget and to permit the desired scope of testing (one-point, three-point and laterally confined) over a range of cure times for the grout core. The selected HSS section was a 127.0 x 50.8 mm section with a 4.78 mm thick wall (5 x 2 inch section with a .188 in. thick wall). The sections used were hot rolled from steel sheet and seam welded at the mid-point of the long side of the rectangular section. The weld conforms to the neutral axis of the beam members. The beam members were not stress relieved prior to filling and testing. The properties of this HSS section as listed in a supplier handbook (Drummond McCall, Reference Book 81-17) are given in Figure 4.1.

Other reasons for the use of the 127 x 50.8 mm x 4.78 mm thick HSS section were:

.a filled tube could be moved by one person.
Larger sizes would require several people or a lifting device once filled (pouring could not be accomplished in the compression frame area),

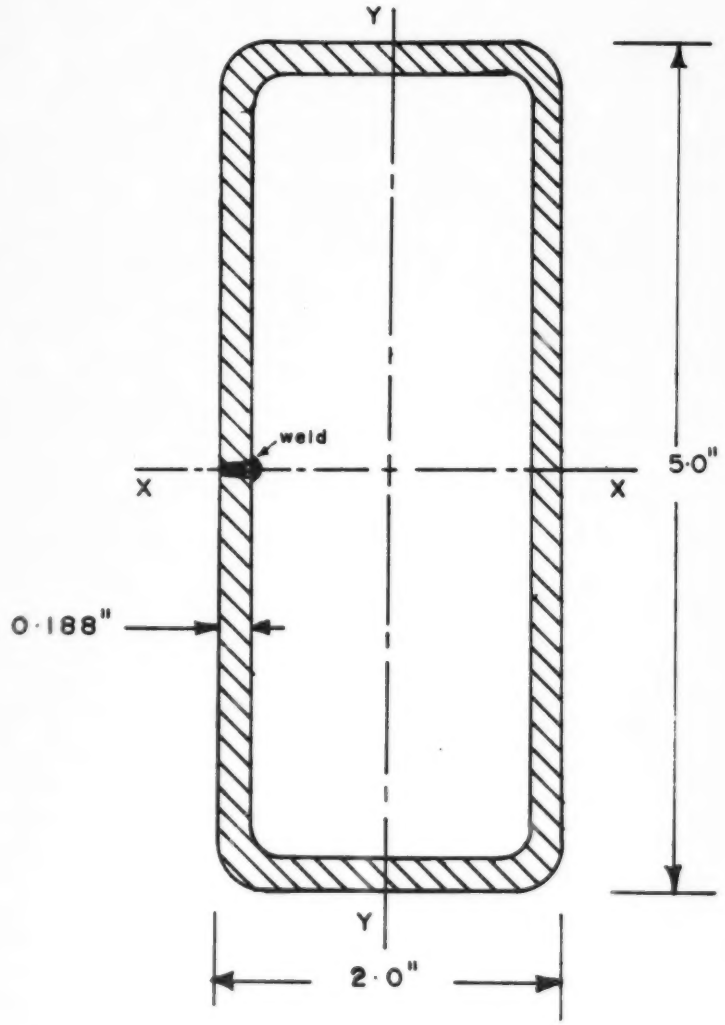

MASS	8.16lbs/ft.
AREA	2.40 in^2
SECTION MODULUS	Sxx - 2.76 in^3 Syy - 1.6 in^3
MOMENT OF INERITIA	Ixx - 6.9in^4 Iyy - 1.6 in^4
RADIUS OF GYRATION	rxx - 1.67in ryy - 0.804in

FIGURE 4.1 HOLLOW STURCTURAL STEEL (HSS) SECTION USED IN LABORATORY INVESTIGATIONS.

.the availability of HSS sections is limited in the Halifax area, the one chosen is in stock locally,

.the concrete filling of the beam member was required to match the one-half cubic foot mixes of grout to

.avoid wastage of the grout material,

.the elastic section modulus (Sxx) of the HSS is approximately 48% lower than the 89 x 89 RSJ chosen for comparisons. Due to the difference in shape factors of the two sections the Plastic Modulus of the HSS (Zxx) is only 30% lower than the 89 x 89 RSJ. This difference in Section and Plastic Modulus between the HSS and the RSJ is necessary to provide a lighter weight section for installation purposes. Indications from the Kato work, where a 50% increased bending resistance for a concrete filled round pipe versus an empty pipe at ultimate load, would suggest that the concrete core can compensate for these reduced moduli values to produce an equivalent strength composite beam as provided by the 89 x 89 RSJ.

Beam Section (mm)	Section Modulus ($10^3 mm^3$)		Shape factor	Plastic Modulus ($10^3 mm^3$)		Weight per linear metre (kg)
	Sxx	Syy		Zxx	Zyy	
89x89 RSJ	67.4	22.4	1.15[1]	77.5	25.8	19.35
127.0x50.8 HSS	45.3	26.2	1.30[2]	58.9	30.9	12·2

[1] Assumed standard for the National Coal Board RSJ design work (Newson)
[2] Canadian Institute of Steel Construction

4.1.1 Computation of Composite Beam Properties

Several cases are proposed to predict the properties of the grout filled HSS beams. Each of

these cases is briefly outlined below and a determination (moment of inertia, section modulus) of the associated beam properties is conducted:

Case I - Transformation of entire grout core to equivalent steel material:

The concrete section can be directly transformed into an equivalent steel material and the composite beam properties (I,S) computed. This case assumes that the concrete material has the same basic strength properties (for the transformed area) as the steel.

Case II - Tranformation of grout core in compression to equivalent steel material:

The grout material is known to have a very poor tensile strength. In recognition of the fact that on bending the steel and grout are likely to be unbonded, it is more likely to consider the material transformation for the concrete to steel as being appropriate for only the compression zones of the beam, not for zones in tension. This

case will alter the centroid and neutral axis of the beam to effect a change in the strength of the beam member.

Case III - Transformation of grout core in compression to equivalent steel material and the use of a reinforcing rod for tensile loads in the bottom of the beam.

The use of a reinforcement member (rod) in the bottom of the beam to serve as a tensile member during bending in conjuction with the material transformation to steel of the concrete in the compression zone of the beam. This situation would similarily modify the centroid and neutral axis of the beam to change the strength of the beam member.

It is noted that for all material transformation calculations, the industry standard value of (E_s/E_c) n=15 is used. The material transformations and modified moment of inertia and section modulus for each case are shown in Figure 4.2.

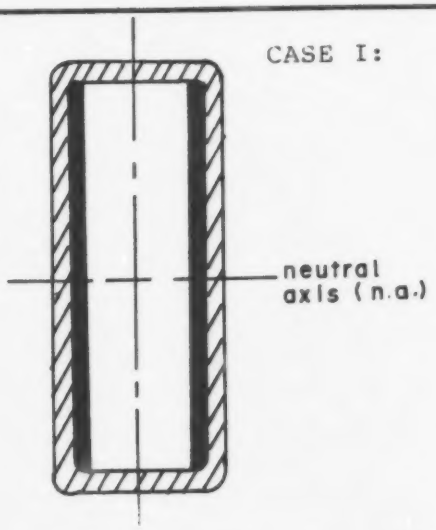

CASE I: Transformation of complete grout core to equivalent steel section

$I_x = 7.79\ in^4$
$S_x = 3.12\ in^3$

(neutral axis unchanges)

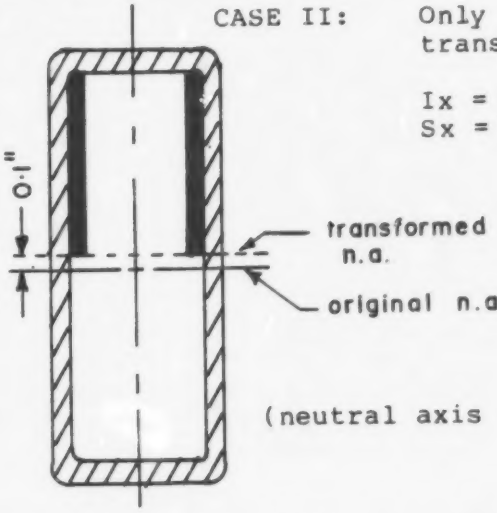

CASE II: Only the grout core in compression transformed to an equivalent steel section

$I_x = 7.29\ in^4$
$S_x = 2.91\ in^3$

(neutral axis moves up 0.1" due to transformed area)

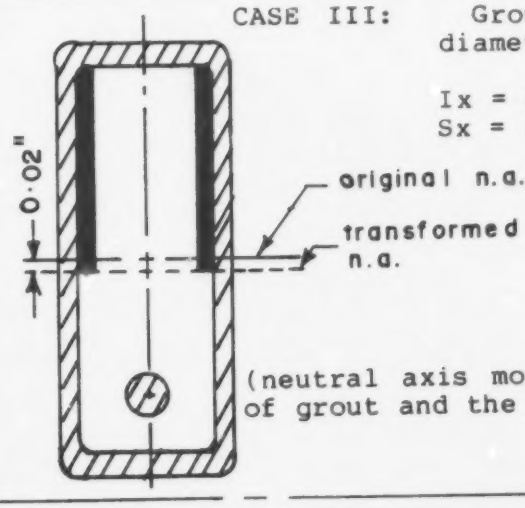

CASE III: Grout core in compression and 1/2 inch diameter rebar reinforcement section

$I_x = 8.08\ in^4$
$S_x = 3.23\ in^3$

(neutral axis moved down 0.02"due to transformed area of grout and the rebar)

FIGURE 4.2 TRANSFORMED AREA CALCULATIONS FOR 3 CASES OF GROUT FILLED HSS BEAMS

4.1.2 Selection of beam length

The beam span was predetermined to be a minimum of 5 feet to accommodate the compression frame and existing bend test fixture. Each beam was fabricated from a six foot section of HSS. The 6 inch overhang on each end of the beam allowed for fabrication of the vent holes and fill tube plus end plate work without disturbing the 5 foot test section. Also, a six foot section of the selected HSS required approximately 0.4 cubic feet of grout to fill it, which was consistent with the 0.5 cubic foot mix batches provided by the 25 kg bags of the grout material.

4.2 Selection of Grout Material

The selection of a grout material was made to ensure standardization of the mix during testing. This was accomplished by using a commercially available pre-mixed cementitious grout (M-BED STANDARD from Sternson Limited) mixed to a specified water/cement ratio. The strength/time curves for M-Bed grout are given in Figure 4.3. At the initial stage of the investigation several water ratios from 3.5 l/25 kg to 4.5 l/25 kg mixes were used to investigate pumping properties of the grout material.

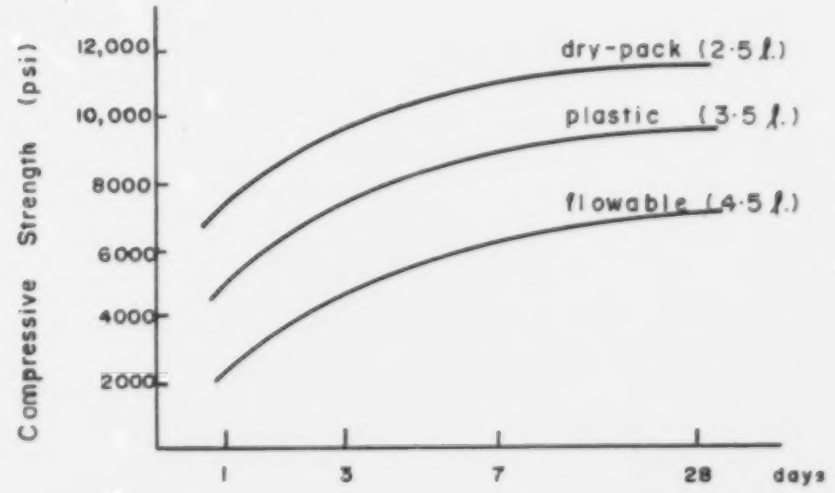

FIGURE 4·3 M-BED STANDARD

During the course of the study, work was done on the effect of the strength of the grout mix on the bending properties of the beams. The various water ratio mixes used for pumping tests previously discussed were used for this purpose. Also, several tests were conducted using a high early strength resin grout (Talygrout 100, Sternson, Limited, Figure 4.4).

4.3 Method of Preparation and Placement of Grout in HSS Sections

The cementitious grout was mixed in accordance with the manufactures specifications by adding the prebagged (25 kg) grout to the selected water volume (4.0 liters for most tests). Mixing was done using a double turbine type grout mixer driven by a variable speed drill press, Photograph 1.

The mixed grout was pumped into prepared HSS beam sections using a Moyno-2L4, Progressing Cavity Pump equipped with a 1 ft^3 grout hopper, Photgraph 2. All beams were fabricated to have a fill point and two vent holes. Filling of the HSS sections was conducted with the beams slightly tipped to ensure that no air became trapped in the grout material Photograph 3. Several beams were pressured grouted at 200 psi to investigate

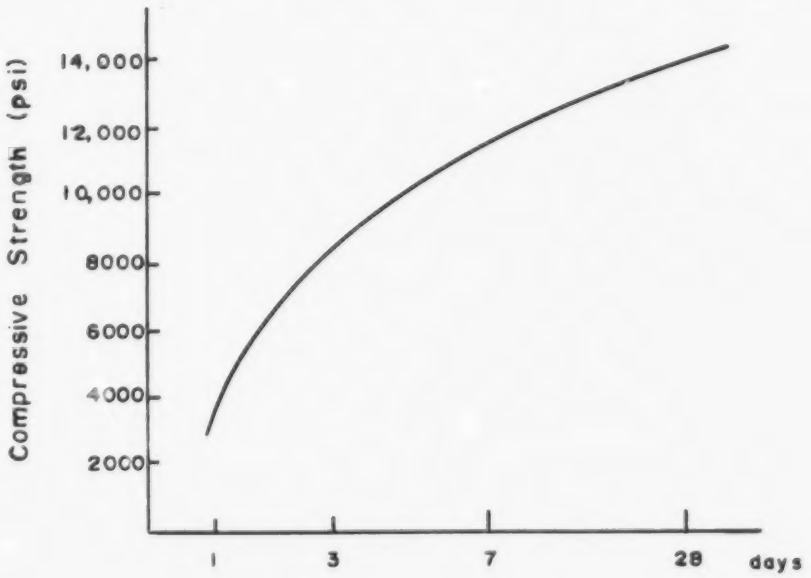

FIGURE 4·4 TALYGROUT 100

Photograph 1. Double turbine grout mixer mounted on a variable speed drill press for mixing grout.

Photograph 4. Moyno 4L4 Progressing Cavity Pump equipped with a 1 ft³ grout hopper. The hopper was equipped with a vibrator to ensure continuous movement of the grout during pumping.

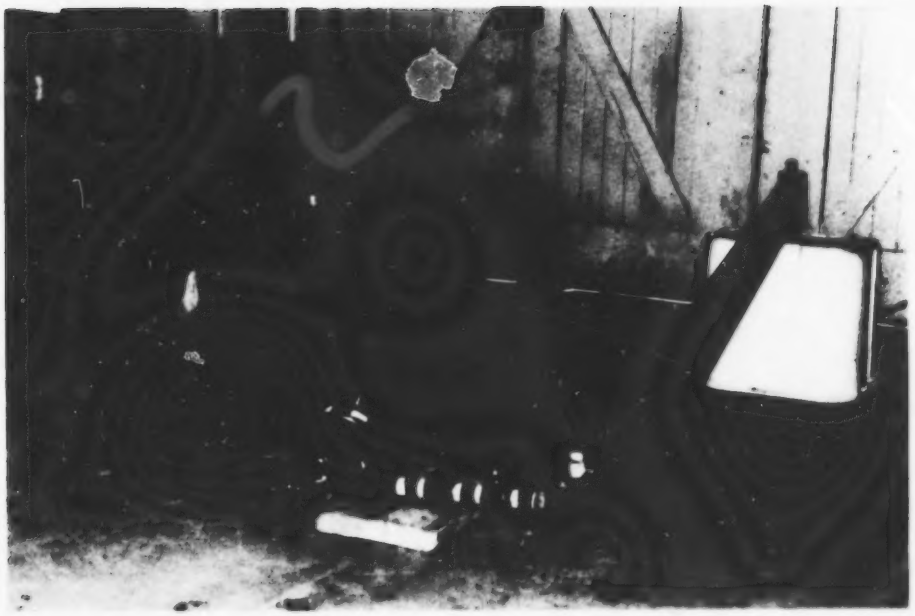

Photograph 3. HSS tube pumping setup showing the inclined beam member used to prevent entrapped air occurring in the grout core. This picture demonstrates a pressurized grout filling setup (the in-line pressure sensor and value assembly would not normally be used).

the effect of a pressurized grout core on the beam strength properties. The grout pressures were recorded by an in-line, isolated pressure sensor (Red Valve, 1"Diameter, Series 30-200 psi maximum), Photograph 4.

No special precautions were taken to ensure humidity control of the beam members during the grout cure period. This procedure was considered suitable as all beams were completely sealed following the grout placement.

4.4 Testing of the Beam Sections

Bending tests were conducted using the following testing machine at the Technical University of Nova Scotia:

Make: Tinius Olsen Universal Testing Machine

Model: 50822

Capacity: 3 ranges: 0 - 44,000 lbs;
0 - 220,000 lbs;
and 0 - 440,000 lbs.

Controls: Mechanical type machine, displacement controlled

Load Rate: .025 in/minute to 2.0 in/minute
(all tests were conducted at a load rate of 0.15 inches/minute).

Photograph 4. In-line isolated pressure sensor and value assembly used for the pressurized grout core filling procedures.

4.4.1 - Simply supported beam tests

Both one-point and three-point bend tests were conducted on simply supported composite beam sections (Photograph 5) at the following grout cure times:

- 1 day
- 3 days
- 7 days
- 28 days

A variety of tests some with strictly a nonpressurized grout core, some with a pressurized grout core and others with a steel rod reinforcement in the tension zone of the beam (Photograph 6) were investigated.

4.4.2 Laterally constrained Beam Tests

A special set of tests were conducted on the composite beam using a specially constructed stiff testing frame to prevent the end rotation of the beam during bending. This frame is shown in Figure 4.5 and in Photograph 7. The tie-rods of the frame were instrumented with electric strain gauges to determine the stresses being transferred into the tie-rods during bending tests Photograph 8. The purpose of the laterally constrained beam was to induce a linear compression arch in the grout material instead of the

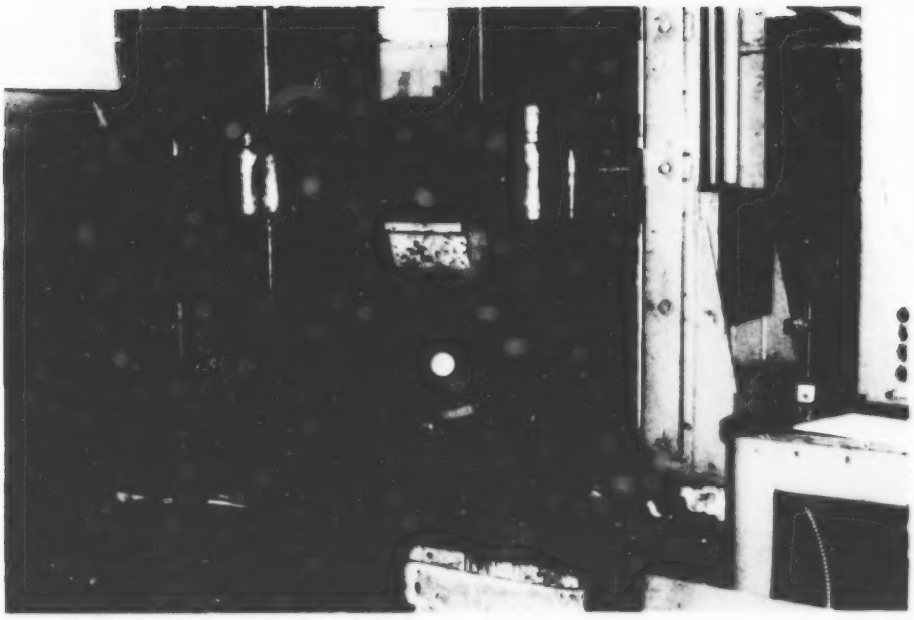

Photograph 5. One-Point Bend Test on a simply supported composite beam member showing dial-gage instrumentation at the centre of the beam.

Photograph 6. Reinforcement rod (1 2 inch diameter installed in the bottom of the beam member with 1/4 inch cover on the sides and bottom.

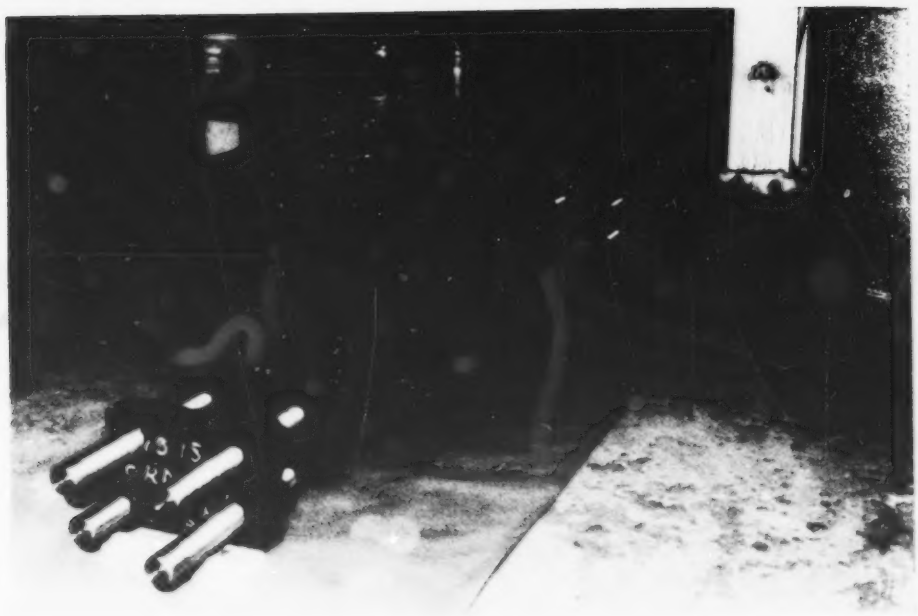

Photograph 7. Laterally confined stiff test frame used to restrict the end-rotation of the beam during bend tests.

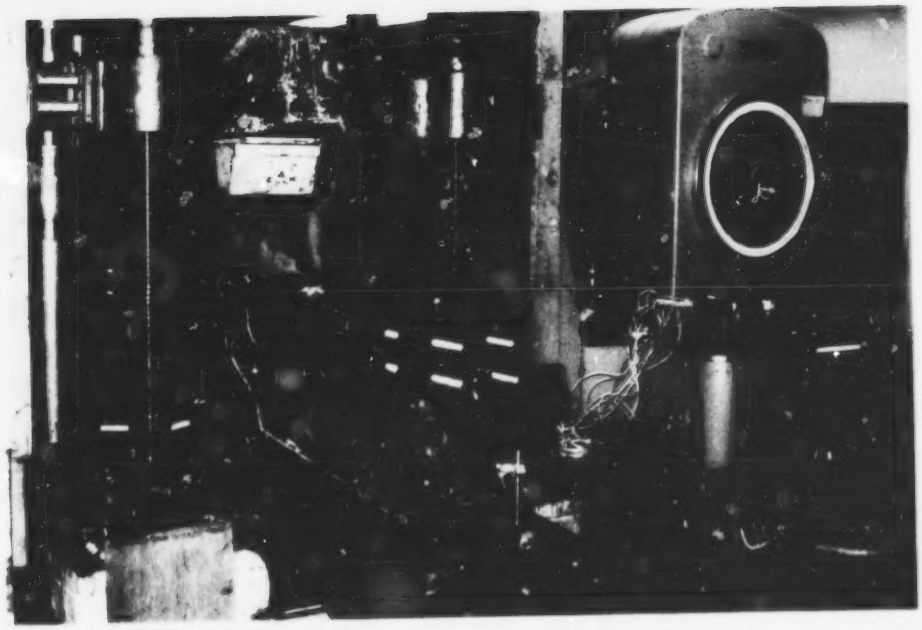

Photograph 8. Three-point bend test on Laterally-constrained beam showing electric strain gage instrumentation of the frame tie rods, centre point deflection dial gage, end point rotation dial gage and test frame load indicator.

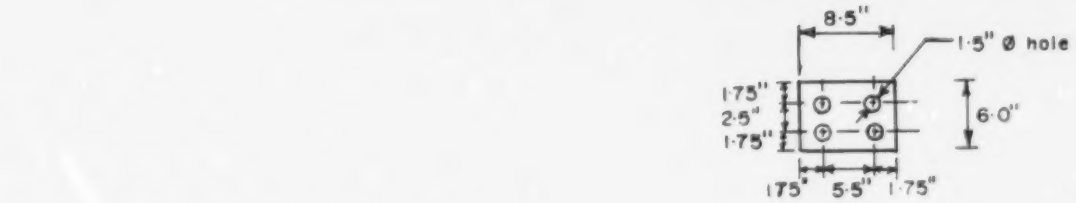

END PLATE DETAIL

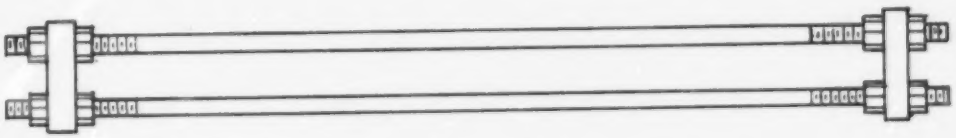

TOP VIEW

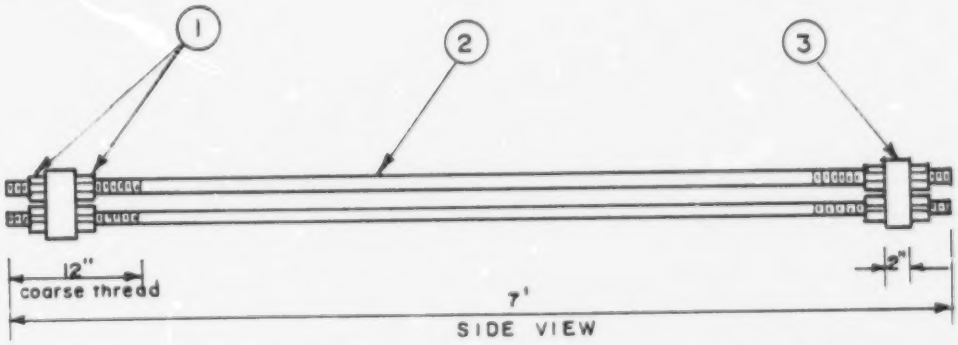

SIDE VIEW

	ITEM	MATERIAL	Qty
1	NUTS	1·5" dia. coarse thread	16
2	TIE ROD	1·5" dia. 'stressproof' steel bar - threaded ends	4
3	END PLATE	2" C.R. steel plate	2

FIGURE 4·5 LATERALLY CONFINED BEAM TEST FRAME

tensile (failure) stress at the center point of simply supported beams. This principle of a linear compression arch induced in a laterally constrained beam member, and the test jig to investigate it are documented by Sterling, 1980. The Sterling investigations were conducted to determine the ultimate load behaviour of laterally constrained rock beams. The concrete core of the grout filled HSS sections represents a similar low tensile strength brittle material similar to rock, and as a result, the laterally constrained beam tests were seen to be consistent with this investigation.

4.5 Results of Laboratory Investigation

The information compiled during the bending tests on the five foot long composite beam members comprise the following data:

- load (force) recorded in 1000 pound-force increments, as indicated on the load indicator of the compression machine,
- center point deflection of the beam determined by dial gauge (.001 inch) at the 1000 pound-force increments discussed above.

Several special tests were also performed to document the deformation of the beam during loading. These tests included the following data:

- rotation at the bottom end points of the simply supported beam during the loading procedure as recorded by a dial gauge (.0001 inch).
- strain measurements by electric strain gages on the instrumented tie rods of the laterally constrained test frame.

Figure 4.6 illustrates the instrumentation utilized during the bend tests to provide data for analysis of the composite beam member.

The test results which were recorded are included in Appendix II, and graphical presentation of the data is included in the following text. Each phase the investigation will be discussed in the following section of the report to detail the observations made from the experimental work.

4.5.1 Selection of the grout material to be used in beam tests

Prior to establishing the grout mix to be used for filling the HSS sections, an investigation was

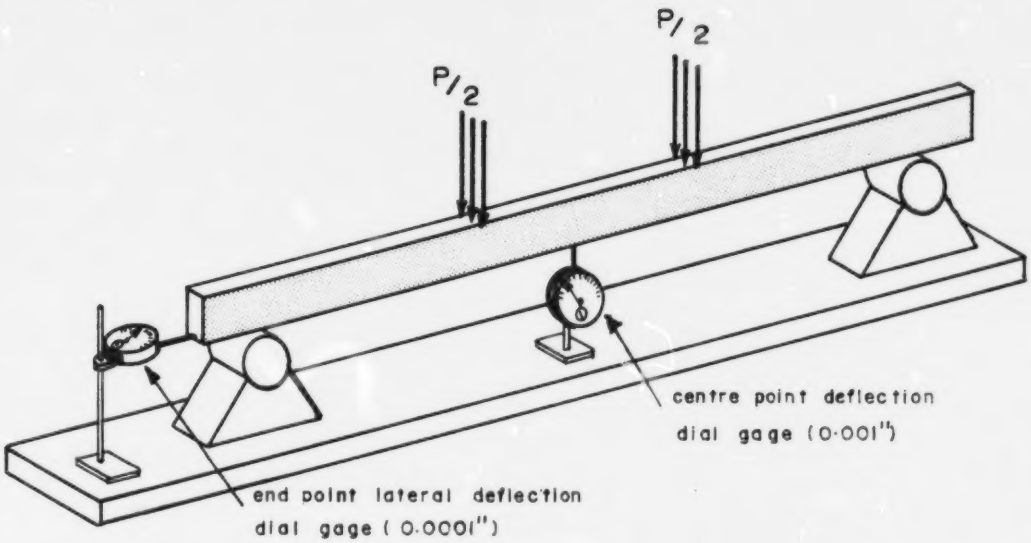

SIMPLY – SUPPORTED BEAM TESTS

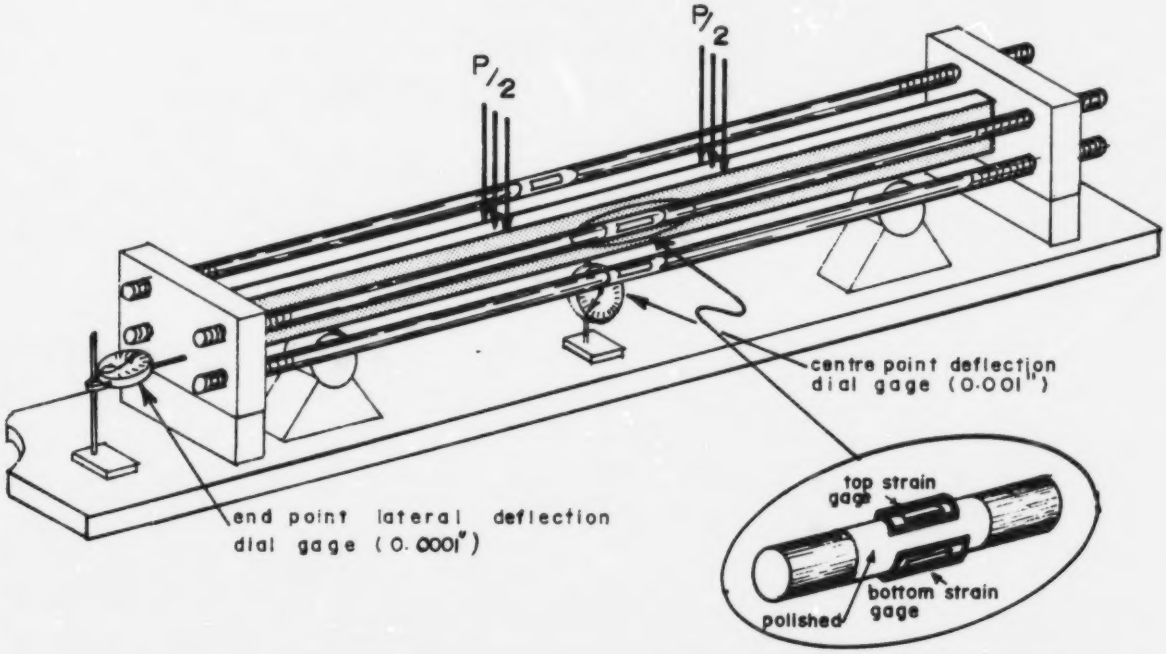

DETAIL – STRAIN GAGE INSTALLATION
(2 gages per tie-rod)

LATERALLY – CONFINED BEAM TESTS

FIGURE 4·6 INSTRUMENTATION USED IN BEAM TESTS

conducted to determine the effect which the strength of the grout material had on the beam performance in center point bending tests. A variety of water volumes (3.5 l, 4.0 l, 4.5 l) per 25 kg bag of M-Bed cementitious grout were used as well as a variety of cure times. To provide a comparison with the cementitious grout (M-bed), tests were also conducted on a high-early strength resin grout filling using another Sternson Limited product Talygrout 100. The results of these tests are shown in Figure 4.7.

Comments:

From an analysis of the beam deflection information it is concluded that there is an increased bending strength with an increased grout strength. When compared with the graph of the empty HSS section beam, all grout filled tubes are seen to provided increased resistance to bending.

It was concluded from this work that the remainder of the tests on grout filled beams would be conducted using M-bed cementitious grout mixed at a water volume of 4.0 l as a standard mix. It was considered undesirable to use the 'Plastic Mix' grout (3.5 l), despite its increased strength, due to problems

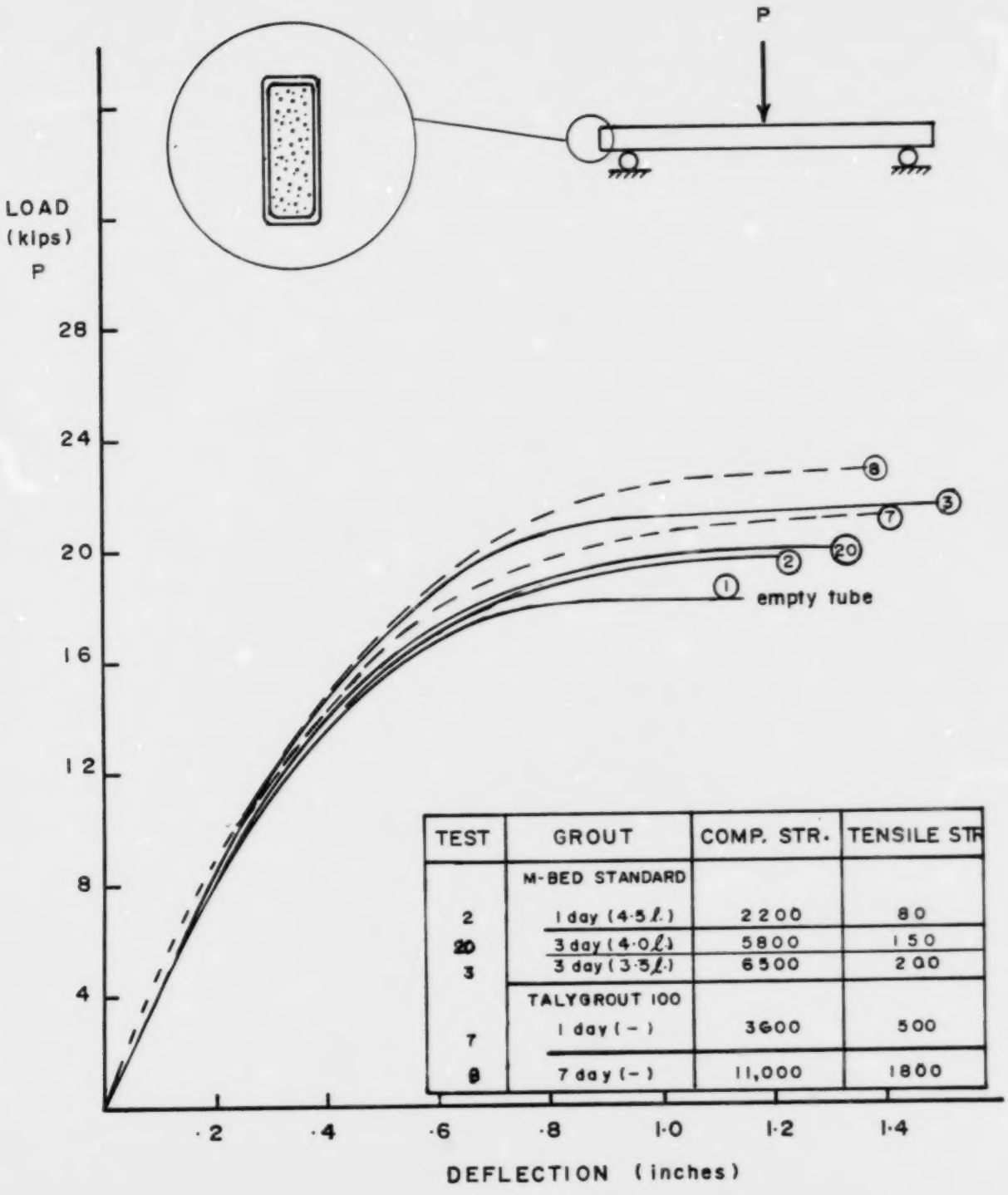

TEST	GROUT	COMP. STR.	TENSILE STR
	M-BED STANDARD		
2	1 day (4·5 ℓ.)	2200	80
20	3 day (4·0 ℓ.)	5800	150
3	3 day (3·5 ℓ.)	6500	200
	TALYGROUT 100		
7	1 day (–)	3600	500
8	7 day (–)	11,000	1800

FIGURE 4·7 EFFECT OF GROUT STRENGTH ON DEFLECTION OF COMPOSITE BEAM IN 1–POINT BEND TESTS

with pumping the very stiff mix into the HSS sections. Consequently, for the remainder of the experimental program mixes of 4.0 l, M-bed grout were used.

The maximum composite beam performance would obviously be achieved using the resin grout (Talygrout 100). This product was studied for comparative reasons only. The excessive cost of a resin grout product would eliminate it from any practical applications for this subject study.

4.5.2 Performance of grout filled (4.0 l M-bed) HSS sections

Following the selection of a filling material, a series of one and three-point bending tests were conducted on grout filled HSS section beams. The one point tests were used to represent the worst condition of loading which could occur on a structural support in the underground environment. The three-point tests were conducted to simulate an evenly distributed load on the beam (the application of an evenly distributed load on the beam was considered unnecessary to be undertaken in this contract due to the complexity and cost of such loading mechanisms).

The results of these tests are shown in Figure 4.8.

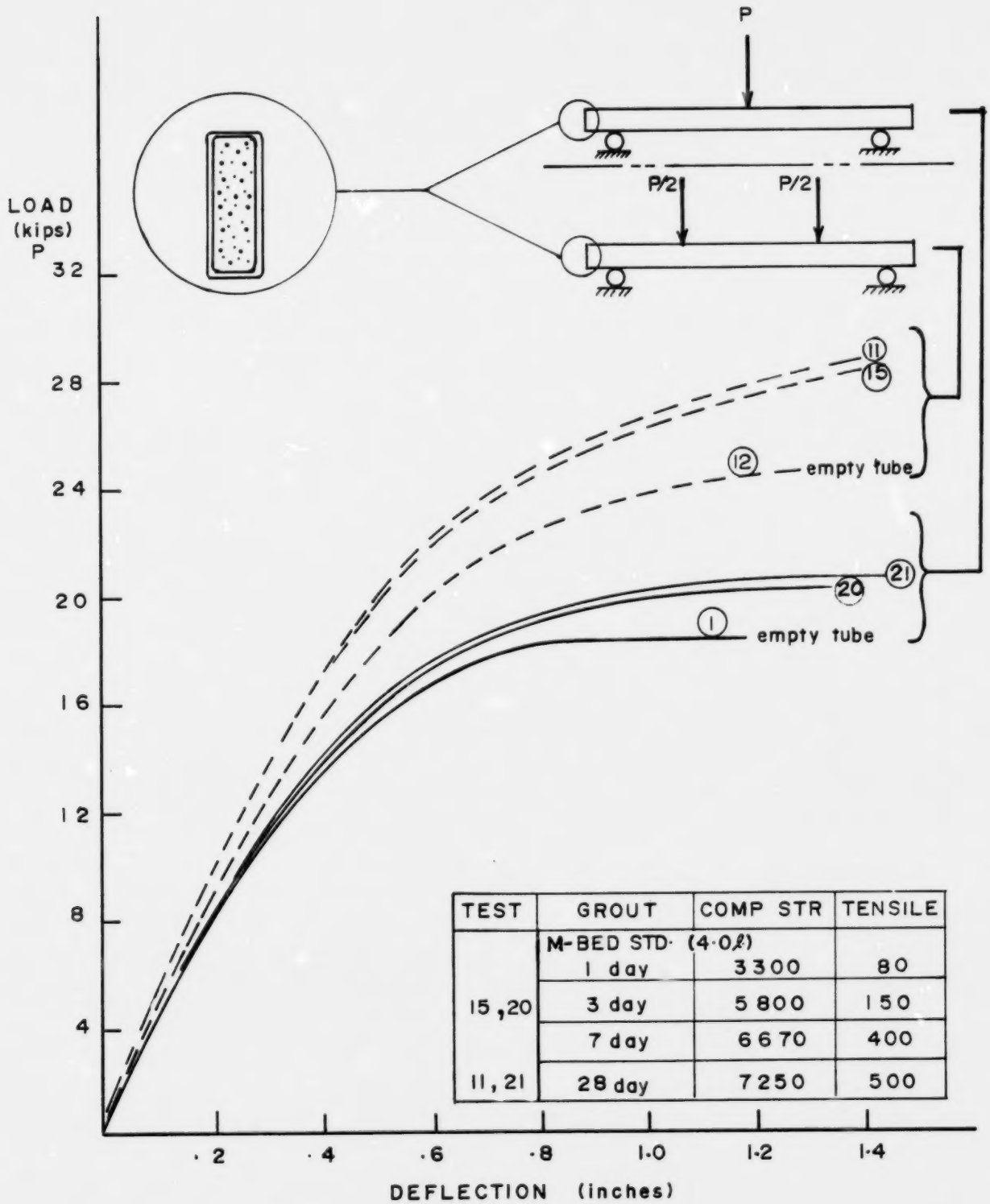

TEST	GROUT	COMP STR	TENSILE
15,20	M-BED STD. (4.0ℓ) 1 day	3300	80
	3 day	5800	150
	7 day	6670	400
11,21	28 day	7250	500

FIGURE 4.8 1 & 3 POINT BEND TESTS ON SIMPLY SUPPORTED COMPOSITE BEAM

Comments:

Preliminary indications from this information are that very limited bending resistance is added to the HSS section beam in the elastic region of the load/deflection curve for the one-point loading tests. For the three-point tests there is a slight shift of the load/deflection curve or stiffening of the composite beam in bending due to the addition of the grout core. In the plastic region of both tests there is an obvious increase in the ability of the composite beam to resist bending loads.

4.5.3 Performance of pressurized grout filled HSS section beam

One-point bending tests were performed on several beams which were pressure grouted to 200 psi with the M-bed grout (4.0 1) mix. This work was conducted to determine if the pressurized core had any effect on the strength of the composite beam.

The results of these tests are plotted in Figure 4.9. Several other related graphs are included in Figure 4.9 for comparison purposes.

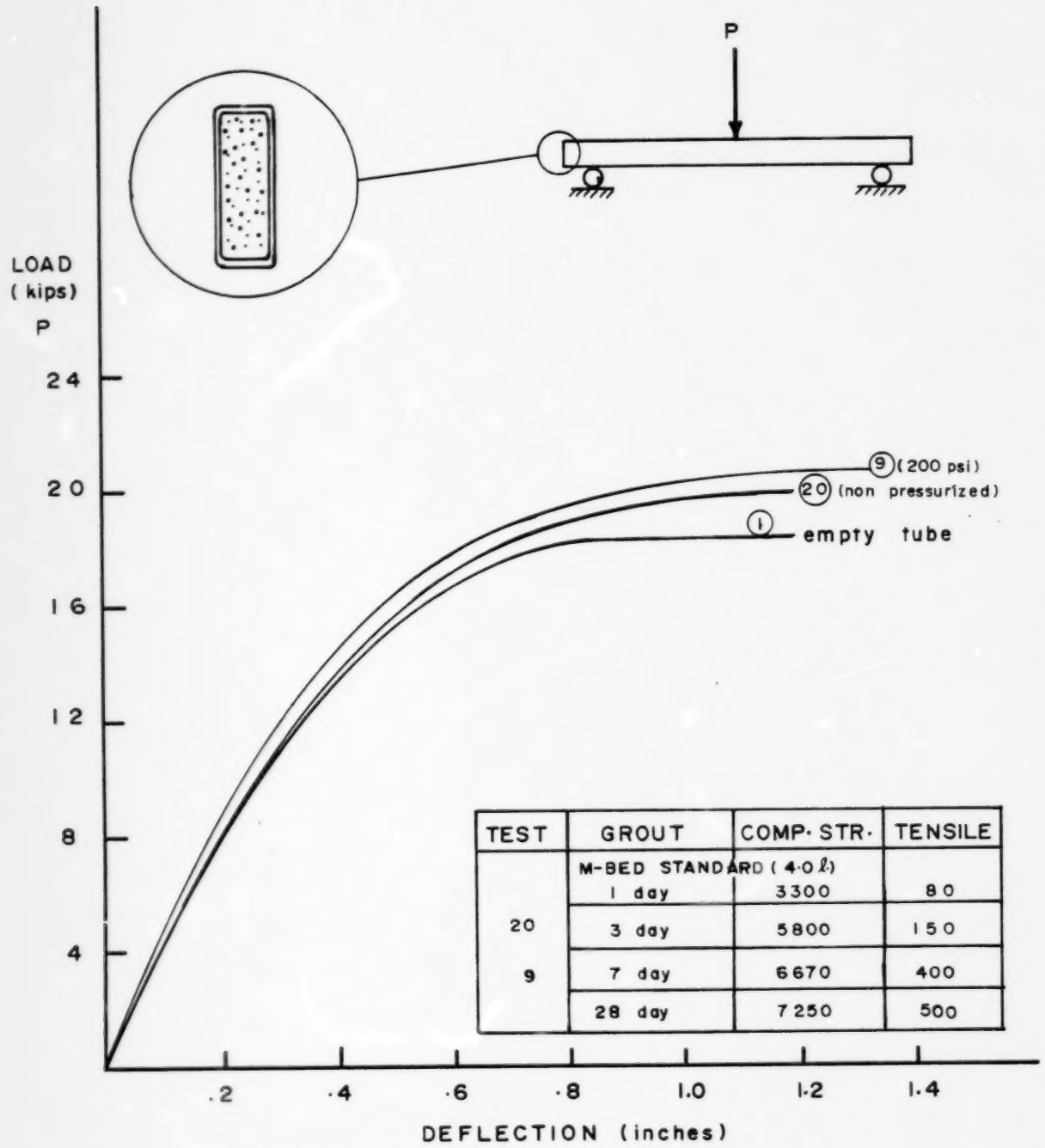

TEST	GROUT	COMP. STR.	TENSILE
	M-BED STANDARD (4.0 ℓ)		
	1 day	3300	80
20	3 day	5800	150
9	7 day	6670	400
	28 day	7250	500

FIGURE 4.9 1- POINT BEND TEST ON PRESSURIZED (200 psi) GROUT CORE IN HSS SECTION

Comments

No apparent change in the strength of the beam was created by pressurizing the grout core.

4.5.4 Performance of reinforced beam grout members

In an effort to generate additional tensile strength in the bottom of the beam (an observed weakness from earlier testing) it was decided to install a 0.5 inch diameter reinforcing bar with a 0.5 inch grout cover (sides and bottom) at the bottom of the beam. It was recognized that the grout cover was insufficient to permit maximum rebar strength development; however, the intent of this group of tests was to provide a preliminary assessment only. If encouraging results were generated by the preliminary testing, more detailed engineering design could be conducted.

As a second phase to the reinforced composite beam evaluation, several tests were conducted with pressurized grout (at 200 psi) and a 0.5 inch diameter reinforcing rod with a 0.5 inch cover.

The results of the testing are presented in Figure 4.10.

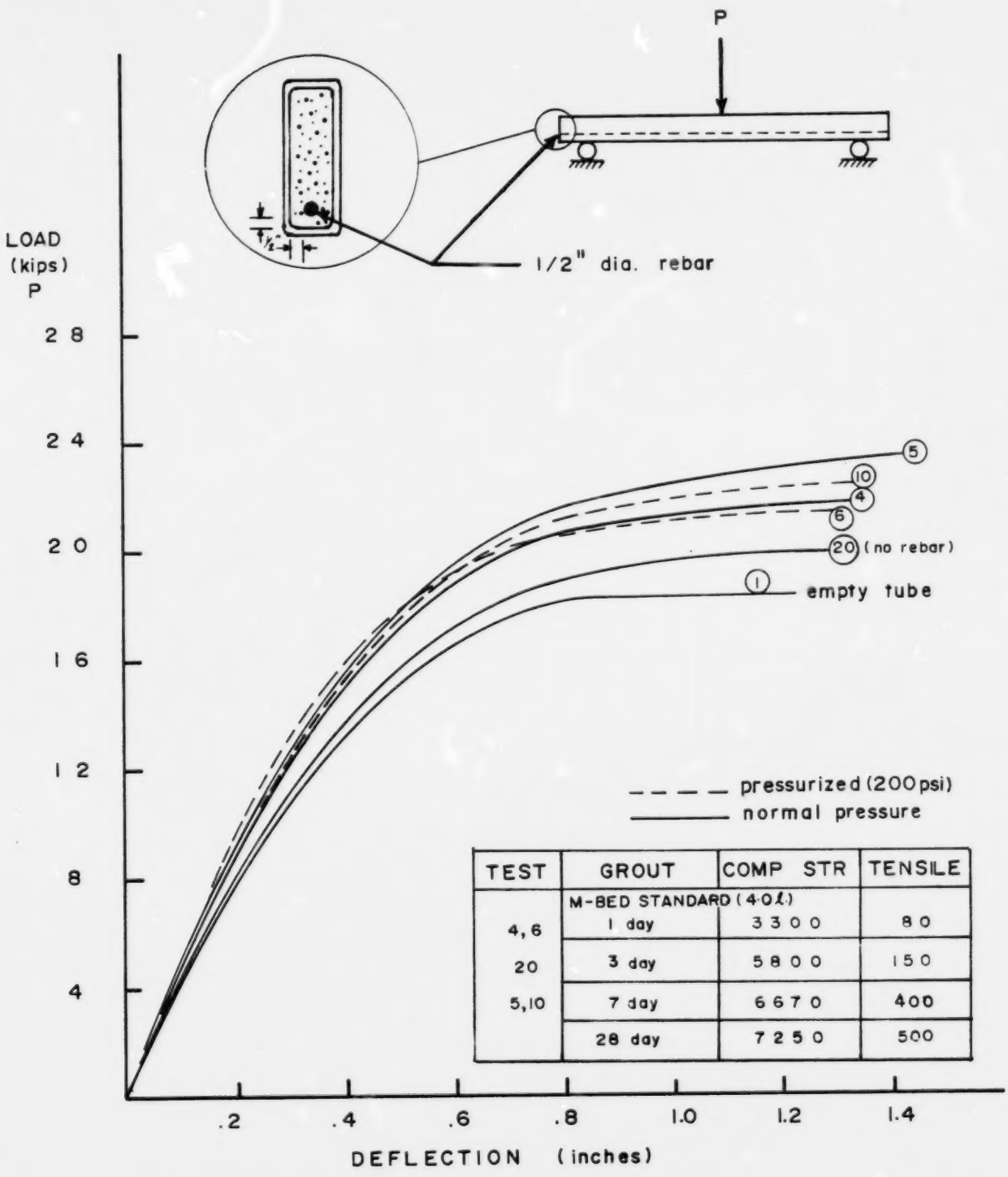

TEST	GROUT	COMP STR	TENSILE
	M-BED STANDARD (4.0ℓ)		
4,6	1 day	3300	80
20	3 day	5800	150
5,10	7 day	6670	400
	28 day	7250	500

FIGURE 4.10 1-POINT BEND TESTS ON GROUT FILLED HSS WITH 1/2 INCH. DIA. REBAR - NORMAL AND PRESSURIZED (200 psi) GROUT CORE

Comments

The addition of the rebar to the bottom of the grout filled HSS beam is observed to stiffen the member within its elastic range, which was not observed in previous testing with only the grout filling. It is also observed that the yield point for the composite member has been increased with the addition of the reinforcing rod. The plastic deformation of the composite member has not been significantly altered by the addition of the reinforcing bar, except it is uniformly elevated in comparison with the grout filled HSS section.

The pressurized grout filled samples of reinforced HSS section beams exhibit a unique property in the bending tests. The elastic region of the load/ deflection curve coincides with the previous reinforced grout filled (unpressurized) composite beams. However, the pressurized, reinforced beams exhibit a lower yield point and a decreased plastic zone compared with the unpressurized samples. For both the 1 and 7 day tests this phenomenon was observed.

4.5.5 Performance of laterally constrained beams

All laterally constrained beams were tested in three-point loading. The lateral constraint of the beam ends was intended to restrict the end rotation during bending and thereby produce a stronger beam member. A record of the displacement at the bottom end points of the beam, when compared with the end rotation of a simply supported beam (filled with Talygrout 100) adequately demonstrate the success of this lateral constraint test frame. It can be observed in Figure 4.11 that the end rotation of the lower extreme fibres at the end of the beam were held within - 0.010 inch to + 0.015 inch during the test. Though there is some end-movement, it is possible to make the case for evaluating the laterally constrained beams as rigid-end beams. Further discussion of this point will be conducted in Section 4.6.

Figure 4.12 demonstrates the performance of the laterally constrained beams for empty and grout filled (1,3,4,5,28 day curves) beams in three-point loading.

Comments

A significant shift of both the elastic and plastic regions of the load/deflection curve are

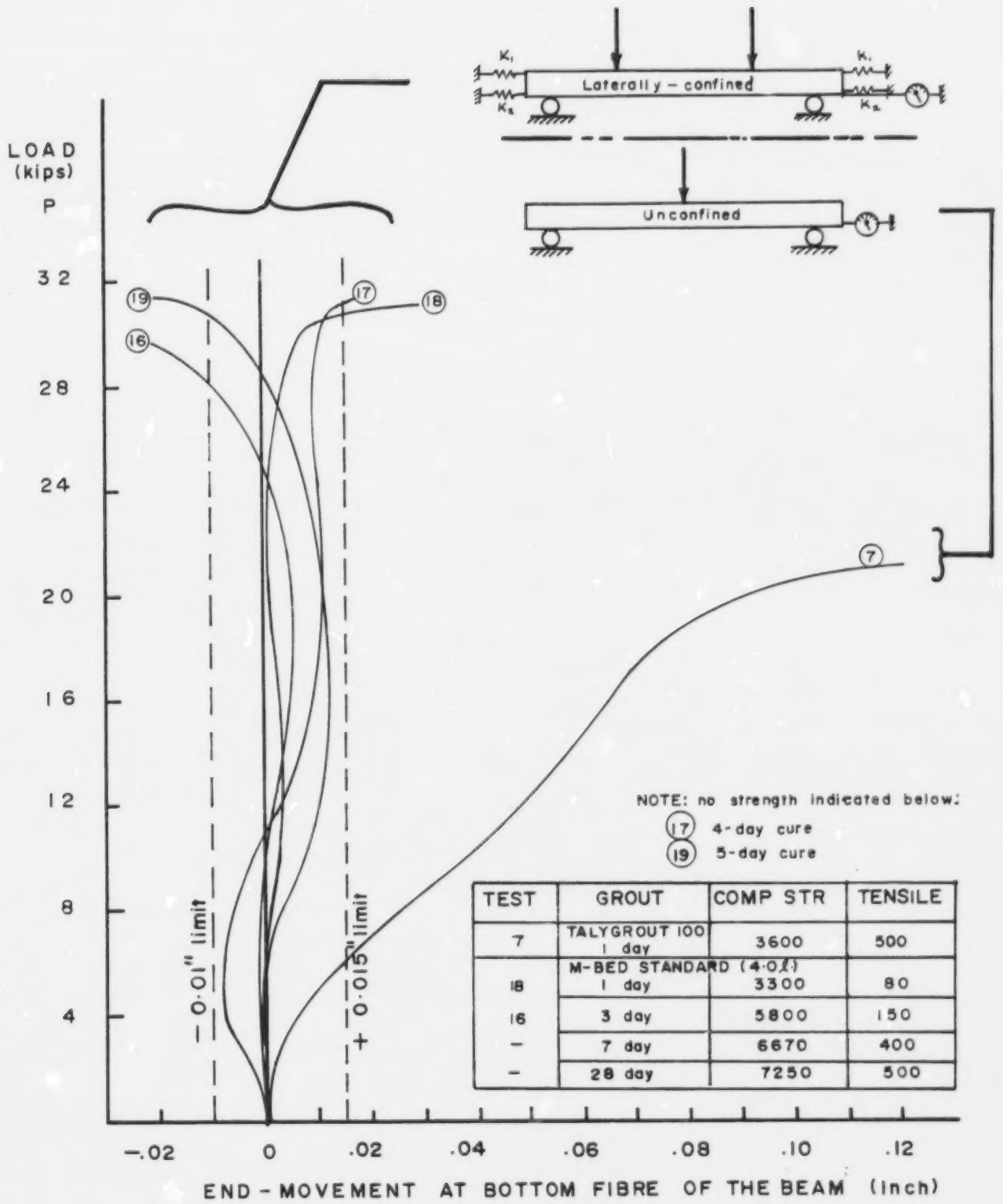

FIGURE 4·11 LATERAL DEFLECTION OF BOTTOM FIBRE OF COMPOSITE BEAMS FOR LATERALLY-CONFINED VS. UNCONFINED BEAM TESTS

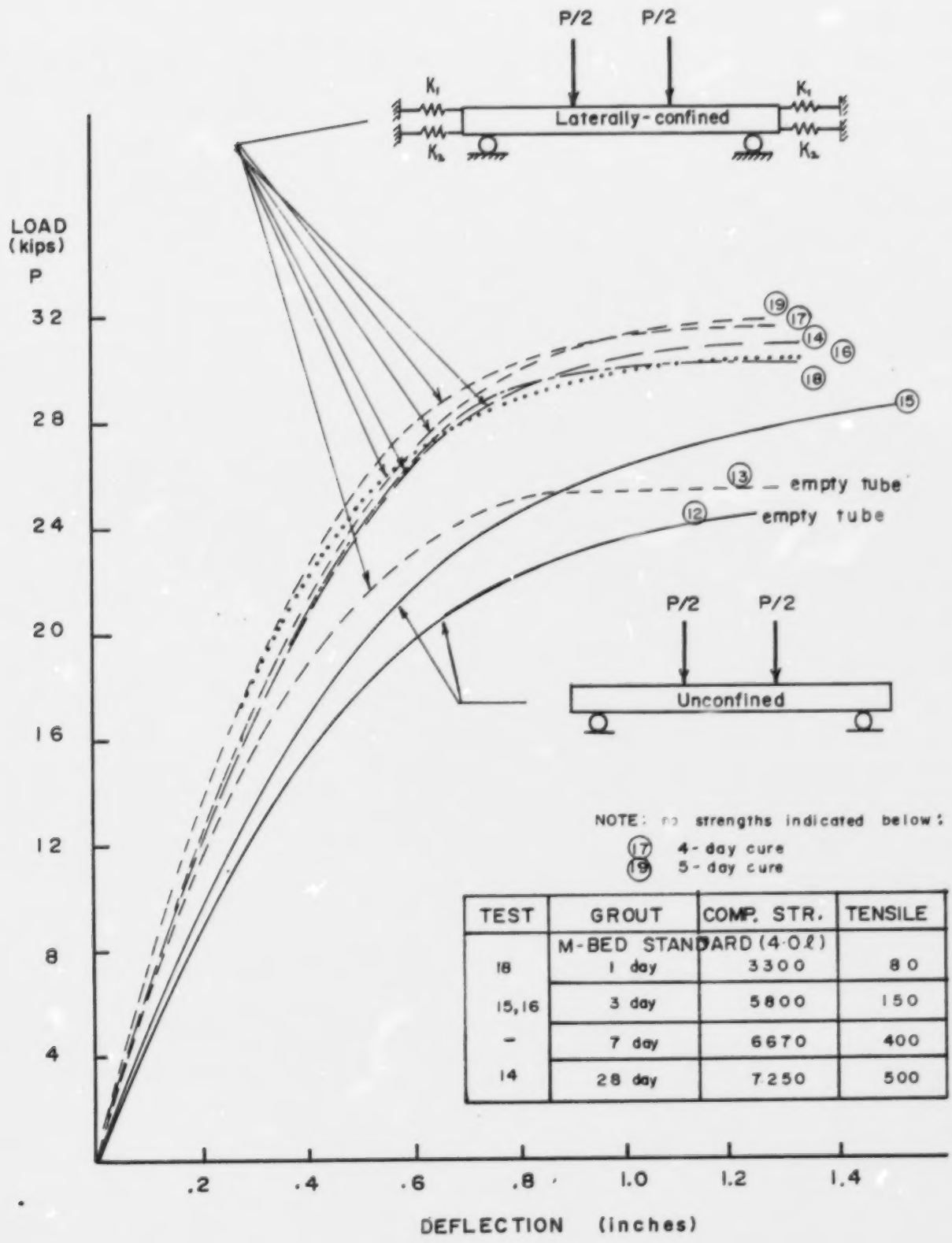

NOTE: 28 strengths indicated below:
17 4-day cure
19 5-day cure

TEST	GROUT	COMP. STR.	TENSILE
	M-BED STANDARD (4·0ℓ)		
18	1 day	3300	80
15,16	3 day	5800	150
–	7 day	6670	400
14	28 day	7250	500

FIGURE 4·12 BEAM DEFLECTION FOR LATERALLY-CONFINED VS. UNCONFINED COMPOSITE BEAMS – GROUT FILLED HSS SECTION

identified in Figure 4.12. It would also appear that the elastic (proportional) limit of the beam has been extended in these tests. The shift of the elastic curve to the left indicates a significant stiffening of the beam member. This factor may be attributed to the increased action of the grout to resist bending through the introduction of thrust forces (due to the induced pressure arch) in the grout with the laterally confined beam in bending; however, such a conclusion would require more extensive testing than was conducted in this study.

4.6 Theoretical Analysis of Laboratory Testing Through Engineering Mechanics of Beam Structures

4.6.1 One and three-point bend tests

Based on standard beam tests for one and three point loading (ASTM C293-79 and C78-84 respectively) centre-point deflections in the beam can be determined within the elastic range by the following formulae:

$$\Delta 1/_2 = \frac{PL^3}{48EI} \quad \text{- one point test}$$

$$\Delta 1/_2 = \frac{23PL^3}{648EI} \quad \text{- three point test (note: the total load on the beam is 2P)}$$

where: P = load on beam (lbs)

L = Span of beam (inches)

E = modulus of elasticity of material (psi)

I = moment of inertia of beam (in^4)

$\Delta l/_2$ = centre-point deflection (in)

The centre-point bending moment and shear values for the simply supported beam subjected to bending are shown in Figure 4.13 for both the one-point and three-point tests, and are as follows:

$$Mc = \frac{Pl}{4} \text{ - one point test}$$

$$Mc = \frac{Pl}{3} \text{ - three point test}$$

Several observations of this analysis are now discussed. In the one-point simply supported beam test the location of maximum bending moment and maximum shear stress coincide. This fact means that the stresses exerted on the centre-point beam fibres in a one-point test are a combination of bending moments and shear stresses. In comparison the three-point simply supported beam is in a state of pure bending (ie. no shear or axial force) at the centre point. The maximum

SIMPLE BEAM—CONCENTRATED LOAD AT CENTER

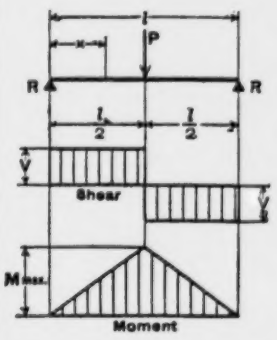

Equivalent Tabular Load . . . . . $= 2P$

$R = V$ . . . . . $= \frac{P}{2}$

M max. (at point of load) . . . . . $= \frac{Pl}{4}$

M_x (when $x < \frac{l}{2}$) . . . . . $= \frac{Px}{2}$

$\Delta max.$ (at point of load) . . . . . $= \frac{Pl^3}{48EI}$

Δ_x (when $x < \frac{l}{2}$) . . . . . $= \frac{Px}{48EI}(3l^2 - 4x^2)$

SIMPLE BEAM—TWO EQUAL CONCENTRATED LOADS SYMMETRICALLY PLACED

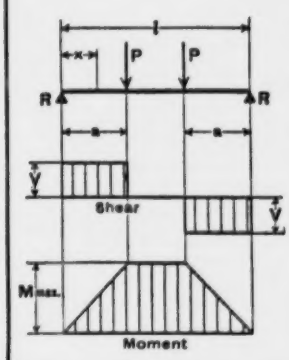

Equivalent Tabular Load . . . . . $= \frac{8Pa}{l}$

$R = V$ . . . . . $= P$

M max. (between loads) . . . . . $= Pa$

M_x (when $x < a$) . . . . . $= Px$

$\Delta max.$ (at center) . . . . . $= \frac{Pa}{24EI}(3l^2 - 4a^2)$

Δ_x (when $x < a$) . . . . . $= \frac{Px}{6EI}(3la - 3a^2 - x^2)$

Δ_x (when $x > a$ and $< (l-a)$) . . $= \frac{Pa}{6EI}(3lx - 3x^2 - a^2)$

FIGURE 4·13 LOADING, SHEAR & MOMENT DIAGRAMS

(Canadian Institute of Steel Construction, CISC)

bending moment which can be sustained by the three-point loaded beam has been previously defined for the elastic analysis to be:

$$M = \frac{\sigma max\ I}{C} \text{ or } M = \sigma max\ S$$

where σmax - maximum fibre stress (psi)

I - moment of Inertia (in^4)

C - distance from neutral axis to extreme fibre of beam (in)

S - section modulus (in^3)

It is recognized that in the one-point bend test the shear force and bending moment coincide at the centre of the beam. It is emphasized that the normal stress induced into the beam in bending as calculated by the equation above are not greatly altered by the presence of the shear stresses. Thus it is justifiable to use the theory of pure bending to calculate the normal stresses in the case of non-uniform bending and it is the accepted practice to do so (Timoshenko, 1968).

4.6.2 Laterally constrained beam tests

The tests conducted using the laterally constraint test frame are not evaluated analytically as a mathematical model is not available for this frame.

The proposed schematic for this testing system is given in Figure 4.14. If the tie rods in the test frame (modelled with springs in Figure 4.14) were infinitely stiff, this test would very closely approximate the rigid-end beam, Figure 4.14. As an approximation for the laterally confined beam the shear, bending moment and deflection of a rigid-end beam in three-point loading will be used. The beam diagram and formulae for shear forces, bending moment and deflection for a three-point load of a laterally confined beam are shown in Figure 4.15, and state that centre-point deflection in the elastic range is defined by the following formula:

$$\Delta l/_2 = \frac{5PL^3}{648EI}$$

and the centre-point bending moment (which is in pure bending) is defined by the following formula:

$$M \text{ (centre-point)} = \frac{PL}{9}$$

4.6.3 Theoretical prediction of beam performance

Based on the preceding deflection and bending moment formulae, for the one-point and three-point flexure tests for simply supported beams and for the three-point flexure test for a rigid-end beam,

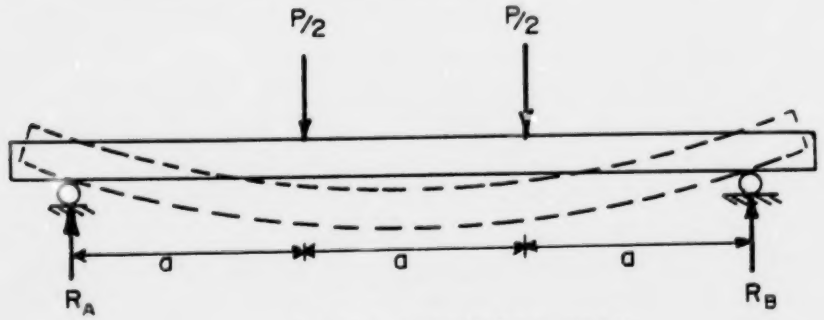

SIMPLY SUPPOPTED BEAM

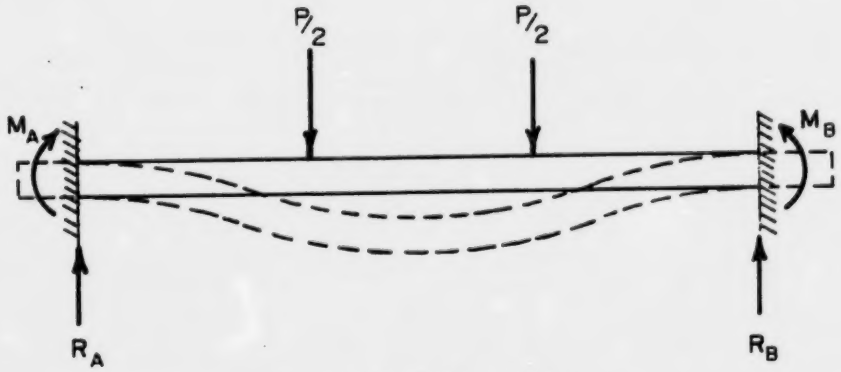

RIGID-END BEAM

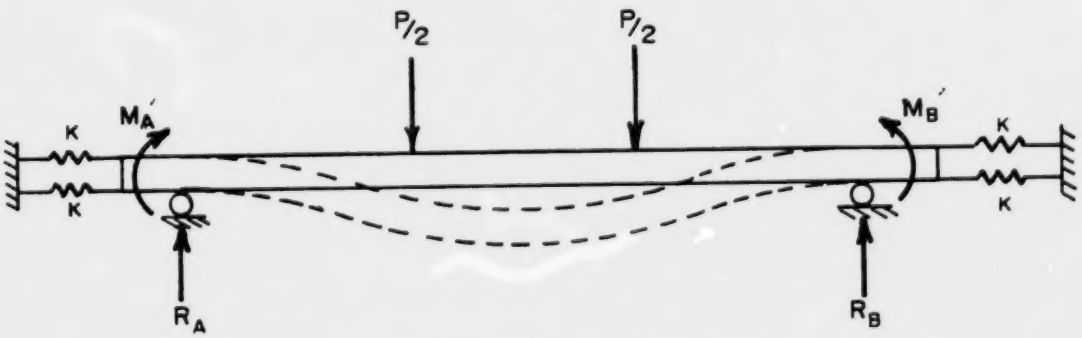

LATERALLY-CONFINED BEAM

FIGURE 4·14 LATERALLY-CONFINED BEAMS AND SIMILARITIES TO RIGID-END BEAMS

BEAM FIXED AT BOTH ENDS—CONCENTRATED LOAD AT ANY POINT

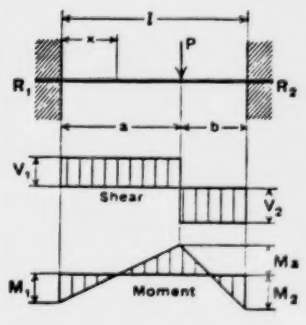

$R_1 = V_1$ (max. when $a < b$) . . . $= \frac{Pb^2}{l^3}(3a + b)$

$R_2 = V_2$ (max. when $a > b$) . . . $= \frac{Pa^2}{l^3}(a + 3b)$

M_1 (max. when $a < b$) . . . $= \frac{Pab^2}{l^2}$

M_2 (max. when $a > b$) . . . $= \frac{Pa^2b}{l^2}$

M_a (at point of load) . . . $= \frac{2Pa^2b^2}{l^3}$

M_x (when $x < a$) . . . . . $= R_1x - \frac{Pab^2}{l^2}$

$\Delta max.$ (when $a > b$ at $x = \frac{2al}{3a+b}$) . $= \frac{2Pa^3b^2}{3EI(3a+b)^2}$

Δa (at point of load) . . . $= \frac{Pa^3b^3}{3EIl^3}$

Δx (when $x < a$) . . . . . $= \frac{Pb^2x^2}{6EIl^3}(3al - 3ax - bx)$

THREE-POINT BENDING - RIGID ENDED

(derrived from above by method of superposition)

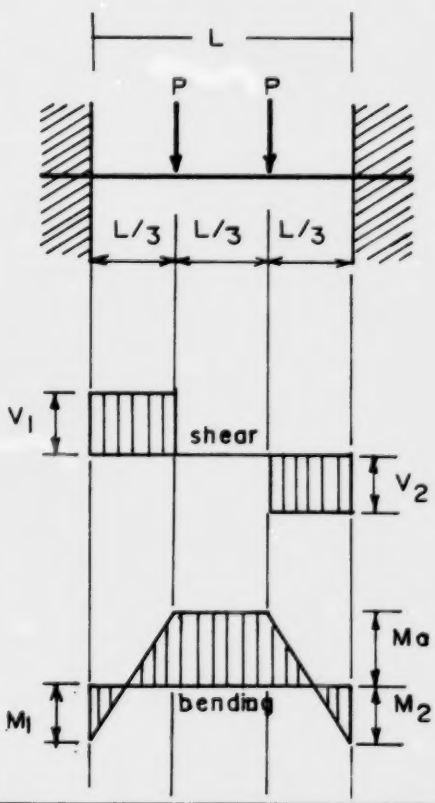

$$R_1 = R_2 = P$$

$$V_1 = V_2 = P$$

$$M_{max\ (ends)} = \frac{2PL}{9}$$

$$M_a(centre) = \frac{PL}{9}$$

$$\Delta max\ (centre) = \frac{5PL^3}{648EI}$$

FIGURE 4·15 LOADING, SHEAR & MOMENT DIAGRAMS FOR RIGID BEAM (CISC)

theoretical estimates for the beam performance (elastic) are determined. Within this theoretical analysis several criteria have been used:

- Maximum Fibre Stress: σmax = 24,000 psi

  (recommended by Proctor and White, 1968 for cold worked steel for elastic analysis of tunnel rib supports). Note:

  $\sigma yield$ = 32,000 psi

  $\sigma ultimate$ = 60,000 psi

- transposed areas of composite beams used

  $n = \frac{E_s}{E_c} = 15$

  (recommended by Thimoshenko, 1968)

The theoretical predictions of load/deflection for the beams to be evaluated in laboratory testing are conducted for the following situations:

. One-Point loading, Simply Supported
  - empty HSS beam
  - grout filled HSS (Transformed Section)
  - Cases I, II & III (section 4.1.1)

. Three-point loading, simply supported
  - empty HSS
  - grout filled HSS (Transformed Section)
  - Cases I, II & III (Section 4.1.1)

. Three-point loading, LATERALLY CONSTRAINED

- Empty HSS
- grout filled HSS Cases I, II (section 4.1.1)

The results of these estimates are given in Tables 4.1a,b and c, consecutively. The results are also plotted in Figures 4.16.

The results of these estimates are given in Tables 4.1a,b and c, consecutively. The results are also plotted in Figures 4.16.

4.7 Comparison of the Composite Beam Theoretical Predictions Versus Test Results of Composite HSS Beams

To provide a comparison between the laboratory testing and the theoretical predictions of beam performance made in Section 4.6; the following analysis is conducted. The performance of 'EMPTY' HSS beams (laboratory versus theoretical) are compared initially to serve as a control point for subsequent comparisons. The performance of the empty beam structures should be highly predictable and serve to confirm the accuracy of the bending tests conducted in the laboratory. Following this analysis, comparisons are made between the laboratory bend test results for the composite beam structures and the CASE I, CASE II,

Table 4.1a. Theoretical Beam Performance For Beams * In 1-Point Loading

Load (pounds)	Center-Point Deflection (inches) $\left[\Delta 1/2 = \frac{Pl^3}{48EI}\right]$			
	Empty Beam	Grout Filled Beams		
		CASE I	CASE II	CASE III
	$I = 6.9\ in^4$ $S = 2.76\ in^3$	$I = 7.79\ in^4$ $S = 3.12\ in^3$	$I = 7.29\ in^4$ $S = 2.91\ in^3$	$I = 8.08\ in^4$ $S = 3.23\ in^3$
1,000	.0218	.0193	.0206	.0186
2,000	.0435	.0385	.0412	.0371
3,000	.0654	.0578	.0618	.0557
4,000	.0870 +	.0770	.0823	.0743
5,000	.1090	.0965 +	.1030 +	.0930 +
6,000	.1305	.1155	.1235	.1114
8,000	.1740	.1540	.1646	.1485
10,000	.2175	.1925	.2058	.1856
Bending Moment at Centre Point $M = \sigma max \cdot S$	66,240	74,880	69,840	77,520
Maximum Load $P = 4\ \frac{Mc}{I}$	4,416	4,992	4,656	5,168

*All beams are analysed for a beam length l = 60 inches
+limit of elastic analysis with maximum fibre strength of steel = 24,000 psi

Table 4.1b. Theoretical Beam Performance For Beams In Three Point Loading

Load* (2P)	Center-Point Deflection (inches) $\left[\Delta 1/_2 = \frac{23Pl^3}{648EI}\right]$			
	Empty Beam	Grout Filled Beams		
		CASE I	CASE II	CASE III
	$I = 6.9\ in^4$ $S = 2.76\ in^3$	$I = 7.79\ in^4$ $S = 3.12\ in^3$	$I = 7.29\ in^4$ $S = 2.91\ in^3$	$I = 8.08\ in^4$ $S = 3.23\ in^3$
1,000	.0185	.0164	.0175	.0158
2,000	.0370	.0328	.0351	.0316
3,000	.0556	.0492	.0526	.0474
4,000	.0741	.0656	.0701	.0633
5,000	.0926	.0820	.0876	.0791
6,000	.1111	.0984	.1052	.0949
7,000	.1296←	.1140	.1227←	.1107
8,000	.1481	.1312 ←	.1402	.1265 ←
Bending Moment at Centre Point $Mc = \sigma max \cdot S$	66,240	74,880	69,840	77,520
Maximum Load $P = 4\ \frac{Mc}{I}$	3,312	3,744	3,492	3,876

*Total Load on the beam = 2P

←limit of elastic analysis with maximum fibre strength of steel = 24,000 psi

Table 4.1c. Theoretical Beam Performance For Beams In Laterally Confined Beam Test (Simulated By Rigid-Ended Beam, 3-Point Loading)

Loads* (pounds) (P)	Center-Point Deflection (inches) $\left[\Delta 1/2 = \frac{5Pl^3}{648EI}\right]$		
	Empty Beam	Grout Filled Beams	
		CASE I	CASE II
	$I = 6.9\ in^4$ $S = 2.76\ in^3$	$I = 7.79\ in^4$ $S = 3.12\ in^3$	$I = 7.29\ in^4$ $S = 2.91\ in^3$
2,000	.0162	.0142	.0152
4,000	.0324	.0284	.0304
6,000	.0486	.0426	.0456
8,000	.0648	.0568	.0608
10,000	.0810 +	.0710	.0760 +
12,000		.0852 +	.0912
Bending Moment at Centre Point $Mc = \sigma max \cdot S$	66,240	74,880	69,840
Maximum Load $P = \frac{9M}{I}$	9,936	11,232	10,476

*Total Load on the beam = P

+limit of elastic analysis with maximum fibre strength of steel = 24,000 psi

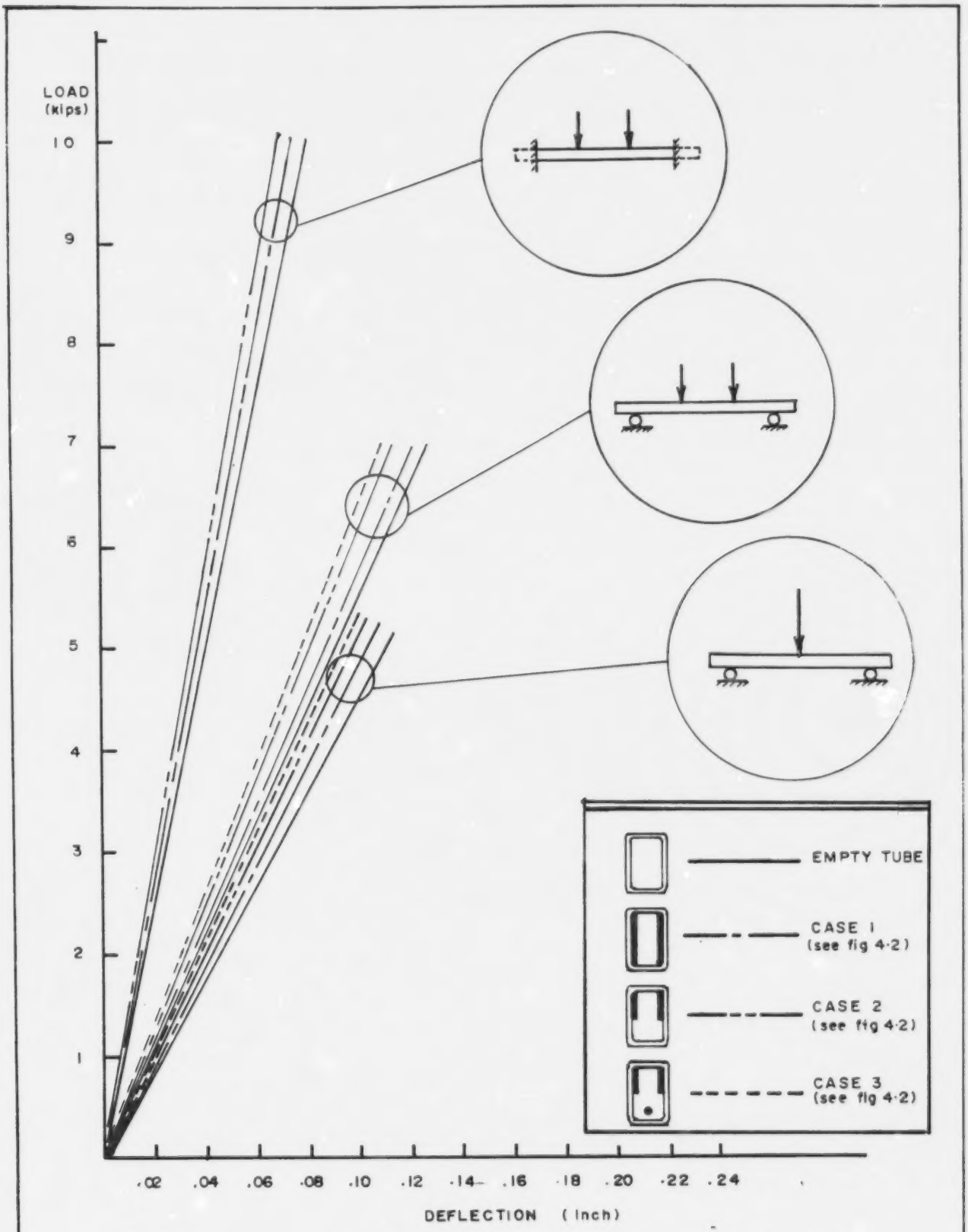

FIGURE 4·16 THEORETICAL LOAD vs. DEFLECTION (ELASTIC) CURVES FOR HSS SECTIONS UNDER STUDY

CASE III theoretical models for composite beam performance proposed in Section 4.1.1. This analysis should confirm which of the proposed models is applicable, if in fact the composite beam theory can be used to predict the performance of a grout filled HSS beam member.

4.7.1 Comparison of empty beam performance

A plot of the theoretical predictions and laboratory test results for the empty beam structure is given in Figure 4.17. It can be concluded from this comparison that the one and three-point bend tests performed on the simply supported empty HSS beams conform with the theoretical predictions. It is noted that the slight variance of the three-point simply supported bend test to the theoretical prediction is likely produced by the use of only one beam member for this test. A series of tests would likely generate results that conform more precisely to the theoretical analysis.

The performance of the laterally constrained empty HSS beam does not correspond with the predicted rigid-end beam structure initially proposed to model this unique beam member. In so far as no better standardized model for beam theory exists to predict

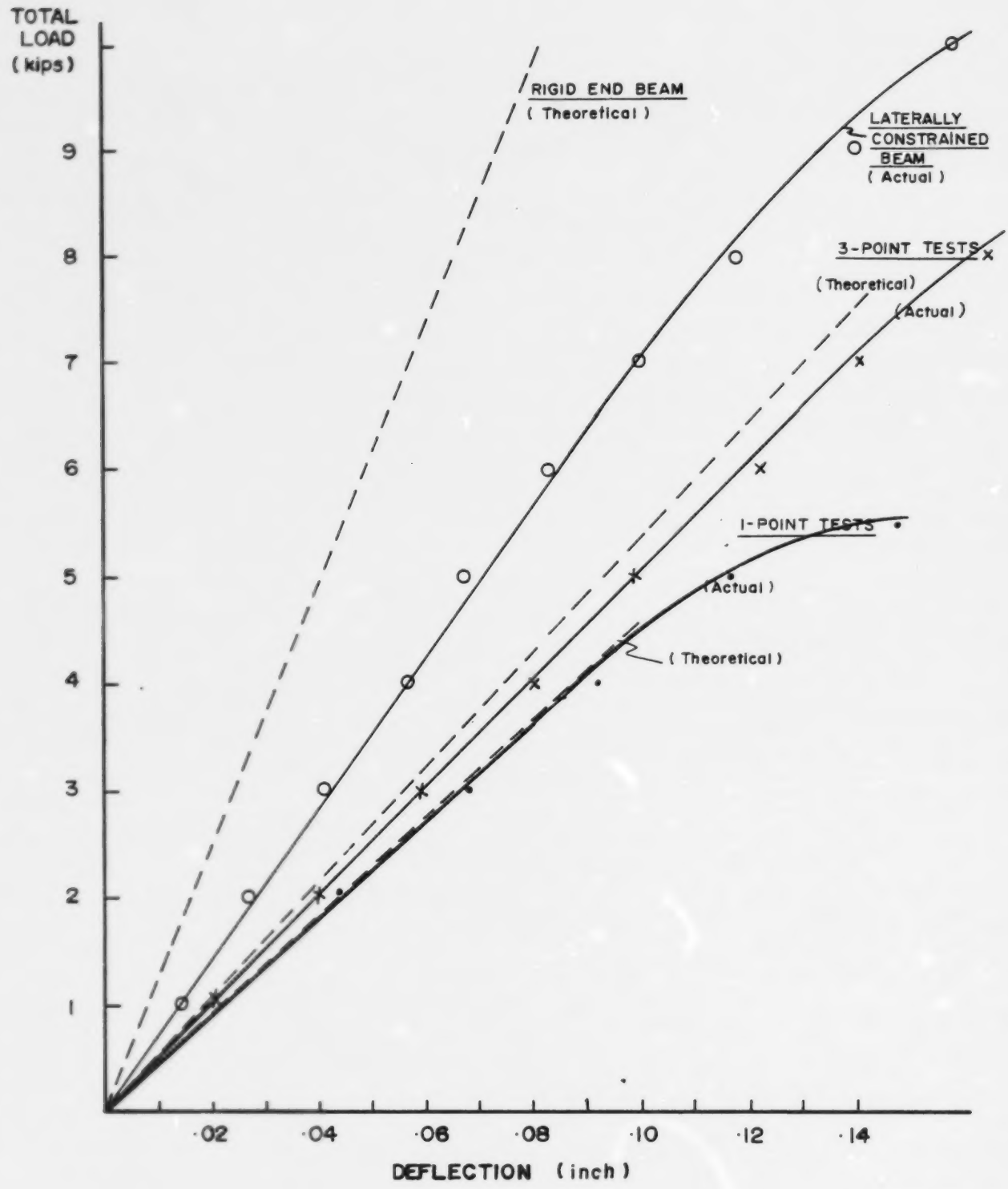

FIGURE 4·17 – COMPARISON OF THEORETICAL PREDICTIONS AND ACTUAL BEND TEST RESULTS ON EMPTY HSS BEAMS WITHIN THE ELASTIC RANGE

the performance of the laterally constrained beam, it is considered unlikely that this beam member can be analytically modelled without extensive testing and standarization of the developed test jig.

4.7.2 Comparison of grout filled HSS beam performance (theoretical predictions vs. test results).

A plot of the results from composite HSS beam tests (3-day cure M-Bed grout core) are shown in Figure 4.18 in conjuction with the theoretical predictions for CASE I and CASE II scenarios as established in Section 4.1.1 of this report. In both the one and three-point simply supported bend tests the composite beam performed below what is predicted by either the CASE I or CASE II theoretical models. It is also noted that for the one-point bend tests within the elastic range of the beam there is no difference in the performance of the beam with or without the grout core.

However, for the three-point bend test there is a noticable stiffening of the beam member with a grout core compared with the empty beam within the elastic range.

The laterally constrained grout filled beam demonstrates a significant stiffening of the beam

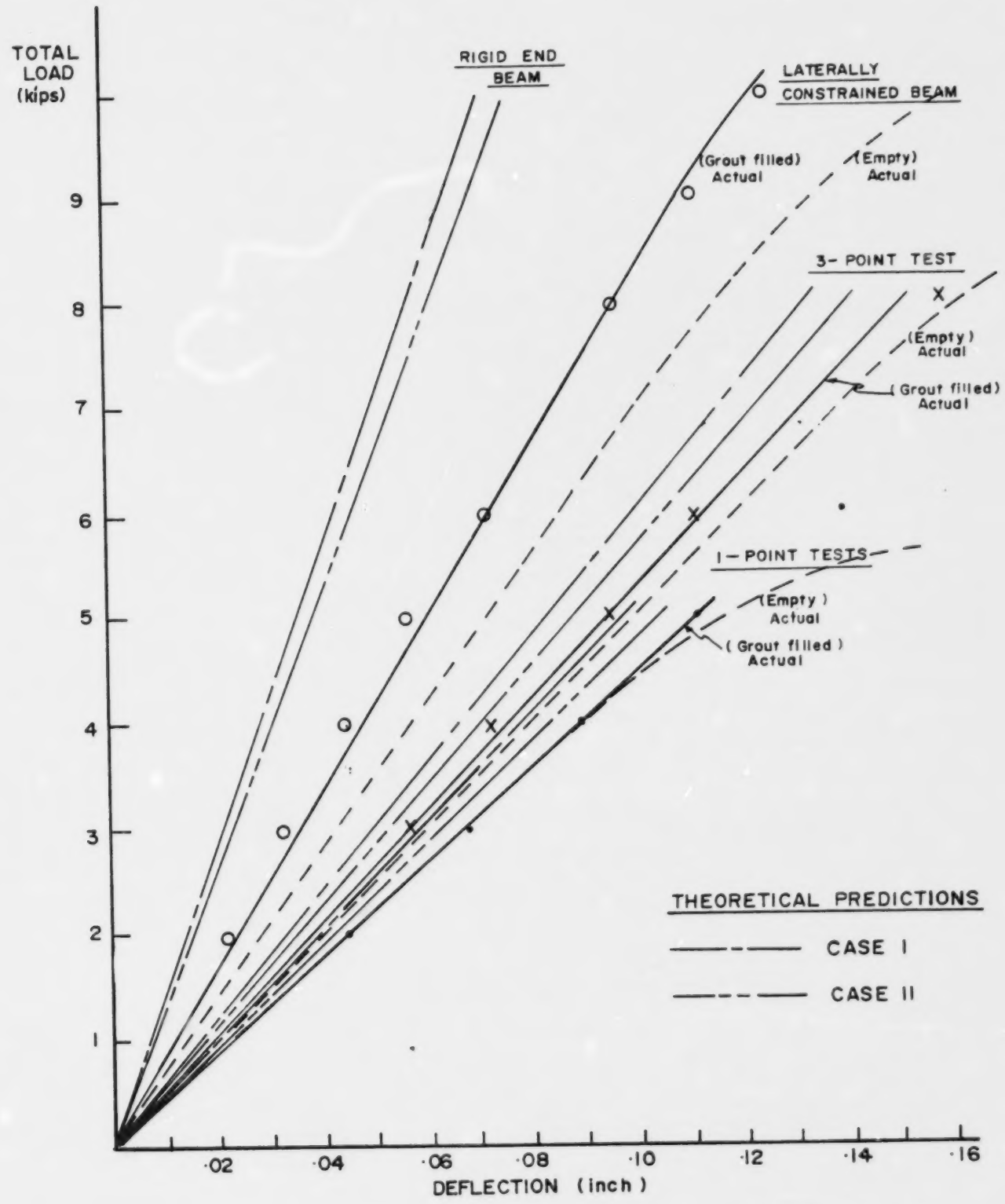

FIGURE 4·18 — COMPARISON OF THEORETICAL PREDICTIONS AND ACTUAL BEND TESTS ON GROUT FILLED HSS COMPOSITE BEAMS WITHIN THE ELASTIC RANGE

within the elastic range compared with the empty HSS. The actual test results do not compare with the CASE I, CASE II models proposed for the laterally constrained grout filled beam. This fact is to be anticipated as the rigid-end beam model proposed for the empty HSS section was noted to be an unsuitable model.

4.7.3 Comparison of theoretical predictions vs test results for reinforced, grout filled HSS beams

The theoretical model proposed for the reinforced grout filled HSS beam in a one-point bend test is plotted with the laboratory bend test results in Figure 4.19. The actual test results are lower than the theoretically predicted performance for the beam.

4.7.4 Conclusions on the proposed theoretical models for composite HSS beam performance.

Based on the preceding discussion of the actual versus theoretical beam performance it is concluded that an accurate prediction of the beam performance in the elastic range cannot be made by the transformed material theory for composite beam structures. This conclusion is likely due to the fact that there is poor bonding of the grout core to the steel, which is a prerequisite of the composite beam theory. It is

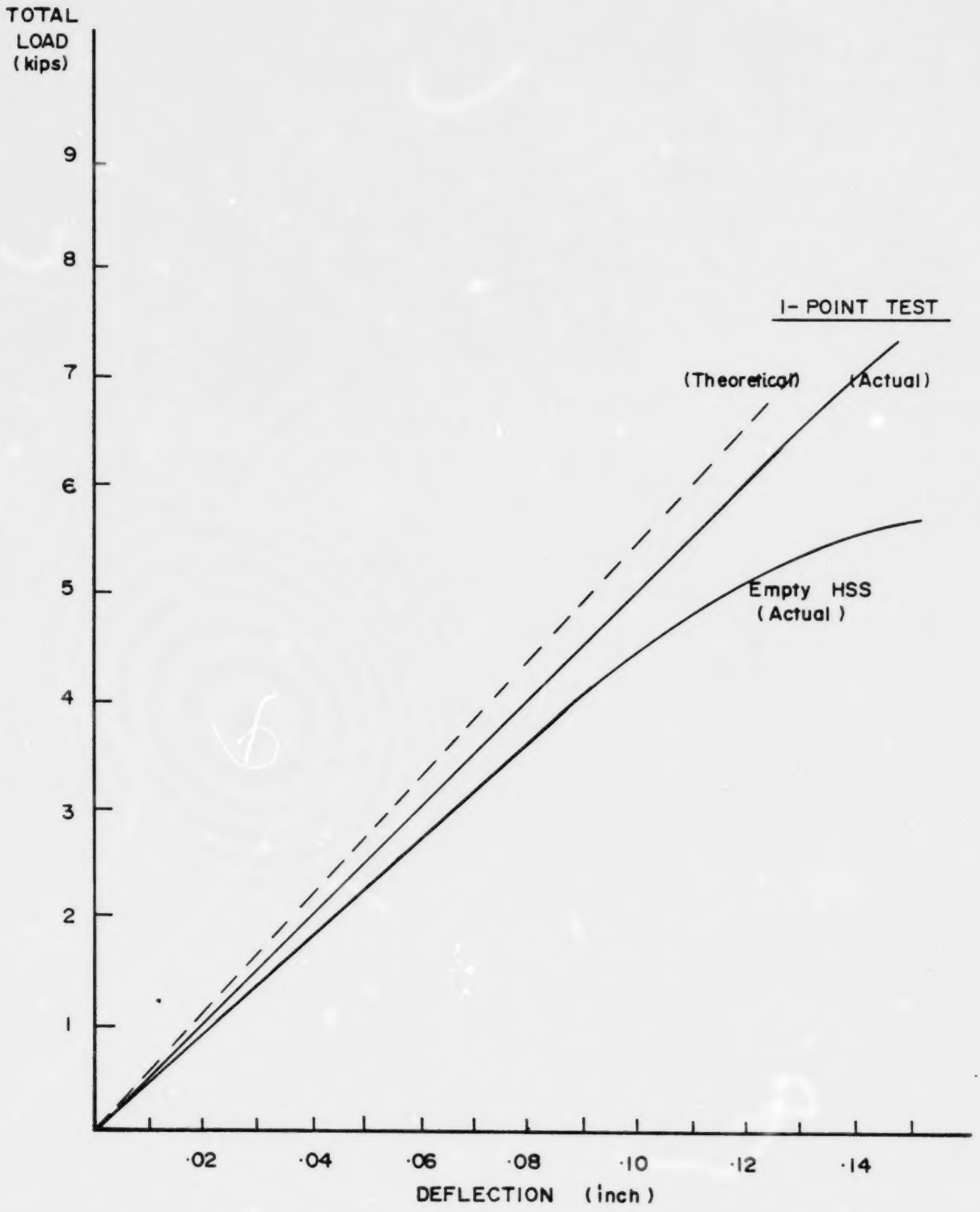

FIGURE 4·19— COMPARISON OF THEORETICAL PREDICTIONS AND ACTUAL BEND TEST ON GROUT FILLED HSS BEAMS WITH 1/2" ø REBAR (WITHIN THE ELASTIC RANGE)

commented that the theoretical beam model which comprehends only the grout core which is subjected to compressive forces, CASE II, is the more accurate model to use if a preliminary estimate of composite HSS beam performance is required. It is cautioned however, that the anticipated beam strengths will be overestimated by this composite beam design technique.

Based on the lack of correlation between the theoretical and actual beam performance in the 'elastic' range, it is considered unjustified to conduct a theoretical vs actual 'plastic' beam analysis.

It is concluded that the performance of a grout filled HSS beam cannot be predicted by the composite beam theory of engineering mechanics. To establish design criteria for elastic and plastic zones of the composite HSS beam extensive testing of this unique composite beam, is required. This conclusion is consistent with the extensive testing and development of design criteria for concrete filled HSS column structures as developed by CIDECT and previously discussed in Section 3.0 of this report. Such testing is considered well beyond the limits of this current work.

4.8 Comparison of the Collapse Loads for Simply Supported RSJ Beams and for Composite HSS Beams

It has been previously discussed that civil engineering tunnel support design is based on elastic theory whereas mining support design is based on plastic deformation and ultimate loads. Considering the negligible improvement in beam performance within the elastic range of the one-point tests for the composite beam member, its application in the civil engineering field is considered unlikely. However, within the mining discipline it is quite possible that such a beam member may have an application. For the one size of HSS beam investigated the following comparison can be made for a 1524 mm (5 ft.) span, simply supported beam with centre-point load.

Beam Section (mm)	Section Modulus (10^3 mm^3)		Wt per Linear m (kg)	Ultimate One-point Load (kN)
	Sxx	Syy		
89x89 RSJ	67.4	22.4	19.35	87.6*
Empty 127.x50.8 HSS (test 1)	58.9	26.4	12.2	80.3**
Composite 127.x50.8 HSS	-	-	12.2	
3 day (test 20)				89.0**
28 day (test 21)				90.1**

* Newson, 1985

** Laboratory Testing ($\frac{\text{Pounds} \times 4.448}{1000}$ = kN)

It is pointed out that with a weight reduction of 7.15 kg per metre of the subject beam (37%), a centre-point ultimate load increase of 2.6 kN (3%) has been achieved with the grout filled HSS beam. The ultimate load of the grout filled HSS beam is 12% higher than for the empty HSS.

In a three-point load situation on simply supported beam structures the following formulae are extended from Elastic and Plastic Beam theory to predict maximum loads:

$$\text{Yield Load (kN)} = \frac{\text{Section Modulus } (cm^3) \times 1530}{\text{span (mm)}}$$

(Elastic Theory)

$$\text{Collapse Load (kN)} = \frac{\text{Section Modulus } (cm^3) \times 2967}{\text{span (mm)}}$$

(Plastic Theory)

These formulae are developed in the same form as presented by Newson, 1985; presented in Section 2.2. The collapse load of a simply supported RSJ (89x89 mm) beam is compared with the empty and composite HSS beams results in three-point loading as follows:

Beam Section (mm)	Plastic Modulus ($10^3 mm^3$) Zxx	Zyy	Wt per Linear m (kg)	Ultimate One-point Load (KN)
89x89 RSJ	77.5	25.8	19.35	131.2*
Empty 127.x50.8 HSS (test 12)	58.9	30.9	12.2	109.0**
Composite 127.x50.8 HSS	-	-	12.2	
3 day (test 15)				129.0**
28 day (test 11)				129.0**

*Calculated by Plastic Theory
**Laboratory Testing ($\frac{\text{Pounds} \times 4.448}{1000} = \text{kN}$)

The results of this comparison indicate that for three-point load tests, the grout filled HSS beam structure provides approximately the same ultimate support capacity (1.7% less) as the 89x89 mm RSJ; however, the HSS beam structure is considerably lighter weight for installation (37% lighter). These results are very similar to those determined for the one-point simply supported beam tests. The ultimate load capacity of the grout filled HSS is 18.3% greater than for the empty HSS. This value is significantly lower than the 50% increased bending strength obtained in the Kato work. This variation can possibly be explained by the rectangular section investigated herein versus the circular pipe section used in the Kato work; however, further work is required to substantiate this conclusion.

5.0 EVALUATION OF THE COMPOSITE HSS BEAM MEMBER FOR MINE SUPPORT

The evaluation of the potential to use a grout filled HSS section for mine support installations has been conducted using a single size HSS beam. This work concluded that it was possible to achieve a support load equivalent to a comparable RSJ with a 37% reduction in the installation weight. To extrapolate this weight reduction factor to any other size grout filled HSS section other than the one which was evaluated is unjustified without further testing. Without this weight reduction factor it is not possible to estimate comparative operating and material costs of tubular HSS and conventional RSJ steel support systems.

However, unit material costs for conventional RSJ steel (not fabricated or rolled) and HSS steel section is indicative of the material costs to be anticipated.

Conventional RSJ steel - $0.39 per lb of steel

Tubular HSS steel - $0.45 per lb of steel

This costing representing a 15% increase in cost per unit weight for HSS steel sections compared with conventional RSJ steel sections.

It is also very difficult to make the comparison of the HSS vs RSJ supports because each 'heavy' RSJ installation is unique. Heavy RSJ sections are designed for specific cases and to estimate the material and operating costs would require a case by case investigation.

In spite of the difficulty to conduct a detailed cost comparison at this time, it is appropriate to indicate that suitable technology does exist to make the composite tubular support member adaptable as a mine support member. In particular, it is required that assembly of the tubular section support and strutting of the support members be accomplished in the mine environment.

5.1 Assembly of Tubular Supports

Fabrication of tubular supports would necessarily require the following:

- filling and bleeding points for the tubular structure,
- tubular to tubular connection for sections which must be joined,
- end caps on open ends of the support to retain the grout,

- vent holes to relieve the potential for an explosion in the event of a fire.

Filling points for the tubular support member can be fabricated by drilling a hole in the tubular section and welding a pipe nipple over this hole. The outside thread on the pipe nipple serves to couple a pipe union on the grout line to the tubular for grout filling and to thread on a pipe cap following the grout filling procedure. Grout filling points should be fabricated at the lowest point of the support member and bleed points at the highest. Tubular filling should be done from the bottom of the support to the top to displace the air inside the tube and thus prevent air gaps in the grout core of the composite support member. Bleed points being at the top of the support member would not require capping and therefore a hole drilled in the tubular structure would be sufficient. If desired, a pipe nipple and cap could be used to seal this hole.

Tubular to tubular connections would be necessary where long tubular sections supports are required. A standard welded end-plate connection used in concrete filled steel tubular columns is shown in Figure 5.1 and could be adopted for this purpose. The requirements for this connection are that it be

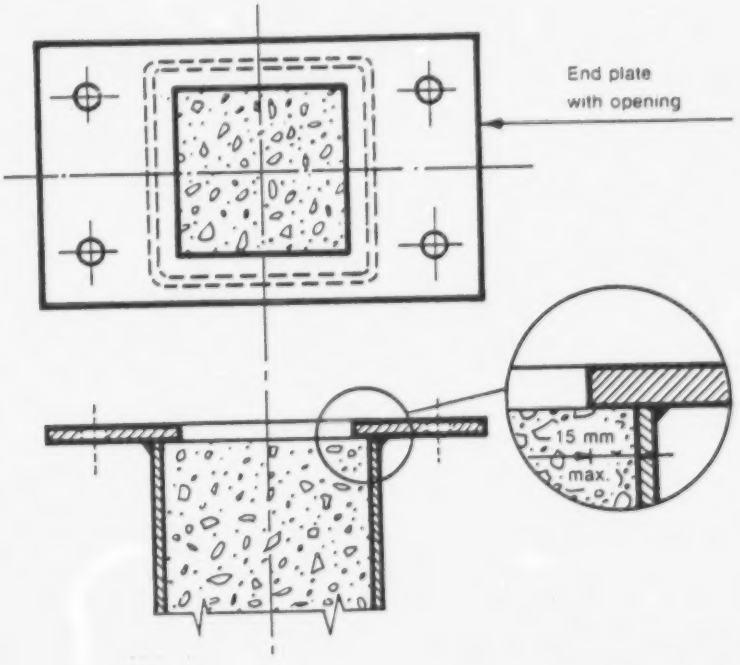

FIGURE 5·1 WELDED END-PLATE CONNECTIONS FOR TUBULAR TO TUBULAR JUNCTIONS (CIDECT)

water-tight and that the connection permit complete filling of the tubular. For composite column members, the restriction on complete filling requires that the welded plate protrude into the grout core not more than 15 mm as shown in Figure 5.1. It is emphasized that this flanged connection would have to be designed to withstand bending stresses not comprehended in the composite column work previously mentioned.

All open end tubular support sections must be end capped to contain the grout. This would include the bottom of the columns on an arch member or the ends of a 'square work' support. This cap would be a welded end plate.

Vent holes are required for all grout (concrete) filled tubular members to permit the escape to steam from the grout core in the event of a fire. Extreme pressures can be generated inside those composite structure which can result in the explosion of the member. This is prevented by providing vent holes to permit the steam to excape. These holes can be drilled in the steel following the filling with grout. If the vent holes were drilled prior to grout filling it would be necessary to cap them until the grout core had set. Based on composite column design work, vent holes need only be small diameter (10 to 15 mm), and should be

placed at least 100-200 mm from the ends of the support and at 2 m intervals in the support.

5.2 Strutting of Tubular Supports

It is a recognized fact that RSJ supports require strutting to prevent lateral movement of the support along the axis of the tunnel. Strutting is a very important function in RSJ supports. This requirement is a result of the low section modulus (Syy) for the RSJ profile that resists 'roll-over' of the support. One major advantage of a composite tubular support is that a tubular section could be used that would provide a much larger Syy-Section Modulus with a very limited increase in the empty tube installation weight, (i.e. select a square section tube not a rectangular section).

Even with the potential to increase the Syy, it may still be necessary to provide struts. Standard welded T-flange connections Figure 5.2 could be used to bolt on angle iron struts. Alignment of these struts would likely present a problem and a flexible sliding connector would possibly provide an improved method of strut connection. This sliding strut connection would

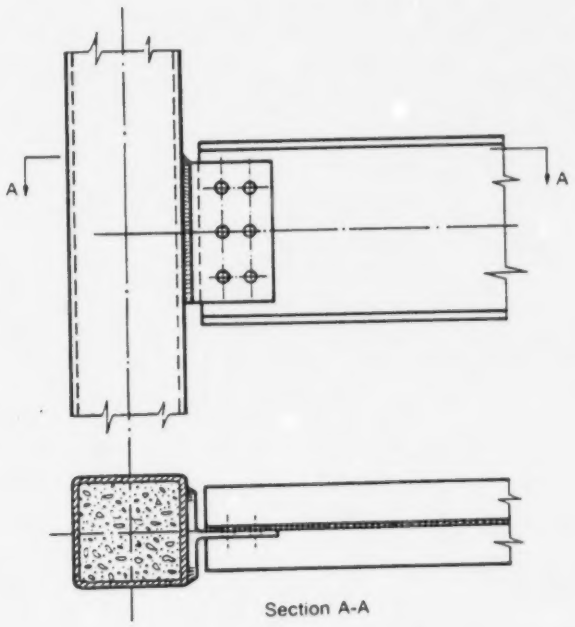

T - CONNECTION

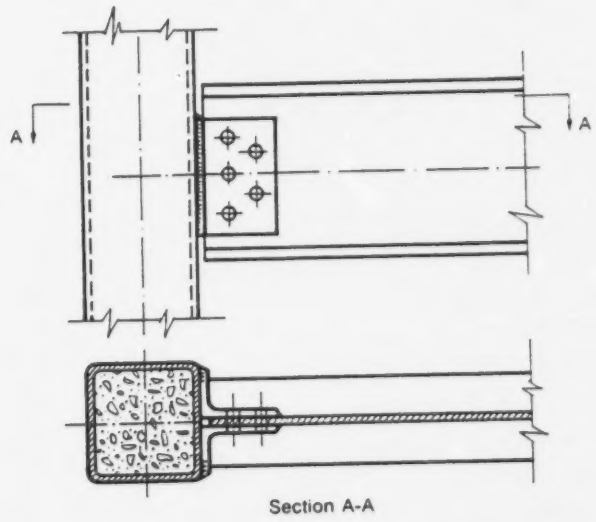

DOUBLE ANGLE CONNECTION

FIGURE 5·2 STANDARD BEAM CONNECTIONS TO CONCRETE FILLED HSS COLUMNS (CIDECT)

comprise two wrap around U-shaped steel sections that could be bolted together around the tubular section and secured after it was adjusted to the proper location on the support.

6.0 CONCLUSIONS

The investigation of grout filled hollow structural steel beam members was conducted using a single size HSS section to ensure standardization of the test results. Based on the performance of the grout filled HSS sections tested it was concluded that the grout filled 127. x 50.8 x 4.78 mm (wall) HSS provided the same ultimate (collapse) load as an 89 x 89 mm RSJ beam in simply supported one and three-point bend tests. The empty HSS section represents a 37% reduction in installation weight compared with the equivalent strength RSJ beam. Based on the equivalent load capacity of the two beam structures, no change in support density is anticipated for the grout filled HSS beam investigated.

A material cost estimate indicated that the subject HSS beam represents a 15% increase in cost per unit weight of steel over the conventional RSJ steel. However, with a 37% weight reduction for the HSS beam there would be a net reduction in steel costs for a equivalent strength beam. This cost saving would likely be sufficient to offset the cost of the grout core in the composite HSS beam. No prediction is made on the labour savings for the installation of the lighter weight HSS beam as this estimate must be costed

on the basis of individual installations, and cannot be generalized for the purpose of this report.

This investigation did not attempt to optimize the design for the grout filled HSS beam. This work would require more extensive testing and further evaluation of the composite beam action.

The attempt to model the beam performance in the elastic range of the grout filled HSS beams by the transformed material composite beam theory was not successful. It was concluded that this technique could not be used for the composite beam performance calculations. Extended tests would be required to develop a criterion which could be used for grout filled HSS composite beam theoretical design.

A review of the current technology for tubular to tubular connections indicated that 2 and 3 piece tubular support structures could be erected in the mine opening and then grout filled. Strutting could be achieved using standard T-flange connections; however, a more flexible strut connection in the form of a two piece sliding flange could be readily designed. The requirement for strutting could be minimized or eliminated by selecting an HSS that would generate a much larger section modulus (Syy) to resist sideway

deformation of the support. This improved lateral strength and possible elimination of struts would further advantage this new composite support member over an equivalent strength RSJ support.

Extended testing of the grout filled HSS section for an arch shaped support member is recommended. The pure bending action of one and three-point tests on a straight beam member subjected the grout core to high tensile stresses for which the grout has very little strength. In an arch structure the grout core would be largely in compression, due to the axial thrust action in the arch, which could result in a very strong support member.

It is concluded from this evaluation of grout filled HSS beam sections that there is potential to develop a unique and new support member for underground mining. Continued testing is required before criteria can be established for the design of these composite support members.

7.0 RECOMMENDATIONS

The investigation conducted on grout filled HSS sections was restricted to straight beam members subjected to pure bending. This loading subjected the grout core to induced tensile loading on the lower half of the core for which the grout material has a very limited strength. Despite the disadvantage imposed on the grout core in pure bending the composite member did generate encouraging results. Investigations could be conducted to further develop a criterion for the optimum design of a 'square work' composite HSS support member. Additional work could also be done using polypropylene and steel fibre grouts which would increase the tensile strength of the grout core up to eight times its normal strength and thereby increase the strength of the composite beam. This conclusion is supported by the limited testing on steel reinforced grout core beams.

In the opinion of the author, it would be much more advantageous if a support profile for the composite beam could be used which would load the grout core in an axial direction not in the transverse direction as is the case with the pure bending tests conducted. The axial loading situation would exist if the composite member profile took the form of an arch or a short radius cambered beam. A review of Section 2.0 of this report will show that for a semi-circular arch which has been suitably blocked, transverse loading of the arch is resolved into a major

compressive thrust component in the axis of the support member, and a much lower magnitude bending moment. This loading situation is referred to as a column-beam member and is identified as a suitable loading mechanism for grout filled HSS sections. Design criteria have been established by CIDECT to predict the performance of grout filled HSS column-beam members; although not for a curved member as is the case with an arch profile.

It is recommended that full scale composite arch sections should be tested to determine the performance of the grout filled HSS beam in a much more compatible loading situation than with a straight beam member. Direct comparison of the composite arch performance with an RSJ arch should be conducted by testing RSJ arches in the same loading situation. It would be advantageous to test several composite arches varying the HSS steel section (a range of Section Moduli for the empty HSS) to predict the performance of the two materials within the composite member. Fibrous grouts could be tested within the arch profile during the full scale tests.

Testing facilities exist in the Timber Structures Laboratory at the Technical University of Nova Scotia (TUNS) to conduct full scale horizontal tests on the arch structures used by the Cape Breton Development Corporation (14 foot splayed-leg arch). This facility consists of a load frame floor with two inch diameter post holes on a two foot grid. Posts inserted in these

holes will be used to block the arch profile during loading to achieve a realistic loading situation. Available space exists on this floor to conduct the full scale arch tests. The necessary hydraulic jacks to load the arches are available at TUNS.

The HSS arch section will require a rolling facility to bend the seven foot radius arch section from straight stock. Such a rolling facility exists at the Dockyard in Halifax and preliminary discussions with Dockyard personnel indicate their cooperation to bend several arches for testing at TUNS. The grout mixing facilites exist and pumping facilities also exits as a result of the current contract to perform the filling of the HSS arches.

In summary, it is recommended to test the composite section in an arch profile, to investigate a much improved loading situation for the composite member. This investigation could generate the opportunity to develop a new underground support technology. It is proposed that these tests be performed at TUNS where existing facilities will minimize the expenditure for such tests to material costs only.

REFERENCES

Biron, C. and Arioglu, E.

1982: Design of Supports in Mines, John Wiley and Sons, p. 61-87.

Choquet, P.

1981: A Failure Criterion of Steel Arch Supports for the Interpretation of Insitu Monitoring Results, proceeding 14th Canadian Rock Mechanics Symposium, Excavation in Surface and Underground Mining Operations, p. 116-122.

Choquet, P.

1984: Design of Steel Arch Supports for Gate Roadways, paper presented at 97th Annual Meeting of the Mining Society of Nova Scotia, June 27-30, 1984.

Furlong, R. W.

1968: Design of Steel-Encased Concrete Beam-Columns Journal of the Structural Division, Proceedings of the American Society of Civil Engineers, Jan. 1968, p. 267-281.

Hoek, E. and Brown, E.

1980: Underground Excavations in Rock, Institute of Mining and Metallurgy, p. 323.

Iyengar, H, et. al.

1979: A specification for the Design of Steel-Concrete Composite Columns, Task Group 20, Structural Stability Research Council, Engineering Journal of American Institute Steel Consruction, Fourth Quarter, p. 101-115.

Jukes, S. G., Hassani, F. and Whittaker, B.

1983: Characteristics of Steel Arch Support Systems For Mine Roadways. Part 1. Modelling Theory, Instrumentation and Preliminary Results, Mining Science and Technology, vol. 1, 1983.

1984: Characteristics of Steel Arch Support Systems For Mine Roadways. Part 2. Effect of Strutting, Mining Science and Technology, vol. 1, 1984, p. 107-121.

Kato, C. et al.,

1981: Steel Pipe with Checkered Projections and its Mechanical Characteristics,

Knowles, R. B. and Parks, R.

1969: Strength of Concrete Filled Steel Tubular Columns, Journal of the Structural Division, Proceedings of the American Society of Civil Engineers, Dec. 1969, p. 2565-2587.

MRDE, NCB

1980: The Development of New and Improved Types of Roadway Support, vol. 1, p. 8.

Newson, S.

1985: The Strength of Roadway Supports, National Coal Board, Headquarters Mining Department, May, 1985.

Peng, S. S.

1978: Coal Mine Ground Control, John Wiley and Sons, p. 406-413.

Proctor, R. and White, T.

1977: Rock Tunnelling with Steel Supports, Commercial Shearing Inc., p. 207-232.

Stelco

1981: Hollow Structural Sections-Design manual for Concrete filled HSS Columns, CIDECT monography #5, Canadian Edition.

Sterling, R. L.

1980: The Ultimate Load Behaviour of Laterally Constrained Rock Beams, Proceedings 21 Symposium on Rock Mechanics, University of Missouri-Rolla, May 28-30, 1980.

Sterling, R. L. and Nelson, C. R.

1978: An Experimental Investigation of the Ultimate Strength of Laterally Constrained Rock Beams, Experimental Mechanics, 1978, p. 261-268.

Timoshenko, S. and Young, D.

1968: Elements of Strength of Materials, Fifth Edition, p. 95-172.

US Army Corp of Engineers

1978: Engineering and Design-Tunnels and Shafts in Rock, EM1110-2-2901, Chapter 3.

Willems, N., Easley, J. and Rolfe, S.

1981: Strength of Materials, McGraw-Hill Book Company, p. 163-239.

APPENDIX I

Section extracted from:

HOLLOW STRUCTURAL SECTIONS

Design Manual For Concrete Filled HSS Columns

(Stelco)

1 Design method

This chapter contains a step by step design method for concrete-filled HSS columns axially loaded or with small real or equivalent eccentricities. Ten load charts are given which take into account the parameters affecting the behavior of these composite columns. Parameters considered include: overall buckling of the column, creep of the concrete, the hoop effect and local buckling of the HSS wall. Complete information concerning the theoretical studies on which the method is based can be found in Appendix II at the end of the manual. It should be noted that Appendix II is also from CIDECT Monograph #5.

It is important to note that the theoretical studies are based on European design rules: Limit States Design method of the ECC (European Committee for Concrete) and the buckling curves of the ECCS (European Convention for Constructional Steelwork).

Knowing the size of the HSS and the mechanical properties of the steel and concrete, it is easy to determine, by means of the charts, the factored resistance of the composite column. Eccentric loading is taken into account by the use of a reduction factor. Also, a preliminary design graph is provided. Typical design examples are given at the end of the chapter.

1.1 Specified material properties: HSS can be either round, square or rectangular in shape. However, the manual has been prepared for round and square HSS only. Stelco's standard HSS conforms to CSA G40.20M Class H. Class H is either hot formed to final shape or cold formed to final shape and then stress relieved. Residual stresses in the Class H product are relatively small and thus Class H gives superior structural performance. Thus, this manual was prepared for, and only applies to, Class H HSS.

The only steel yield strength considered is: F_y = 350 MPa which is a standard grade for HSS.

The concrete used for filling HSS columns should be structural concrete manufactured with standard aggregates, though lightweight concrete can also be used. Appendix I on concrete filling gives details of concrete mixes. It should be noted that Appendix I is also from CIDECT Monograph #5.

The basic mechanical property of concrete considered in this design method is its specified compressive strength, f'_c, as measured by cylindrical test specimens in accordance with CSA Standard CAN3-A23.2, Methods of Tests for Concrete[3].

Concrete strengths considered are: f'_c = 20, 25, 30, 35 and 40 MPa which correspond to standard concrete grades normally available in Canada.

There generally is an obvious economic advantage in selecting a higher strength concrete. This makes it possible to appreciably increase the load carrying capacity of the column, while keeping the steel used to a minimum.

1.2 Performance factors for steel and concrete: As specified in CSA Standard CAN3-S16.1M, performance factors are applied to both the specified compressive strength of concrete, f'_c, and the specified minimum yield strength of steel, F_y, to take into account the variability of material properties, dimensions, workmanship, type of failure, and uncertainty in prediction of member resistance.

These performance factors are ϕ = 0.90 for steel and ϕ_c = 0.67 for concrete and have been incorporated into the load charts.

1.3 Eccentricity: In order to produce a rational method for eccentrically loaded columns, it has been necessary to use the equivalent loading concept. When only a part of the load is acting eccentrically or when end moments are present, it is necessary to calculate an equivalent eccentricity.

Determination of the real or equivalent eccentricity, e, under factored loading conditions is shown for 3 cases in Figure 1.

1.4 Load charts description: Non-dimensional load charts are given in Figures 2.1 to 2.10 (section 1.7, pages 8 to 22). They are aimed at simplifying the designer's work and give the direct graphical equivalent of numerical results. They have been prepared for both circular and square HSS and, since permanent loads are the significant ones in most practical cases, the load charts have been presented only for long term loads and therefore take concrete creep into account. The load charts also account for the overall buckling of the column, the local buckling of both circular and square HSS and the hoop effect for short circular columns.

For each type of section, circular or square, load charts have been drawn covering one specified minimum yield strength of steel and five specified compressive strengths of concrete.

The load charts give the factored compressive resistance, C_r, of concrete-filled HSS columns subject to axial loading. The following parameters are required for use of the load charts:

1 Type of section: square or circular
2 Specified minimum yield strength of steel: F_y
3 Specified compressive strength of concrete: f'_c
4 Effective length of the column: KL
5 Diameter or width of the HSS (outside dimension): D or b
6 Thickness of the HSS wall: t

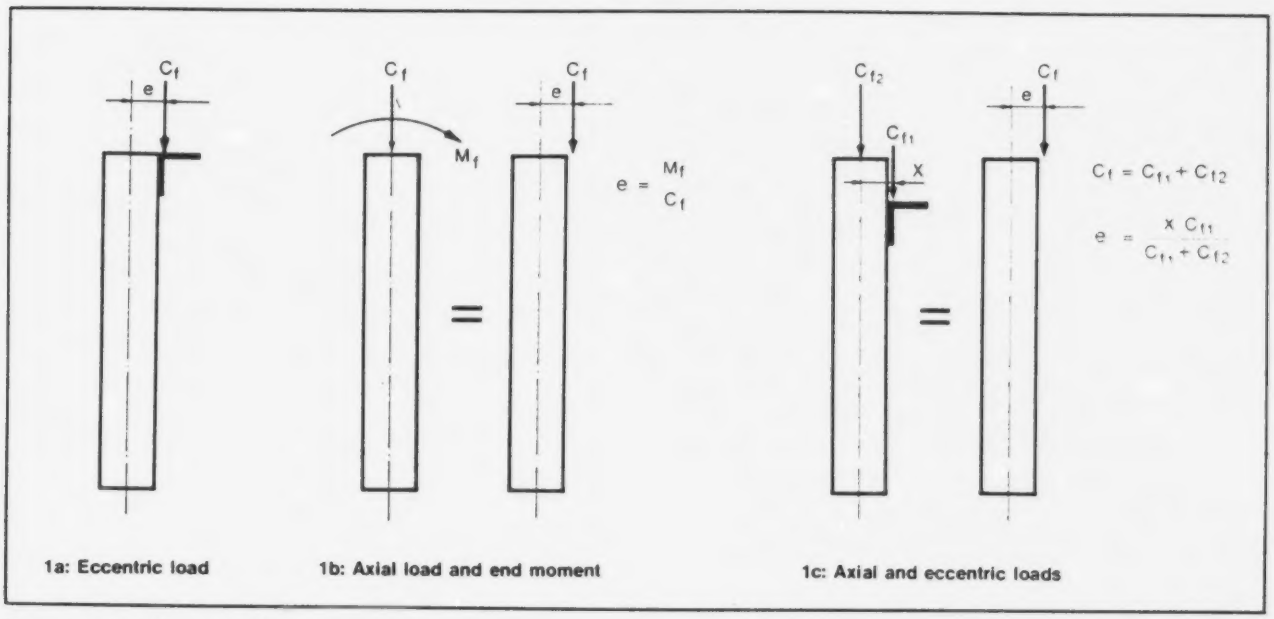

1a: Eccentric load — 1b: Axial load and end moment — 1c: Axial and eccentric loads

Figure 1: Equivalent eccentricity.

The appropriate load chart is chosen according to parameters 1, 2 and 3. Two ratios are necessary to determine the factored compressive resistance C_r and the parameters 4, 5 and 6 are used to determine these ratios:

- Effective length to diameter or width ratio: KL/D or KL/b,
- diameter or width to thickness ratio: D/t or b/t.

These two ratios are then used in the appropriate load chart to determine the value of y.

$$y = \frac{C_r}{t^2}$$

hence: $C_r = yt^2$

where: C_r = factored compressive resistance of the concrete-filled HSS column under axial loading (kN)*

t = thickness of the HSS wall (mm)

y = value obtained from the load chart

*It should be noted that the factored compressive resistance of the concrete-filled HSS column found in this way from the charts includes the performance factors for steel (ϕ) and concrete (ϕ_c)

1.5 Eccentricity reduction factor: The eccentricity reduction factor α is found from Figure 3 (section 1.7, page 23). This graph is based on a linear interaction formula and leads to conservative values of the factored resistance of a column of given length when subjected to a real or equivalent loading eccentricity. More information concerning the description of this graph is given in Appendix II

The values required for using Figure 3 are:

- The real or equivalent eccentricity: e,
- the effective length of the column: KL,
- the diameter or width of the HSS (outside dimension): D or b.

Figure 3 gives the coefficient α in relation to the ratios KL/D or KL/b and e/D or e/b. α is a reduction factor which is applied to the factored compressive resistance of the column C_r to take account of the real or equivalent eccentricity.

1.6 Preliminary design graph description: A preliminary design graph is given in Figure 4 (section 1.7, page 24). It is used to obtain a trial composite section which can then be checked by using the load charts. The formulae used for this graph are based on the following:

- Loading is purely axial. However, when using this preliminary design method, the eccentricity reduction factor α is used to take into account eccentricity,
- the steel and concrete are limited to maximum stress levels of ϕF_y and $\phi_c f'_c$
- the ratio between the area of the steel section A_s and the area of the concrete section A_c is in the range of: $5\% A_c \leqq A_s \leqq 25\% A_c$.

For the sake of simplicity, the following phenomena were approximately taken into account in the preparation of the preliminary design graph by use of a built-in factor: Column buckling, concrete creep, local buckling of the HSS wall and hoop effect.

Important note: The preliminary design graph is only intended to give an estimate of the size of section needed for the loading considered. The section size obtained with the preliminary design graph must be checked with the load charts and the eccentricity reduction factor.

1.7 Load charts and graphs: Pages 8 to 22 provide the necessary load charts and graphs for design purposes.

stelco

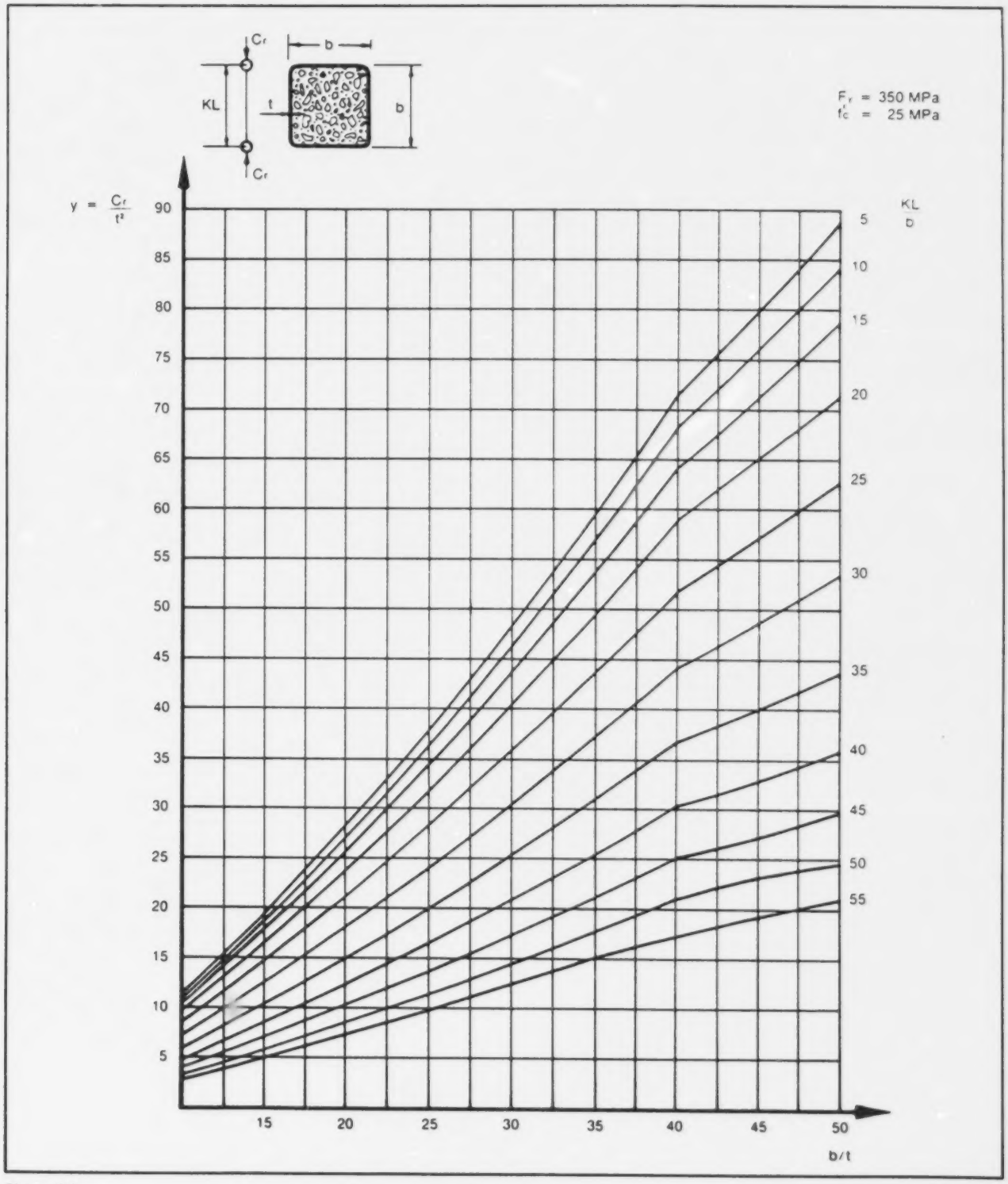

Figure 2.2

APPENDIX II

TEST RESULTS

TEST NUMBER 1

TEST BEAM . 5 x 2 inch HSS with 0.188 inch wall
. Empty

BEAM LENGTH . 5.0 ft or 60. inches

LOAD MECHANISM . 1-Point Test
Simply Supported

Load (pounds)	Centre Point Dial Gage Reading (inches)	Centre Point Deflection (inches)
0	.800	-
1000	.818	.018
2000	.841	.041
3000	.868	.068
4000	.892	.092
5000	.917	.117
6000	.948	.148
7000	.975	.175
8000	1.005	.205
9000	1.038	.238
10,000	1.065	.265
11,000	1.102	.302
12,000	1.139	.339
13,000	1.180	.380
14,000	1.225	.425
15,000	1.280	.480
16,000	1.350	.550
17,000	1.428	.628
18,000	1.585	.785
18,05[illegible]	1.662	.962
18,050	1.805	1.005
18,000	1.860	1.060

Terminated

TEST NUMBER 2

TEST BEAM . 5 x 2 inch HSS with 0.188 inch wall
. M-Bed (4.51) - 1 Day Cure

BEAM LENGTH . 5.0 ft or 60. inches

LOAD MECHANISM . 1-Point Test
Simply Supported

Load (pounds)	Centre Point Dial Gage Reading (inches)	Centre Point Deflection (inches)
0	.800	-
1000	.815	.015
2000	.836	.036
3000	.859	.059
4000	.877	.077
5000	.912	.112
6000	.940	.140
7000	.950	.150
8000	.980	.180
9000	1.010	.210
10,000	1.077	.277
11,000	1.112	.312
12,000	1.139	.339
13,000	1.175	.375
14,000	1.228	.428
15,000	1.267	.467
16,000	1.322	.522
17,000	1.430	.630
18,000	1.550	.750
19,000	1.678	.878
19,200	1.795	.995
19,300	1.865	1.065
19,400	1.875	1.075

Terminated

TEST NUMBER 3

TEST BEAM . 5 x 2 inch HSS with 0.188 inch wall
. M-Bed (3.51) - 3 Day Cure

BEAM LENGTH . 5.0 ft or 60. inches

LOAD MECHANISM . 1-Point Test
Simply Supported

Load (pounds)	Centre Point Dial Gage Reading (inches)	Centre Point Deflection (inches)
0	.600	-
1000	.610	.010
2000	.634	.034
3000	.660	.060
4000	.681	.081
5000	.706	.106
6000	.726	.126
7000	.752	.152
8000	.770	.170
9000	.803	.203
10,000	.833	.233
11,000	.864	.264
12,000	.898	.298
13,000	.936	.336
14,000	.973	.373
15,000	1.015	.415
16,000	1.056	.456
17,000	1.106	.506
18,000	1.173	.573
18,750	1.231	.631
19,500	1.253	.653
19,750	1.289	.689
20,000	1.320	.720
20,500	1.372	.772
20,750	1.427	.827
21,000	1.500	.900
21,400	1.855	1.355
21,500	2.085	1.485

Terminated

TEST NUMBER 4

TEST BEAM
- 5 x 2 inch HSS with 0.188 inch wall
- M-Bed (4.01) - 1 Day Cure
- 1/2 inch Rebar - 1/2 inch grout cover

BEAM LENGTH
- 5.0 ft or 60. inches

LOAD MECHANISM
- 1-Point Test
- Simply Supported

Load (pounds)	Centre Point Dial Gage Reading (inches)	Centre Point Deflection (inches)
0	.600	-
1000	.611	.011
2000	.630	.030
3000	.651	.051
4000	.667	.067
5000	.688	.088
6000	.715	.115
7000	.739	.139
8000	.763	.163
9000	.789	.189
10,000	.820	.220
11,000	.849	.249
12,000	.880	.280
13,000	.920	.320
14,000	.955	.355
15,000	.994	.394
16,000	1.033	.433
17,000	1.087	.487
18,000	1.141	.541
19,000	1.215	.615
20,000	1.310	.710
21,000	1.500	.900
21,600	1.800	1.200

Terminated

TEST NUMBER 5

TEST BEAM . 5 x 2 inch HSS with 0.188 inch wall
. M-Bed (4.01) - 7 Day Cure
. 1/2 inch Rebar - 1/2 inch grout cover

BEAM LENGTH . 5.0 ft or 60. inches

LOAD MECHANISM . 1-Point Test
Simply Supported

Load (pounds)	Centre Point Dial Gage Reading (inches)	Centre Point Deflection (inches)
0	.700	-
1000	.721	.021
2000	.740	.040
3000	.765	.065
4000	.780	.080
5000	.802	.102
6000	.820	.120
7000	.842	.142
8000	.869	.169
9000	.894	.194
10,000	.923	.223
11,000	.948	.248
12,000	.977	.277
13,000	1.014	.314
14,000	1.047	.347
15,000	1.083	.384
16,000	1.122	.422
17,000	1.170	.470
18,000	1.215	.515
19,000	1.273	.573
20,000	1.340	.640
21,000	1.428	.728
22,000	1.576	.876
22,400	1.680	.980
22,800	1.828	1.128
23,000	1.904	1.204
23,350	2.173	1.473
23,500	2.215	1.515

Terminated

TEST NUMBER 6

TEST BEAM
- 5 x 2 inch HSS with 0.188 inch wall
- M-Bed (4.01) - 1 Day Cure
- 1/2 inch Rebar - 1/2 inch grout cover
- Pressurized (200 psi)

BEAM LENGTH
- 5.0 ft or 60. inches

LOAD MECHANISM
- 1-Point Test
- Simply Supported

Load (pounds)	Centre Point Dial Gage Reading (inches)	Centre Point Deflection (inches)
0	.700	-
1000	.716	.016
2000	.737	.037
3000	.756	.056
4000	.775	.075
5000	.798	.098
6000	.816	.116
7000	.841	.141
8000	.867	.167
9000	.888	.188
10,000	.908	.208
11,000	.933	.233
12,000	.964	.264
13,000	.997	.297
14,000	1.035	.335
15,000	1.075	.375
16,000	1.140	.440
17,000	1.163	.463
18,000	1.232	.532
19,000	1.318	.618
20,000	1.424	.724
21,000	1.659	.959
21,400	1.900	1.200
21,420	2.071	1.371

Terminated

TEST BEAM

BEAM LENGTH

LOAD MECHANIS

Load (pounds)	Centre Point Dial Gage Reading (inches)	Ce D
0	.580	
1000	.595	
2000	.620	
3000	.645	
4000	.660	
5000	.681	
6000	.708	
7000	.738	
8000	.758	
9000	.785	
10,000	.814	
11,000	.844	
12,000	.875	
13,000	.913	
14,000	.958	
15,000	1.005	
16,000	1.056	
17,000	1.120	
18,000	1.190	
19,000	1.295	
20,000	1.458	
20,800	1.759	
21,000	1.826	
21,400	2.125	

Terminated

TEST NUMBER 7

TEST BEAM . 5 x 2 inch HSS with 0.188 inch wall
. Talygrout 100 - 1 Day Cure

BEAM LENGTH . 5.0 ft or 60. inches

LOAD MECHANISM . 1-Point Test
. Simply Supported

tre Point Gage Reading inches)	Centre Point Deflection (inches)	End Point - Bottom Fibre Dial Gage Reading (inches)	End Point - Bottom Fibre Deflection (inches)
80	-	.0020	-
95	.015	.0020	.0000
20	.040	.0022	.0002
45	.065	.0037	.0017
60	.080	.0050	.0030
81	.101	.0082	.0062
08	.128	.0160	.0140
38	.158	-	-
58	.178	-	-
85	.205	.0311	.0291
4	.234	.0374	.0354
4	.264	.0432	.0412
5	.295	.0480	.0460
3	.333	.0538	.0518
8	.378	.0582	.0562
5	.425	.0605	.0585
6	.476	.0660	.0640
0	.540	.0711	.0691
0	.610	.0741	.0721
3	.713	.0769	.0749
8	.878	.0882	.0862
9	1.179	.1052	.1032
6	1.246	.1110	.1090
5	1.595	.1303	.1283

TEST NUMBER 8

TEST BEAM . 5 x 2 inch HSS with 0.188 inch wall
. Taly Grout 100 - 7 Day Cure

BEAM LENGTH . 5.0 ft or 60. inches

LOAD MECHANISM . 1-Point Test
. Simply Supported

Load (pounds)	Centre Point Dial Gage Reading (inches)	Centre Point Deflection (inches)
0	.700	-
1000		
2000		
3000		
4000		
5000		
6000		
7000		
8000		
9000	N/A	N/A
10,000		
11,000		
12,000		
13,000		
14,000		
15,000		
16,000		
17,000		
18,000		
19,000		
20,000		
21,000	1.470	.770
22,000	1.574	.874
22,500	1.725	1.025
22,760	1.910	1.210
23,000	2.090	1.390

Terminated

TEST NUMBER 9

TEST BEAM . 5 x 2 inch HSS with 0.188 inch wall
. M-Bed (4.01) - 7 Day Cure
. Pressurized (200 psi)

BEAM LENGTH . 5.0 ft or 60. inches

LOAD MECHANISM . 1-Point Test
Simply Supported

Load (pounds)	Centre Point Dial Gage Reading (inches)	Centre Point Deflection (inches)
0	.700	-
1000	.715	.015
2000	.741	.041
3000	.767	.067
4000	.785	.085
5000	.802	.102
6000	.828	.128
7000	.859	.159
8000	.875	.175
9000	.902	.202
10,000	.928	.228
11,000	.962	.262
12,000	.998	.298
13,000	1.038	.338
14,000	1.080	.380
15,000	1.124	.424
16,000	1.180	.480
17,000	1.245	.545
18,000	1.330	.630
19,000	1.432	.732
20,000	1.617	.917
20,600	1.965	1.265
21,000	2.300	1.600

Terminated

TEST NUMBER 10

TEST BEAM
- 5 x 2 inch HSS with 0.188 inch wall
- M-Bed (4.01) - 7 Day Cure
- 1/2 inch Rebar - 1/2 inch grout cover
- Pressurized (200 psi)

BEAM LENGTH
- 5.0 ft or 60. inches

LOAD MECHANISM
- 1-Point Test
- Simply Supported

Load (pounds)	Centre Point Dial Gage Reading (inches)	Centre Point Deflection (inches)
0	.690	-
1000	.710	.020
2000	.720	.030
3000	.750	.060
4000	.779	.089
5000	.784	.094
6000	.807	.117
7000	.828	.138
8000	.855	.165
9000	.881	.191
10,000	.910	.220
11,000	.941	.251
12,000	.971	.281
13,000	1.008	.318
14,000	1.040	.350
15,000	1.081	.391
16,000	1.115	.425
17,000	1.161	.471
18,000	1.216	.526
19,000	1.290	.600
20,000	1.380	.690
21,000	1.495	.805
21,600	1.675	.985
22,000	1.742	1.052
22,300	2.045	1.355
22,500	2.155	1.465

Terminated

TEST NUMBER 11

TEST BEAM . 5 x 2 inch HSS with 0.188 inch wall
. M-Bed (4.01) - 28 Day Cure

BEAM LENGTH . 5.0 ft or 60. inches

LOAD MECHANISM . 3-Point Test
. Simply Supported

Load (pounds)	Centre Point Dial Gage Reading (inches)	Centre Point Deflection (inches)
0	1.470	-
1000	-	-
2000	-	-
3000	1.523	.053
4000	1.548	.078
5000	1.565	.095
6000	1.582	.112
7000	1.605	.135
8000	1.625	.155
9000	1.645	.175
10,000	1.669	.199
11,000	1.699	.229
12,000	1.723	.253
13,000	1.751	.281
14,000	1.780	.310
15,000	1.805	.335
16,000	1.835	.365
17,000	1.865	.395
18,000	1.990	.430
19,000	1.937	.467
20,000	1.981	.511
21,000	2.026	.556
22,000	2.069	.599
23,000	2.129	.659
24,000	2.209	.739
25,000	2.296	.826
26,000	2.411	.941
27,000	2.557	1.087
28,000	2.730	1.260
28,500	2.855	1.385
28,750	3.160	1.690
29,000	3.250	1.780

Terminated

TEST NUMBER 12

TEST BEAM . 5 x 2 inch HSS with 0.188 inch wall
. Empty Beam

BEAM LENGTH . 5.0 ft or 60. inches

LOAD MECHANISM . 3-Point Test
. Simply Supported

Load (pounds)	Centre Point Dial Gage Reading (inches)	Centre Point Deflection (inches)
0	1.500	-
1000	1.521	.021
2000	1.540	.040
3000	1.559	.059
4000	1.580	.080
5000	1.599	.099
6000	1.623	.123
7000	1.641	.141
8000	1.665	.165
9000	1.689	.189
10,000	1.720	.220
11,000	1.748	.248
12,000	1.785	.285
13,000	1.818	.318
14,000	1.852	.352
15,000	1.884	.384
16,000	1.926	.426
17,000	1.967	.467
18,000	2.011	.511
19,000	2.059	.559
20,000	2.130	.630
21,000	2.202	.702
22,000	2.275	.775
23,000	2.389	.889
24,000	2.532	1.032
24,500	2.671	1.171
24,500	2.785	1.285
24,500	2.830	1.330

Terminated

TEST NUMBER 13

TEST BEAM . 5 x 2 inch HSS with 0.188 inch wall
. Empty Beam

BEAM LENGTH . 5.0 ft or 60. inches

LOAD MECHANISM . 3-Point Test
. Simply Supported
. Laterally Confined

Load (pounds)	Centre Point Dial Gage Reading (inches)	Centre Point Deflection (inches)
0	1.489	-
1000	1.503	.014
2000	1.516	.027
3000	1.530	.041
4000	1.545	.056
5000	1.556	.067
6000	1.572	.083
7000	1.589	.100
8000	1.607	.118
9000	1.629	.140
10,000	1.647	.158
11,000	1.669	.180
12,000	1.691	.202
13,000	1.716	.227
14,000	1.741	.252
15,000	1.771	.282
16,000	1.796	.307
17,000	1.824	.335
18,000	1.854	.365
19,000	1.887	.398
20,000	1.930	.441
21,000	1.975	.486
22,000	2.025	.536
23,000	2.090	.601
24,000	2.162	.673
25,000	2.284	.795
25,400	2.493	1.004

Terminated

TEST NUMBER 14

TEST BEAM . 5 x 2 inch HSS with 0.188 inch wall
. M-Bed (4.01) - 28 Day Cure

BEAM LENGTH . 5.0 ft or 60. inches

LOAD MECHANISM . 3-Point Test
. Simply Supported
. Laterally Confined

Load (pounds)	Centre Point Dial Gage Reading (inches)	Centre Point Deflection (inches)
0	1.610	-
1000	1.624	.014
2000	1.636	.026
3000	1.648	.038
4000	1.663	.053
5000	1.676	.066
6000	1.690	.080
7000	1.707	.097
8000	1.728	.118
9000	1.742	.132
10,000	1.762	.152
11,000	1.780	.170
12,000	1.800	.190
13,000	1.821	.211
14,000	1.841	.231
15,000	1.865	.255
16,000	1.886	.276
17,000	1.908	.298
18,000	1.933	.323
19,000	1.959	.349
20,000	1.988	.378
21,000	2.019	.409
22,000	2.044	.434
23,000	2.075	.465
24,000	2.114	.504
25,000	2.153	.543
26,000	2.198	.588
27,000	2.252	.642
28,000	2.315	.705
29,000	2.397	.787
30,000	2.534	.924
30,500	2.685	1.075
30,750	2.750	1.140
30,900	2.937	1.327
30,900	3.003	1.393

Terminated

TEST NUMBER 15

TEST BEAM . 5 x 2 inch HSS with 0.188 inch wall
. M-Bed (4.01) - 3 Day Cure

BEAM LENGTH . 5.0 ft or 60. inches

LOAD MECHANISM . 3-Point Test
. Simply Supported

Load (pounds)	Centre Point Dial Gage Reading (inches)	Centre Point Deflection (inches)
0	1.600	-
1000	1.615	.015
2000	1.630	.030
3000	1.657	.057
4000	1.682	.082
5000	1.695	.095
6000	1.715	.115
7000	1.736	.136
8000	1.759	.159
9000	1.784	.184
10,000	1.804	.204
11,000	1.830	.230
12,000	1.856	.256
13,000	1.880	.280
14,000	1.910	.310
15,000	1.937	.337
16,000	1.973	.373
17,000	2.003	.403
18,000	2.041	.441
19,000	2.078	.478
20,000	2.120	.520
21,000	2.166	.566
22,000	2.219	.619
23,000	2.278	.678
24,000	2.355	.755
25,000	2.444	.844
26,000	2.547	.947
27,000	2.675	1.075
27,500	2.762	1.162
27,750	2.840	1.240
28,000	2.948	1.348
28,500	3.040	1.440
28,750	3.100	1.500
29,000	3.300	1.700

Terminated

TEST BEAM

BEAM LENGTH

LOAD MECHANI

Load (pounds)	Centre Point Dial Gage Reading (inches)	C
0	1.623	
1000	1.635	
2000	1.645	
3000	1.656	
4000	1.668	
5000	1.680	
6000	1.695	
7000	-	
8000	1.720	
9000	1.735	
10,000	1.749	
11,000	1.770	
12,000	1.786	
13,000	1.804	
14,000	1.822	
15,000	1.846	
16,000	1.870	
17,000	1.895	
18,000	1.920	
19,000	1.950	
20,000	1.977	
21,000	2.005	
22,000	2.038	
23,000	2.080	
24,000	2.110	
25,000	2.148	
26,000	2.193	
27,000	2.248	
28,000	2.325	
29,000	2.433	
29,750	2.575	
30,000	2.642	
30,200	2.775	
30,300	2.857	

Terminated

TEST NUMBER 16

T BEAM . 5 x 2 inch HSS with 0.188 inch wall
. M-Bed (4.01) - 3 day Cure

M LENGTH . 5.0 ft or 60. inches

D MECHANISM . 3-Point Test
. Simply Supported
. Laterally Confined

nt ading	Centre Point Deflection (inches)	End Point - Bottom Fibre Dial Gage Reading (inches)	End Point - Bottom Fibre Deflection (inches)
	-	.0558	-
	.012	-	-
	.022	-	-
	.033	-	-
	.045	-	-
	.057	-	-
	.072	.0557	-.0001
	-	-	-
	.097	-	-
	.112	-	-
	.126	.0565	+.0007
	.147	-	-
	.163	-	-
	.181	-	-
	.199	-	-
	.223	-	-
	.247	-	-
	.272	.0609	+.0059
	.297	-	-
	.327	-	-
	.354	-	-
	.382	-	-
	.415	.0601	+.0043
	.457	-	-
	.487	-	-
	.525	-	-
	.570	.0540	-.0018
	.625	-	-
	.702	-	-
	.810	.0349	-.0209
	.952	-	-
	1.019	-	-
	1.152	-	-
	1.234	-	-

TEST BEAM .

BEAM LENGTH .

LOAD MECHANISM .

Load (pounds)	Deflection Mid-Span (inch)	End-Movement At Bottom Due To Rotation (inch)
0	.000	
1000	.016	
2000	.027	-.0007
3000	.041	
4000	.056	-.0084
5000	.066	
6000	.080	-.0077
7000	.094	
8000	.107	-.0050
9000	.123	
10,000	.139	-.0016
11,000	.156	
12,000	.172	-.0017
13,000	.189	
14,000	.205	+.0050
15,000	.230	
16,000	.247	+.0083
17,000	.267	
18,000	.288	+.0093
19,000	.311	
20,000	.334	+.0110
21,000	.357	
22,000	.389	+.0111
23,000	.422	
24,000	.449	+.0109
25,000	.482	
26,000	.512	+.0099
27,000	.557	
28,000	.608	+.0099
29,000	.677	
30,000	.760	+.0100
31,000	.939	
31,500	.967	+.0124

TEST NUMBER 17

BEAM . 5 x 2 inch HSS with 0.188 inch wall
. M-Bed (4.01) - 4 Day Cure

M LENGTH . 5.0 ft or 60. inches

D MECHANISM . 3-Point Test
. Simply Supported
. Laterally Confined

nd-Movement t Bottom Due To Rotation (inch)	Micro-Strains Recorded In Tie-Rods (με)				Force In Tie Rods (-) Compression; (+) tension (pounds - force)			
	1	2	3	4	1	2	3	4
-.0007	-29	-16	+18	+28	-1537	-848	+954	+1484
-.0084	-43	-24	+31	+39	-2280	-1272	+1643	+2068
-.0077	-56	-40	+52	+59	-2969	-2121	+2757	+3128
-.0050	-61	-47	+70	+79	-3234	-2492	+3711	+4188
-.0016	-63	-56	+96	+106	-3340	-2969	+5089	+5620
-.0017	-71	-60	+117	+125	-3764	-3181	+6203	+6628
+.0050	-64	-61	+135	+147	-3393	-3234	+7157	+7793
+.0083	-76	-74	+170	+178	-4029	-3923	+9012	+9437
+.0093	-83	-72	+194	+200	-4400	-3817	+10,285	+10,603
+.0110	-86	-71	+221	+230	-4559	-3764	+11,716	+12,193
+.0111	-90	-78	+251	+268	-4771	-4135	+13,307	+14,208
+.0109	-94	-82	+273	+287	-4983	-4347	+14,473	+15,215
+.0099	-102	-86	+308	+314	-5407	-4559	+16,328	+16,647
+.0099	-105	-90	+347	+357	-5567	-4771	+18,396	+18,926
+.0100	-112	-95	+383	+394	-5938	-5036	+20,305	+20,880
	-111	-105	+440	+444	-5885	-5567	+23,326	+23,538
+.0124	-120	-105	+429	+414	-6362	-5567	+22,743	+21,948

TEST BEAM

BEAM LENGTH

LOAD MECHANIS

Load (pounds)	Deflection Mid-Span (inch)	End-Moveme At Bottom To Rotati (inch)
0	.000	
1000	.011	
2000	.026	+.0002
3000	.041	
4000	.056	-.0012
5000	.069	
6000	.082	-.0010
7000	.100	
8000	.110	+.0015
9000	.125	
10,000	.141	+.0031
11,000	.165	
12,000	.178	+.0032
13,000	.199	
14,000	.215	+.0032
15,000	.241	
16,000	.254	+.0030
17,000	.280	
18,000	.304	+.0017
19,000	.332	
20,000	.351	+.0008
21,000	.382	
22,000	.411	+.0006
23,000	.447	
24,000	.474	+.0006
25,000	.522	
26,000	.561	+.0021
27,000	.612	
28,000	.677	+.0037
29,000	.767	
30,000	.956	+.0069
30,400	1.312	+.0292

TEST NUMBER 18

TEST BEAM . 5 x 2 inch HSS with 0.188 inch wall
. M-Bed (4.01) - 1 Day Cure

BEAM LENGTH . 5.0 ft or 60. inches

LOAD MECHANISM . 3-Point Test
. Simply Supported
. Laterally Confined

ection -Span nch)	End-Movement At Bottom Due To Rotation (inch)	Micro-Strains Recorded In Tie-Rods (με)				Force In Tie Rods (-) Compression; (+) tension (pounds - force)			
		1	2	3	4	1	2	3	4
000									
011									
026	+.0002	-17	-11	+15	+9	-901	-583	+795	+477
041									
056	-.0012	-34	-21	+33	+40	-1802	-1113	+1749	+2121
069									
082	-.0010	-35	-21	+49	+47	-1855	-1113	+2598	+2492
100									
110	+.0015	-30	-29	+73	+66	-1590	-1537	+3870	+3499
125									
141	+.0031	-42	-34	+92	+96	-2227	-1802	+4877	+5089
165									
178	+.0032	-46	-36	+116	+121	-2439	-1909	+6150	+6414
199									
215	+.0032	-48	-45	+143	+143	-2545	-2386	+7581	+7581
241									
254	+.0030	-51	-50	+164	+164	-2704	-2651	+8694	+8694
280									
304	+.0017	-54	-53	+188	+190	-2863	-2810	+9967	+10,073
332									
351	+.0008	-58	-57	+215	+220	-3075	-3022	+11,398	+11,663
382									
411	+.0006	-65	-61	+246	+247	-3446	-3234	+13,042	+13,095
447									
474	+.0006	-68	-62	+270	+265	-3605	-3287	+14,314	+14,049
522									
561	+.0021	-73	-67	+297	+293	-3870	-3552	+15,745	+15,533
612									
677	+.0037	-75	-71	+324	+325	-3976	-3764	+17,177	+17,230
767									
956	+.0069	-80	-75	+376	+376	-4241	-3976	+19,933	+19,933
312	+.0292	-85	-81	+368	+370	-4506	-4294	+19,509	+19,615

TEST BEAM

BEAM LENG

LOAD MECHA

Load (pounds)	Deflection Mid-Span (inch)	End-Mov At Bott To Rot (inc
0	.000	
1000	.020	
2000	.026	+.00
3000	.039	
4000	.044	-.00
5000	.067	
6000	.082	-.00
7000	.096	
8000	.113	+.00
9000	.130	
10,000	.144	+.00
11,000	.163	
12,000	.182	+.01
13,000	.204	
14,000	.223	+.01
15,000	.244	
16,000	.267	+.01
17,000	.292	
18,000	.316	+.01
19,000	.342	
20,000	.364	+.01
21,000	.391	
22,000	.421	+.00
23,000	.448	
24,000	.474	+.00
25,000	.525	
26,000	.552	+.00
27,000	.598	
28,000	.647	+.00
29,000	.712	
30,000	.786	-.00
31,000	.927	
31,500	1.025	-.01
31,750	1.220	-.03

TEST NUMBER 19

TEST BEAM . 5 x 2 inch HSS with 0.188 inch wall
. M-Bed (4.01) - 5 Day Cure

BEAM LENGTH . 5.0 ft or 60. inches

LOAD MECHANISM . 3-Point Test
. Simply Supported
. Laterally Confined

End-Movement At Bottom Due To Rotation (inch)	Micro-Strains Recorded In Tie-Rods ($\mu\xi$)				Force In Tie Rods (-) Compression; (+) tension (pounds - force)			
	1	2	3	4	1	2	3	4
+.0001	-17	-16	+16	+18	-901	-848	+848	+954
-.0014	-31	-30	+31	+35	-1643	-1590	+1643	+1855
-.0009	-38	-39	+48	+64	-2015	-2068	+2545	+3393
+.0034	-42	-43	+65	+59	-2227	-2280	+3446	+3126
+.0072	-51	-55	+77	+75	-2704	-2915	+4082	+3976
+.0117	-56	-61	+99	+93	-2969	-3234	+5248	+4930
+.0128	-59	-67	+121	+112	-3128	-3552	+6415	+5938
+.0128	-65	-73	+143	+137	-3446	-3870	+7581	+7263
+.0128	-70	-79	+172	+159	-3711	-4188	+9118	+8429
+.0118	-76	-87	+199	+183	-4029	-4612	+10,550	+9702
+.0097	-84	-93	+228	+211	-4453	-4930	+12,087	+11,186
+.0074	-88	-100	+258	+241	-4665	-5301	+13,678	+12,776
+.0046	-94	-109	+290	+278	-4983	-5779	+15,374	+14,738
+.0016	-105	-119	+327	+322	-5567	-6309	+17,336	+17,071
-.0051	-110	-124	+367	+371	-5832	-6574	+19,456	+19,668
-.0183	-115	-141	+423	+442	-6097	-7475	+22,425	+23,432
-.0351	-127	-150	+423	+437	-6733	-7952	+22,425	+23,167

TEST NUMBER 20

TEST BEAM . 5 x 2 inch HSS with 0.188 inch wall
. M-Bed (4.01) - 3 Day Cure

BEAM LENGTH . 5.0 ft or 60. inches

LOAD MECHANISM . 1-Point Load Test
. Simply Supported

Load (pounds)	Centre Point Dial Gage Reading (inches)	Centre Point Deflection (inches)
0	.450	-
1000	.470	0.020
2000	.495	0.045
3000	.518	0.068
4000	.540	0.090
5000	.562	0.112
6000	.590	0.140
7000	.625	0.175
8000	.649	0.199
9000	.680	0.230
10,000	.710	0.260
11,000	.743	0.293
12,000	.792	0.342
13,000	.822	0.372
14,000	.860	0.410
15,000	.915	0.465
16,000	.967	0.517
17,000	1.035	0.585
18,000	1.125	0.675
19,000	1.283	0.833
20,000	1.771	1.321

Terminated

TEST NUMBER 21

TEST BEAM . 5 x 2 inch HSS with 0.188 inch wall
. M-Bed (4.01) - 28 Day Cure

BEAM LENGTH . 5.0 ft or 60. inches

LOAD MECHANISM . 1-Point Load Test
. Simply Supported

Load (pounds)	Centre Point Dial Gage Reading (inches)	Centre Point Deflection (inches)
0	.498	-
1000	.521	.023
2000	.546	.048
3000	.571	.073
4000	.607	.109
5000	.621	.123
6000	.648	.150
7000	.675	.177
8000	.708	.210
9000	.738	.240
10,000	.775	.277
11,000	.807	.309
12,000	.845	.347
13,000	.889	.391
14,000	.932	.434
15,000	.980	.482
16,000	1.034	.536
17,000	1.088	.590
18,000	1.170	.672
19,000	1.300	.802
20,000	1.590	1.092
20,250	1.795	1.297
20,250	2.090	1.592

Terminated